The immunomodulatory properties of the IgM- and IgA-enriched immunoglobulin preparation trimodulin

Dissertation
Fabian Bohländer

TECHNISCHE UNIVERSITÄT DARMSTADT

Vom Fachbereich Biochemie
der Technischen Universität Darmstadt

zur Erlangung des Grades
Doctor rerum naturalium
(Dr. rer. nat.)

Dissertation
von Fabian Bohländer

1. Gutachter: Prof. Dr. Harald Kolmar
2. Gutachter: PD Dr. med. Jörg Schüttrumpf

Darmstadt 2021

Erklärungen laut Promotionsordnung

Erklärung gemäß §8 Abs. 1 lit. c PromO

Ich versichere hiermit, dass die elektronische Version meiner Dissertation mit der schriftlichen Version übereinstimmt und für die Durchführung des Promotionsverfahrens vorliegt.

Erklärung gemäß §8 Abs. 1 lit. c PromO

Ich versichere hiermit, dass zu einem vorherigen Zeitpunkt noch keine Promotion versucht wurde und zu keinem früheren Zeitpunkt an einer in- oder ausländischen Hochschule eingereicht wurde. In diesem Fall sind nähere Angaben über Zeitpunkt, Hochschule, Dissertationsthema und Ergebnis dieses Versuchs mitzuteilen.

Erklärung gemäß §9 Abs. 1 PromO

Ich versichere hiermit, dass die vorliegende Dissertation selbstständig und nur unter Verwendung der angegebenen Quellen verfasst wurde.

Erklärung gemäß §9 Abs. 2 PromO

Die Arbeit hat bisher noch nicht zu Prüfungszwecken gedient.

Darmstadt, 06. Juli 2021

_____
Unterschrift

Zusammenfassung

Schwere Infektionserkrankungen wie Sepsis oder sCAP sind bekannte Probleme im Gesundheitswesen. Mit dem Ausbruch von SARS-CoV-2 und COVID-19 ist eine weitere Infektionserkrankung mit dramatischen Einfluss auf Gesundheit und Wirtschaft weltweit in den Fokus gerückt. Schwere Fälle von Sepsis, sCAP und COVID-19 führen zu einer entarteten Immunreaktion, die mit einer überschießenden Entzündungsreaktion einhergeht. Daher ist die Modulation des hyperinflammatorischen Immunsystems ein Hauptziel der Therapie. Eine vielversprechende adjuvante Therapieoption stellt Trimodulin dar, ein IgM- und IgA-angereichertes Immunglobulinpräparat (mit ~21 % IgM, 23 % IgA und 56 % IgG) in klinischer Entwicklung. Verfügbare funktionelle Studien identifizierten mehrere Wirkmechanismen die hauptsächlich der IgG und IgM Komponente zugeordnet werden konnten. Im Gegensatz dazu konnte die Rolle der IgA Komponente bisher nicht identifiziert werden.

Das Ziel dieser Arbeit ist es, die immunmodulatorischen Eigenschaften von Trimodulin im Kontext schwerer Infektionserkrankungen zu untersuchen. Ein besonderer Fokus wurde dabei auf die funktionelle Rolle der IgA Komponente gelegt.

Zunächst wurde ein zelluläres Modelsystem basierend auf neutrophil-ähnlichen HL-60 Zellen etabliert und umfänglich charakterisiert. Die Induktion einer Entzündungsreaktion durch bakterielle Stimuli (LPS und *S.aureus*) oder durch SARS-CoV-2 ähnliche Partikel wurde untersucht und die zugrunde liegenden Mechanismen (wie FcR Abhängigkeit und Signalwege) identifiziert. Als nächstes wurden die anti-inflammatorischen Effekte von Trimodulin sowohl auf ruhende Zellen- , als auch auf inflammatorisch aktivierte Zellen analysiert. Für die Immunomodulation durch Trimodulin konnten die folgenden fünf synergistischen Mechanismen gezeigt werden:

(1) Die direkte Bindung inflammatorischer Zytokine. (2) Das Ansteuern des ITAMi Signalweges durch monomere IgG und IgA Spezies. (3) Die Aktivierung des inhibitorischen ITIM Signalweges und verstärkte FcγRIIB Expression. (4) Modulation des Zellphänotyps durch verringerte FcγRIIA und FcαRI Expression. (5) Die Verdrängung von Immunkomplexen und reduzierte Phagozytose.

Durch den Vergleich der immunmodulatorischen Eigenschaften mit einem klassischen IVIg konnte demonstriert werden, dass Trimodulin stärkere Immunmodulation induziert. Trimodulin zeigte eine bessere direkte Bindung von Zytokinen, stärkere Phänotyp Modulation und Aktivierung des ITAMi Signalweges. Weiterhin konnte beobachtet werden, dass die IgA Komponente von Trimodulin mit dem FcαRI interagiert und FcαRI abhängige Phagozytose induziert.

Zusammenfassend lässt sich sagen, dass mehrere synergistische Wirkmechanismen durch Trimodulin induziert werden und dadurch eine starke Immunmodulation hervorrufen. Vorteilhafte Effekte im Vergleich zu einem IVIg können der zusätzlichen IgA Komponente zugeschrieben werden, durch die der FcαRI und dessen inhibitorische Signalwege angesteuert werden. Unterschiede in der IgG Subklassenverteilung und synergistische Effekte zwischen monomären und multimeren IgG, IgA und

IgM Spezies in Trimodulin könnten weitere Gründe für verbesserte Immunomodulation durch Trimodulin sein.

Die *in vitro* Modelle dieser Arbeit demonstrieren wirkungsvolle Immunmodulation durch Trimodulin im Kontext von Sepsis, sCAP und COVID-19. Nichts desto trotz beschränken sich diese Modelle auf lediglich einen Zelltyp und eine limitierte Anzahl zellulärer Effektorfunktionen. Weitere Forschungsarbeit ist notwendig um die Daten um weitere Zelltypen und Wirkmechanismen zu erweitern. Nur mit einem umfassenden Wissen über die Wirkmechanismen *in vitro* können die klinischen Daten von Sepsis, sCAP oder COVID-19 Patienten unterstützt und erklärt werden.

Abstract

Severe infection diseases, like sepsis or sCAP, are well-known problems for public health. With the outbreak of SARS-CoV-2 and COVID-19, another infection disease with a dramatic impact on health and the economy comes into focus. Severe cases of sepsis, sCAP and COVID-19 lead to a dysregulated immune response associated with overwhelming inflammation. Modulation of the hyperinflammatory immune system is, therefore, a major goal of therapy. A promising option is the adjunctive therapy with trimodulin, an IgM- and IgA-enriched immunoglobulin preparation in clinical testing (comprising ~21 % IgM, 23 % IgA, and 56 % IgG). Available functional studies identify several modes of action, which were mainly attributed to the IgG or IgM component. In contrast, the role of IgA in these preparations was not unraveled yet. This thesis aim is to investigate the immunomodulatory properties of trimodulin in the context of severe infection diseases. A specific focus was set on the identification of functional roles for the additional IgA component.

First, a cellular model system based on neutrophil-like HL-60 cells was established and comprehensively characterized. The induction of inflammation by bacterial stimuli (LPS and *S.aureus*) or by SARS-CoV-2-like particles was investigated and the underlying mechanism (FcR dependency, signaling pathways) identified. Next, anti-inflammatory effects of trimodulin on resting cells, as well as on inflammatory activated cells were analyzed. The following five synergistic mechanisms for immunomodulation by trimodulin were shown:

(1) The direct binding of pro-inflammatory cytokines. **(2)** Targeting of ITAMi signaling by monomeric IgG and IgA species. **(3)** Activation of inhibitory ITIM signaling and increased FcγRIIB expression. **(4)** Modulation of cell phenotype by decreased FcγRIIA and FcαRI expression. **(5)** Displacement of immune complex and reduced phagocytosis. By comparing immunomodulatory effects to classical IVIg, trimodulin was shown to mediate stronger immunomodulation by better binding of cytokines, enhanced phenotype modulation, and activation of ITAMi signaling. Furthermore, the IgA component of trimodulin interacts with the FcαRI receptor and mediates FcαRI dependent phagocytosis of *S.aureus*.

In conclusion, several synergistic modes of action are induced by trimodulin mediating powerful immunomodulation. Beneficial effects in comparison to IVIg can be attributed to the additional IgA component, by targeting FcαRI and inhibitory signaling. Differences in IgG subclass distribution and synergistic effects between monomeric and multimeric IgG, IgA, and IgM in trimodulin could be further reasons for improved immunomodulation by trimodulin.

The *in vitro* models of this work depicting sepsis, sCAP and COVID-19 demonstrated potent immunomodulation of trimodulin. Nevertheless, these models are restricted by testing only one cell type and a limited number of cellular effector outcomes. Further work is necessary to extend the data set to further cell types and modes of action. Only with comprehensive knowledge about the modes of action *in vitro*, clinical data for sepsis, sCAP or COVID-19 patients can be supported and explained.

Table of contents

1. Introduction

1.1. Basics: the immune system, antibodies and Fc-receptors

1.1.1. The immune system

The human immune system has the primary function to defeat invading pathogens like bacteria, fungi or viruses. But also the protection against toxins or degenerated body cells (cancer cells) is important [1]. To elicit these functions our body uses a complex network consisting of structural and chemical barriers (e.g. skin or mucosa), small molecules and soluble proteins (e.g. complement proteins, cytokines or antibodies) and a variety of immune effector cells (e.g. macrophages, dendritic cells, granulocytes, T-cells and B-cells) [1,2].

These components of the immune system work in two fundamental groups; innate and adaptive immunity. Innate immunity is (besides structural barriers) the first line in defense against invading pathogens. The innate response is a fast, antigen-independent mechanism responding within hours [2,3]. The basis for this fast response is the recognition of common pathogen structures by receptors on innate immune cells. When this network is not sufficient to eliminate invading pathogens, adaptive immunity is activated [1]. Adaptive immunity is an antigen-specific response that requires longer times to fight infection [2,3]. Central for adaptive immunity is the production of antigen-specific antibodies by plasma cells. The adaptive immune response uses two – interacting – mechanisms, the humoral- (based on soluble molecules like antibodies) and the cellular immunity (based on immune cells) [4].

Although innate and adaptive immunity are two different mechanisms, they are tightly connected and act together [2]. An example of this interplay are neutrophils. Neutrophils are the most abundant circulating leukocytes, which represent 60 % of total white blood cells. They act in innate immunity as the first line in the fight against invading pathogens. In addition, they mediate crucial functions in adaptive immunity, by interacting e.g. with antibodies [5,6].

The central mechanism that enables adequate immune function is the discrimination between self and non-self structures. Disorders of these mechanisms can lead to autoimmune diseases, like *multiple sclerosis* (MS) or *rheumatoid arthritis* (RA) [2,3]. Further, imbalances of the immune system can lead to either overwhelming inflammatory responses or compromised immune responses, known as immune deficiencies [1].

1.1.2. Immunoglobulins: central for adaptive immune response

In response to invading pathogens, adaptive immunity is activated. B-cells can recognize pathogen-specific antigens directly or by interacting with antigen-presenting cells (APCs). Cell proliferation and antibody production are then triggered by T-helper cells. Five antibody isotypes can be secreted by plasma cells: Immunoglobulin (Ig) G, IgA, IgM, IgD and IgE (compare Figure 1-1). Whereby each class

interacts with different partners and mediates a plethora of effector functions [1,7]. Antibodies of IgG class can be divided into four subclasses (IgG1-4), IgA antibodies in two subclasses (IgA1-2).

Because IgD and IgE antibodies were neither found in relevant concentrations in human plasma donations nor in immunoglobulin preparations those isotypes are not discussed in this work [7,8].

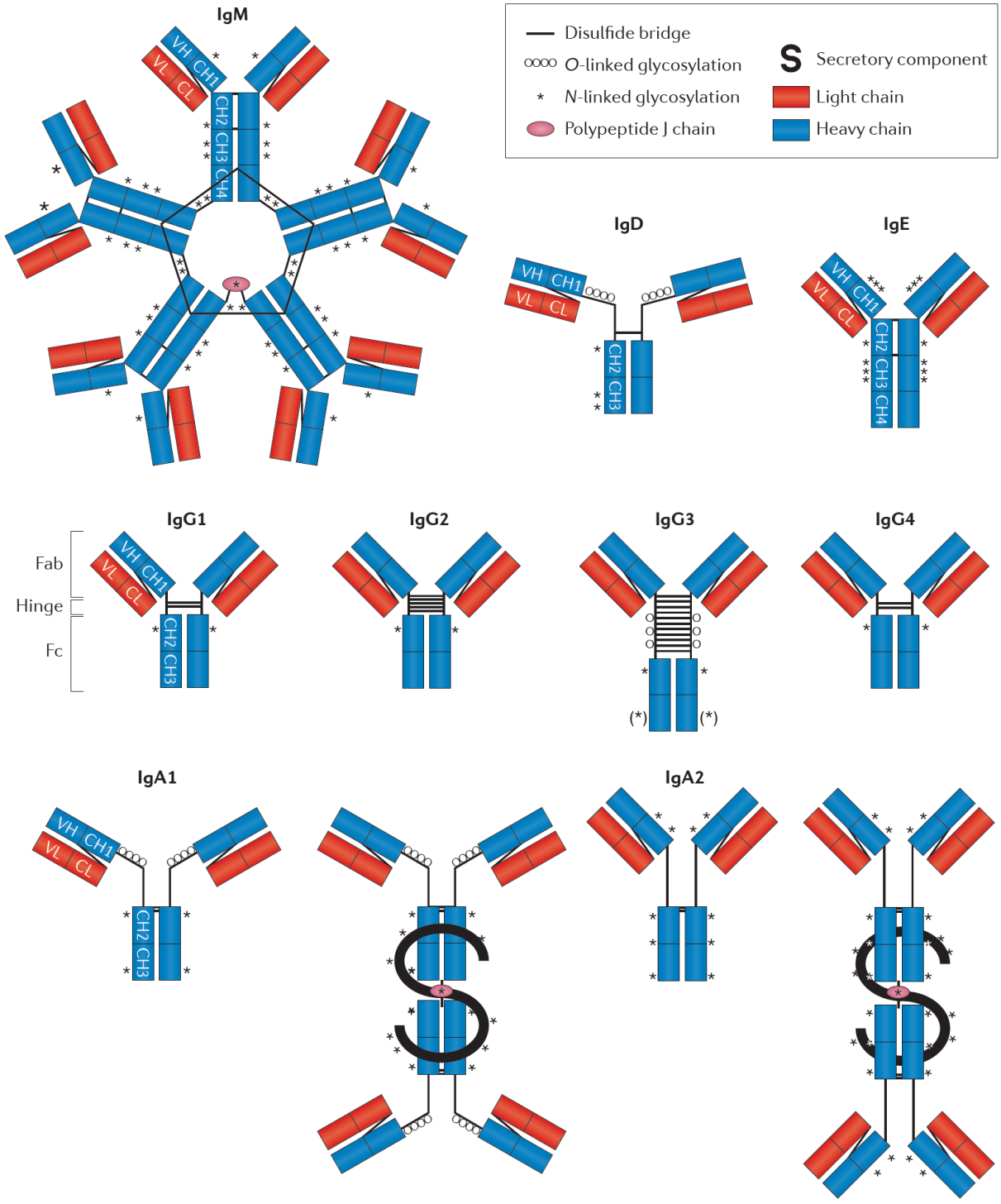

Figure 1-1: Schematic overview of human immunoglobulin isotypes and their subclasses. Each immunoglobulin monomer consists of two heavy (blue) and light chains (red) connected by disulfide bridges. Light and heavy chains are divided into the variable region (Fab-part), which mediates antigen binding and the constant region (Fc-part), which mediates binding to

Fc-receptors (FcR). Antibody isotypes differ in their constant chains. Each isotype is modified by glycosylation (stars and circles). IgG can be divided into four subclasses (IgG1-4), IgA into two subclasses (IgA1-2). IgM is secreted as a multimer, IgD, IgE and IgG as monomers. IgA is present as monomers and multimers. Multimeric forms of IgM and IgA are connected by the joining-chain (J-chain). Secretory dimeric IgA is associated with the secretory component (SC). Figure according to [7].

Each basic immunoglobulin molecule is a heterodimeric protein consisting of two identical heavy and light chains, connected by disulfide bridges. These chains can be divided into variable domains, which mediate antigen binding (Fab-region) and constant domains, which mediate distinct effector functions (Fc-region). Fab- and Fc-region are connected by a hinge region. The antibody molecule has two Fab- and one Fc-region resulting in a "Y"- or "T"-shaped structure, compare Figure 1-1 [7–9]. The immunoglobulin isotypes differ in their specific Fc-regions, multimerization, glycosylation and subclasses; this leads to differing biological effector functions. In the following section IgM, IgG and IgA isotypes are described more in detail.

During an immune response, **Immunoglobulin M** (IgM) is the first antibody produced by naive B-cells. First IgM is present as a membrane-bound form on the B-cell surface, but during the immune response, IgM is secreted into the blood. IgM is the third most abundant immunoglobulin isotype and represents ~10 % of human serum immunoglobulins (normal serum range 0.34-2.1 g/L) [8,9]. Secreted IgM is only present in multimeric form as pentamer or hexamer (>950 kDa). IgM monomers are linked by disulfide bounds and exclusively the pentamer with an additional joining-chain (J-chain). The J-chain facilitates multimerization and secretion into the mucosa but is not necessary [9–12].
IgM antibodies are expressed early after contact with antigens; variable regions do not undergo many somatic mutations during isotype switch, resulting in polyreactive antibodies. These low-affinity antibodies are known as natural antibodies. In contrast, during affinity maturation and isotype switching highly specific antibodies are developed, called immune antibodies [9,13,14].
While pentameric IgM comprises ten antigen-binding sites, high avidity binding to antigens is possible. The multimeric interaction of the IgM-Fab-regions with antigens and IgM-Fc-regions with FcR or complement system induces an early, powerful immune response [7,9,14]. Therefore, IgM activates 400-times stronger complement and induces 1000-fold stronger opsonization and agglutination of pathogens than monomeric IgG [15]. In response to stimulation with antigens and cytokines, plasma cells undergo isotype switching from IgM to IgG or IgA isotype, simultaneously variable regions undergo somatic mutations leading to affinity maturation [9].

Immunoglobulin G (IgG) is the most abundant antibody isotype which represents 75-80 % of serum immunoglobulins (normal range of 7-14 g/L). IgG is exclusively found as a monomer with ~ 150 kDa (IgG3 ~170 kDa) and is divided into four subclasses based on structural and functional differences [8,9,16,17]. IgG subclasses are ordered according to their abundance in serum (IgG1, 60-70 % > IgG2, 20-30 % > IgG3, 5-8 % > IgG4, 5 %) [17,18]. The subclasses have more than 90 % identity in

amino acid sequence and mainly differ in their hinge regions [17]. Especially IgG3 differs structurally because of its elongated hinge region, this makes IgG3 more prone for proteolytic degradation and reduces serum half-life [7]. Half-life of IgG1, 2 and 4 is about 20 days, whereas IgG3 has a half-life of 7 days [16]. According to the abundance and high stability, IgG1 antibodies are the best-studied and most frequently used antibody isotype in research [9]. Although structural differences between IgG subclasses are small, the interaction with antigens, FcRs or complement differs, which has a noteworthy influence on effector outcome. Functionally IgG3, followed by IgG1, has the greatest potency; IgG2 and IgG4 show a lower ability to activate immune cells. The mechanistic explanation behind this is a more flexible structure enables better ability to interact with antigens or FcR, leading to enhanced effector functions [7,9,17,18].

The human body produces higher amounts of **Immunoglobulin A** (IgA) than all other immunoglobulin isotypes together. Therefore, IgA is the predominant antibody on mucosa and secretions (~74 % IgA, 25 % IgG, 1.5 % IgM) and with 15 % the second most in serum (normal range 0.88-4.1 g/L) [8,9,19,20]. IgA exists in two subclasses IgA1 and IgA2; structurally both differ mainly in the hinge region, where IgA1 has an elongated hinge region. The elongated hinge enhances the potency of IgA1 to induce effector functions but makes it more prone for proteolytic degradation [9,21,22]. This is likely a reason for the distribution of IgA subclasses in plasma and secretions: in plasma, IgA1 is dominant (90 % IgA1; 10 % IgA2), whereas in secretions the IgA2 portion is, depending on the specific location, higher (20-60 % IgA2). IgA is the most heterogenic isotype which is found in two subclasses, as a monomer (~150 kDa), dimer (~ 385 kDa), higher-order multimers (mainly tetramers), secretory forms and further different glycoforms [19–21,23].

Multimeric forms of IgA (mainly dimers) are covalently linked by the J-chain. Although multimerization does not require J-chain, it facilitates multimerization and transport into mucosa by polymeric immunoglobulin receptor (pIgR) [10,20,24]. Multimeric IgA has, similar to IgM, an enhanced avidity and, therefore, increased antigen binding and effector functions [24,25], e.g. *in vitro* data reveal that IgA dimers have a 15-fold stronger neutralizing capacity than monomeric IgA [26]. **Secretory IgA (SIgA)** is crucial for the protection of mucosa by three mechanisms: immune exclusion, intracellular neutralization and antigen excretion [24,27]. Therefore, SIgA is discussed to be a central player in pulmonary diseases [23,26,28,29].

In contrast to IgA on the mucosa, the role of **serum IgA** is not well investigated. This depends on discrepancies within IgA receptors of humans and animal models [21]. Despite in mucosa, serum IgA is mainly monomeric, but also dimeric and multimeric IgA were found (~15 % of IgA) [19,21,30]. Serum IgA can mediate multifaceted roles by interacting with its main receptor FcαRI. Dependent on the interaction IgA can mediate potent inflammatory or immunomodulatory functions [21,31–33]. In contrast to IgG and IgM, IgA cannot activate the classical complement pathway, whereas IgA can activate the lectin pathway [34].

1.1.3. Immunoglobulin interaction partners: Fc-receptors

Antibodies bind to different receptors via their Fc-part; those include Fc-receptors (FcR), C-type lectin receptors, TRIM21 or pIgR. Among them, FcR has an outstanding function by connecting the humoral immune response (mediated by antibodies) with the cellular immune response (FcR bearing immune cells) [35,36]. Most cells of the immune system and especially leucocytes, for example, B-cells, NK-cells, macrophages, neutrophils, mast-cells or platelets, express at least one class of FcR [35,37,38].

FcR mediated effector functions depend on the type of receptor and the valency of antibody interaction [39]. To understand antibody-mediated effector functions it is important to know the key receptors for IgG, IgA and IgM on immune cells. Figure 1-2 gives an overview of relevant leucocyte FcRs. Because of the major role of neutrophils in immune response, the following detailed description of FcR is focused on this cell type.

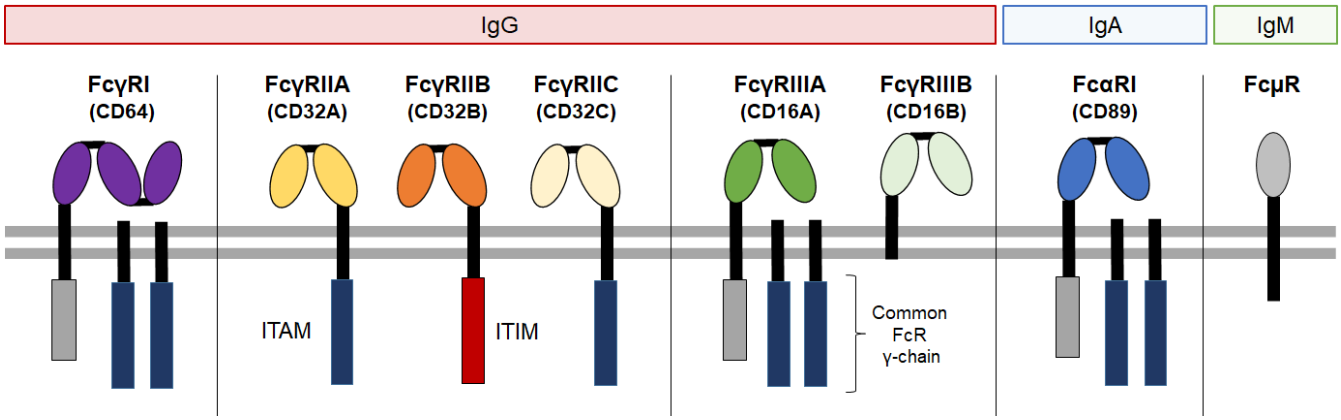

Figure 1-2: Overview of leucocytes Fc receptors (FcR). FcR consist of two extracellular immunoglobulin-binding domains, with exception, FcγRI consists of three binding domains. Signal transduction of the activating FcR is mediated via immunoreceptor tyrosine-based activation motif (ITAM); transduction for inhibitory FcγRIIB is mediated by immunoreceptor tyrosine-based inhibition motif (ITIM). FcγRIIA/B/C have no additional FcR-γ-chain; the signaling motif is contained in the ligand-binding chain. Figure based on [35,40].

IgG-FcγR are divided into three classes, FcγRI (CD64), FcγRII (CD32) and FcγRIII (CD16) with six subtypes (FcγRI, FcγRIIA, B, C and FcγRIIIA, B). The number of FcγR on the cellular surface is varying between different immune cells. Neutrophils express most abundant FcγRIIIB, followed by FcγRIIA, FcγRI and FcγRIIB [41]. With exception of FcγRIIB, all IgG-FcγR are activating receptors, signaling via immunoreceptor tyrosine-based activation motif (ITAM) that in turn activates inflammatory effector outcomes. In contrast, FcγRIIB signals via inhibitory immunoreceptor tyrosine-based inhibition motif (ITIM) mediating anti-inflammatory effects on immune cells [42].

FcγRI (CD64) is the only high-affinity receptor for IgG, thereby, enabling it to bind monomeric IgG, whereas all other FcRs have to interact with multimeric immune complex for appropriate signaling and activation [42,43]. FcγRI shows an additional immunoglobulin-binding domain, which endows this receptor

a high affinity to IgG in the nanomolar range. Low-affinity FcγR show affinity for IgG in the micromolar range [43]. In comparison to FcγRII, FcγRI has no intracellular ITAM motif but is associated with the ITAM-containing common FcR-γ-chain, like FcγRIIIA and FcαRI (compare Figure 1-2) [35]. FcγRI expression is relatively low on resting neutrophils but is cytokine-inducible [44].

Low-affinity receptors for IgG include **FcγRIIA** (CD32A), **FcγRIIB** (CD32B) and **FcγRIIC** (CD32C). These receptors have a fundamental difference in their intracellular motifs. FcγRIIA is like other FcγRs an activating receptor with intracellular ITAM-motif. FcγRIIA is constitutively expressed and the most important receptor for immune complex binding on neutrophils [44,45]. In comparison, FcγRIIB with inhibitory ITIM-motif is a potent negative regulator of immune cell signaling. The relatively unknown FcγRIIC has similarities to both FcγRIIA and B but is equipped with an activating ITAM motif [35]. Expression of FcγRIIC is restricted to NK-cells and B-cells on 7-15 % of the human population [46].

Another low-affinity FcγR is FcγRIII (CD16) with the subtypes FcγRIIIA/B. **FcγRIIIA** (CD16A) is expressed on natural killer NK-cells and macrophages, but not on neutrophils. The main function of FcγRIIIA is clearance of immune complex via its intracellular ITAM-motif [44]. In comparison, **FcγRIIIB** (CD16B) is strongly expressed on the surface of human neutrophils [44,47]. FcγRIIIB has no intracellular motif and no direct signaling function [43]. FcγRIIIB is shed upon activation from the cell surface by proteolytic cleavage [46,48,49]. The soluble form of FcγRIIIB modulates the immune system by interacting with various cell types causing the release of interleukin (IL)-6 and IL-8 [46].
The affinity of the FcγR to IgG subclasses is different and influences effector outcome [35]. Multiple reviews exists discussing the IgG subclass interaction with FcγR [16,17,35,46,50].

Besides the well-described IgG FcRs and the known functions of IgA in mucosal immunity, the role of IgA-FcαRI and the importance of serum IgA in immunity is underrated [21,51]. The **IgA-FcαRI** (CD89) is the most important receptor for IgA effector functions in serum. FcαRI is constitutively expressed on immune cells including neutrophils and macrophages [52]. However, FcαRI expression can be modulated by various stimuli like cytokines or inflammatory mediators. Further, the interaction capacity between IgA and FcαRI is enhanced on stimulated cells, a process known as inside-out signaling [36,52–54].
Monomeric and dimeric IgA bind FcαRI with moderate affinity, IgA immune complex bind with high avidity. IgA subclasses interact with FcαRI under similar affinity [21,55]. In contrast, secretory IgA with the attached secretory component cannot bind due to sterically hindrance. In line with this, FcαRI is not found on cells in mucosal areas [52].
FcαRI is associated like FcγRI and FcγRIII with the common FcR-γ-chain transducing ITAM signaling [52,56]. FcαRI binds its ligand IgA in a 2:1 stoichiometry (two FcαRI bind one IgA-Fc), whereas the FcγR binds in 1:1 stoichiometry the ligand IgG. In line with this, the IgA binding site differs from binding of IgG to their FcγR. [52,57].

In 2009, an authentic FcR for IgM, called **IgM-FcμR**, was discovered by Kubagawa *et al*. [58]. Expression of FcμR is restricted to B-cells, T-cells, natural killer cells and is not reported for macrophages and neutrophils [40,59,60]. IgM FcμR is distinct from other immunoglobulin FcRs, the restricted expression and absence of ITAM or ITIM motifs seem to be unique features in conjunction with the ligand IgM, which appears only during early immune response [59]. FcμR may induce signaling via its own cytoplasmic tail or a yet unknown adaptor protein. Functionally FcμR seems to be important for B-cell development and control of autoantibodies [59].

1.2. Immunoglobulins as therapeutics

There are different approaches to use immunoglobulins as therapeutics. Besides monoclonal and recombinant produced immunoglobulins (almost completely from IgG isotype), native human immunoglobulins can be used. Native human immunoglobulins were used for convalescent plasma therapy e.g. in coronavirus induced diseases 2019 (COVID-19) [61]. Alternatively, human immunoglobulins can be isolated from pooled plasma donations and purified to immunoglobulin preparations. Immunoglobulin preparations are produced from pooled plasma donations of over 1000 healthy donors [62,63]. This pooling provides a high diversity and expands the immunoglobulin repertoire of a single individual [64].

1.2.1. Intravenous immunoglobulin preparations (IVIg)

The classical IVIg preparations contain >95 % IgG antibodies with a plasma-like subclass distribution, a small percentage of IgG dimers and only traces of IgA and IgM antibodies [65,66]. IVIg are used in low doses as replacement therapy for immunoglobulin deficiency since 1952. Additionally, potent effects of IVIg in *immune thrombocytopenia purpura* (ITP) were shown in 1981. Following this, the therapeutic field of IVIg was continuously expanded to the high-dose treatment of autoimmune and inflammatory diseases [63,64]. IVIg preparations nowadays are used as an immunomodulator for treatment of more than 30 indications approved by the FDA and additional off-label use. Common indications of inflammatory and autoimmune diseases are ITP, RA, *systemic lupus erythematosus* (SLE), *Kawasaki disease*, or *Guillain–Barré syndrome* [63–66]. In addition, IVIg are used as adjunctive therapy in sepsis patients [62,67].

The heterogeneity of diseases treated by IVIg is an indicator for the complexity of IVIg mediated functions. A variety of studies aimed to unravel modes of action behind IVIg-preparations. Several Fab- or Fc-part mediated mechanisms were shown, but no central mode of action is clarified. Instead, the modes of action are multifaceted, like the antibody effector functions *in vivo*, to fulfill their beneficial clinical effects. The modes of action can be classified in anti-pathogenic and immunomodulatory effects, whereby the clinical outcome depends on the dose and individual immune status of the patient. This shows the great variety and heterogeneity of this product class [62–64,66,68,69]. To improve the understanding of how IVIg work, different experimental setups with comparable data are necessary.

Although IVIg therapy is used for decades and is considered safe and effective, some limitations remain. These include the dependency on plasma donations, the high doses for treatment and in consequence high costs of therapy [64,70,71]. To circumvent supply problems, alternative recombinant molecules were developed. Those compromise recombinant Fc-multimers, neonatal FcR- or FcγR-targeting therapeutics [68,71,72]. Another approach is to extend the repertoire of immunoglobulins in IVIg by the addition of IgM- and IgA-components [64,73].

1.2.2. IgM- and IgA-enriched immunoglobulin: trimodulin

Usage of IgM- and IgA-enriched immunoglobulin preparations are promising because of (1) the possibility to treat patients with IgM- or IgA-deficiencies and (2) the usage of beneficial properties of IgM and IgA in comparison to IgG [64,73,74].

The only commercially available IgM- and IgA-enriched preparation is Pentaglobin®, a preparation with 16 % IgA, 12 % IgM and 72 % IgG [74]. With trimodulin another IgM- and IgA-enriched immunoglobulin is in clinical development. Trimodulin is a normal polyvalent antibody preparation derived from plasma for intravenous administration. Trimodulin has a unique composition and contains immunoglobulins IgM (~23 %), IgA (~21 %) and IgG (~56 %), which is nearly the physiological distribution of immunoglobulin isotypes in plasma [74].

As highlighted in many reviews, the addition of IgM and IgA to standard IVIg preparations enhance the therapeutic efficacy for the treatment of inflammatory diseases like sepsis [62,64,67,73–75]. Because trimodulin is currently in development, a lot of knowledge originates from studies using Pentaglobin®. Several *in vitro* and *in vivo* studies showed superior effects of Pentaglobin® in the treatment of inflammatory diseases in comparison to standard IVIg therapy [15,76–80].

The anti-pathogenic effects of trimodulin were shown in a rabbit endotoxemia model [81]. Further, trimodulin was shown to be effective in subgroups of ventilated severe community-acquired pneumonia (sCAP) patients with high inflammation and/or low IgM levels (CIGMA-study) [82]. Trimodulin is therefore in clinical testing for related COVID-19 disease (ESsCOVID-study) [83]. *In vitro,* several studies showed immunomodulatory properties of trimodulin. It was shown that trimodulin can modulate inflammatory cytokine release and cell phenotype of endotoxin challenged lymphocytes [84]. Trimodulin can protect platelets from pneumolysin-induced damage [85] and avoid excessive activation of the complement system (*manuscript submitted*).

Based on the complexity of this product additional *in vitro* studies are required for a better understanding of the differences concerning the modes of action between trimodulin and standard IVIg.

IgA: the underrated component?

The importance of each immunoglobulin component in IgM- and IgA-enriched immunoglobulins is still under investigation. The great diversity and heterogeneity of immunoglobulin species make a separation of the IgM, IgA and IgG components challenging, impeding research.

The previous investigations address beneficial effects to the known effector functions of IgG and IgM [15,76,78–80,84]. The underrated role of IgA in these studies is reasoned in the limited knowledge and the general issues of IgA in research: (1) Differences between animal models and humans (FcαRI is missing in most rodents, IgA is a polymeric molecule in serum of animals, whereas IgA is monomeric in human serum). (2) Difficulties in the recombinant production of IgA, due to high and heterogeneous

glycosylation. (3) IgA has a low stability and short serum half-life [21,52,86–88]. Furthermore, IgA has a difficult stand in immunoglobulin therapy, as IgA was related as a potential risk factor in individuals with IgA nephropathy based on anti-IgA antibodies [64,74].
Despite these challenges, some work focuses on plasma-derived IgA preparations and demonstrates promising anti-pathogenic and anti-inflammatory effects [89–94]. Therefore, further studies regarding IgA function in immunoglobulin preparations are urgently needed.

The following important modes of action are identified for immunoglobulin preparations and will be discussed more in detail: Anti-pathogenic activities, which promote the clearance of pathogens (chapter 1.2.3) and immunomodulatory activities counteracting inflammatory processes (chapter 1.4.3).

1.2.3. The anti-pathogenic activity of immunoglobulin preparations

Generally, immunoglobulin preparations act via antibody-mediated effector functions. These can be structured into [95]: Direct neutralization of toxins and agglutination of pathogens (Figure 1-3A/B), complement-dependent cytotoxicity (CDC) (Figure 1-3C) and FcR mediated cytotoxicity (Figure 1-3D).

This work focuses on FcR mediated effector functions because of the great importance of immunoglobulin-FcR interaction and the resulting effector functions as a link between innate and adaptive immunity. Immunoglobulin preparations have various antimicrobial activities, based on the broad spectrum of antibody specificities in the donor plasma. Antimicrobial effects are generally observed at low doses of IVIg treatment [63,69].
Figure 1-3 gives an overview of the most important anti-pathogenic properties of antibodies, as well as immunoglobulin preparations:

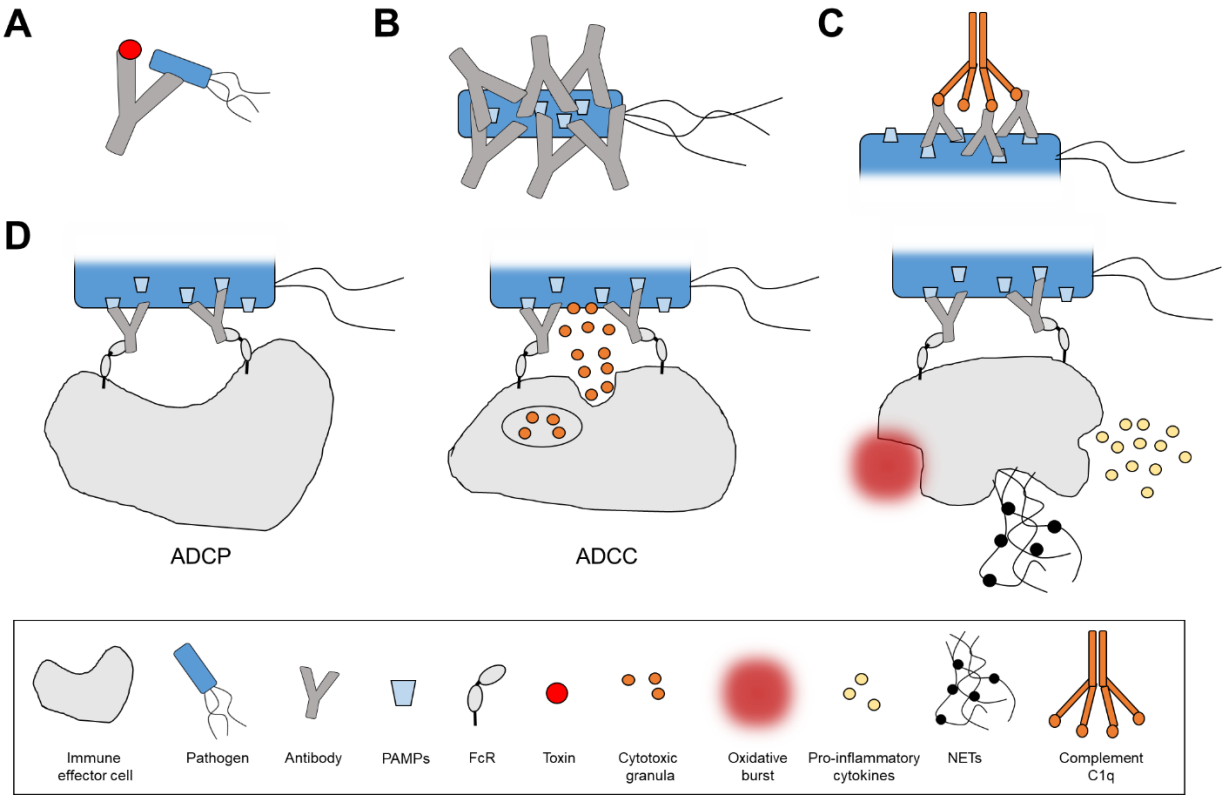

Figure 1-3: Anti-pathogenic effector functions of antibodies. **(A)** Antibodies can directly neutralize toxins or pathogens. **(B)** Direct binding of antibodies to pathogen-associated molecular patterns (PAMPs) induces agglutination of bacteria. **(C)** Opsonization of pathogens can activate the complement system by antibody binding to C1q. **(D)** Fc-receptor (FcR) mediated effects induce anti-pathogenic effects. Antibody-dependent phagocytosis (ADCP), cytotoxicity (ADCC), oxidative burst or release of neutrophil extracellular traps (NETs) and pro-inflammatory cytokines lead to clearance of pathogens. Figure based on [39,54,95].

(A) Neutralization of toxins and pathogens: Immunoglobulin preparations can neutralize bacterial endo- and exotoxins or pathogens by direct binding of natural antibodies [96,97] or specific antibodies [39]. Multimeric IgM and IgA species in IgM- and IgA-enriched immunoglobulins seem to have a better neutralization capacity than standard IVIg [78,80].

(B) Agglutination of bacteria: Direct binding of native IgG, IgA or IgM or specific antibodies to pathogen-associated molecular patterns (PAMPs) delivered by immunoglobulin preparations led to agglutination of bacteria, resulting in increased clearance by immune cells or the respiratory tract [62]. Here, multimeric IgA and IgM species were shown to be more efficient than monomeric IgG [15,73,76].

(C) Activation of the complement system: IgG and IgM antibodies can opsonize pathogenic particles for complement component C1q, thereby promoting CDC [95]. Studies comparing standard IVIg with IgM- and IgA-enriched immunoglobulin preparations showed that the complement opsonic capacity is significantly higher than standard IVIg. Reason is the 400-times stronger activation of C1q by IgM compared to IgG [15,76].

(D) Enhancement of FcR mediated cytotoxicity: Antibodies administered in immunoglobulin preparations can opsonize various bacterial-, fungal- or viral pathogens, thereby marking the pathogens for phagocytosis or neutralization by immune effector cells [62]. FcR mediated effector functions include a broad field of inflammatory cellular outcomes, such as antibody-dependent cellular phagocytosis (ADCP), antibody-dependent cellular cytotoxicity (ADCC), pro-inflammatory cytokine release, oxidative burst (release of reactive oxygen species (ROS)), degranulation or neutrophil extracellular traps (NETs) [39,54,95]. Recently, it was shown that IgA enhances ADCP and ADCC more efficiently than IgG [86,98,99].

1.3. Immunoglobulins and neutrophils in severe infection diseases

An often-used therapeutic field for immunoglobulin preparations are severe infection diseases. In such diseases, patients require intensive care and mechanical ventilation. Although the number of patients and mortality is high, there is a limited clinical success, regarding adjunctive therapies. Considering the major healthcare problem arising with these diseases, new therapeutic options are urgently needed. In the following section immunological features, the role of immunoglobulins, neutrophils and the opportunities for immunoglobulin therapy are discussed for sepsis, sCAP and COVID-19.

1.3.1. The role of neutrophils

While neutrophils are central players of innate and adaptive immunity, as well as inflammation, they can also mediate crucial tissue damage when the immune system is exhausted [6,100,101]. Neutrophils mediate central antibody-mediated effector functions like ADCP, ADCC or release of anti-pathogenic granulas or NETs [5].

Neutrophils bear a plethora of receptors involved in anti-pathogenic immune response; those include receptors for primary recognition of pathogen structures, like toll-like-receptors (TLR) or C-type lectins; receptors for interaction with the inflammatory environment, like cytokine receptors and receptors for the interaction with the adaptive immune system, like FcR [101]. Latter are crucial for the interaction with immunoglobulins, elimination of immune complex and modulation of the immune response.

Based on their fundamental role, neutrophils are involved in several autoimmune and inflammatory disorders, like RA, SLE or acute respiratory distress syndrome (ARDS) [6,101]. Understanding the mechanism responsible for neutrophil activation (in the case of pathogen elimination) and over-activation (in the case of disorders) is crucial for successful immunotherapy. Basis for these mechanisms are receptors and signaling pathways on neutrophil cells.

1.3.2. Sepsis

Sepsis is defined as a life-threatening organ dysfunction caused by a dysregulated immune response to infection [102]. Dysregulation of immune response differs sepsis from normal infections. Sepsis is one of the most common diseases worldwide, affecting ~49 million people and causing ~11 million deaths per year. Sepsis is a main cause of deaths in intensive care units (ICU) mortality rates ranging between ~20 % for sepsis, ~40 % for severe sepsis and >60 % for septic shock patients. In contrast to sepsis, severe sepsis is associated with organ dysfunction and hypoxemia. Ongoing diseases can lead to septic shock, a multiple organ dysfunction frequently associated with worse clinical outcomes. Despite advances in ICU treatment, there is limited progress in adjunctive therapies and mortality rates remain high [67,74,103–105].

Sepsis is induced by an invading pathogen (e.g. bacteria, fungi or virus); typical molecular patterns activate the innate immune response (via pattern recognition receptors (PRR)) and induce inflammatory cytokine release. When the initial host response to an infection is being amplified and dysregulated, often due to a combination of a compromised immune system with persistent and multiresistant pathogens, sepsis develops [103–105]. The imbalanced immune system typically generates a biphasic immune response during sepsis (Figure 1-4):

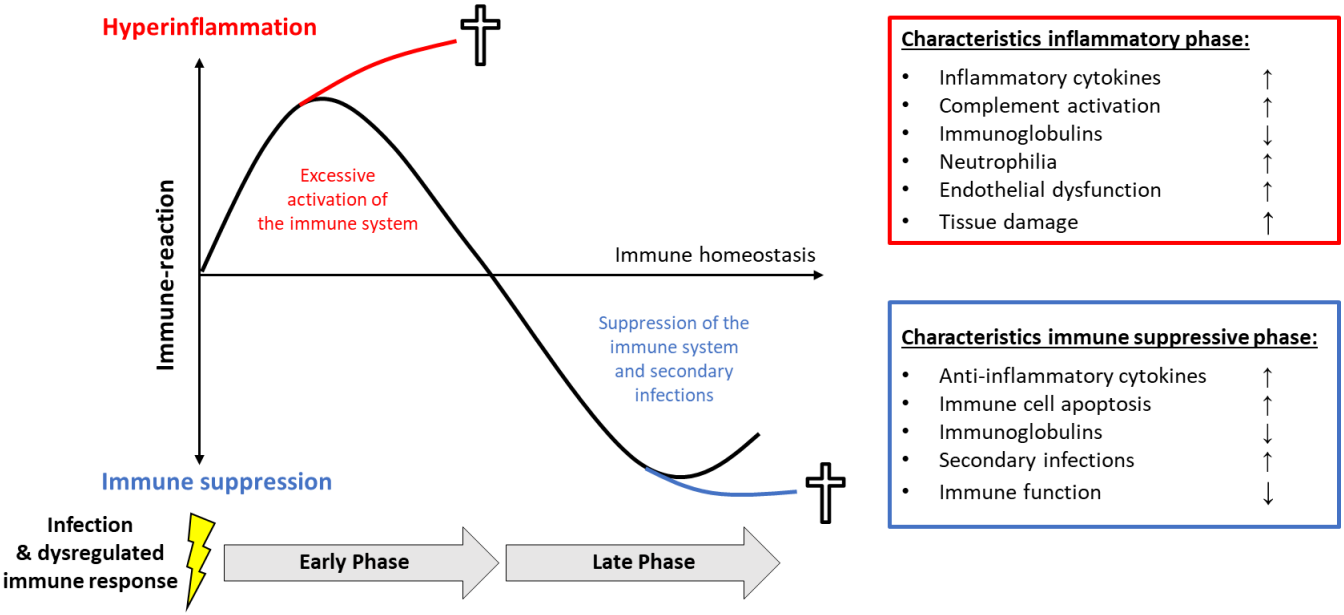

Figure 1-4: Biphasic immune response during sepsis. Sepsis is induced by persistent infection in combination with a dysregulated immune system. Due to infection, an overwhelming inflammatory phase develops, leading to hyperinflammation and tissue damage. Counteraction of the immune system can lead to contrary effects resulting in immune suppression and facilitating secondary infections. Figure based on [106,107].

As shown in Figure 1-4 the typical immune response during sepsis begins with an infection followed by (1) the inflammatory phase. In this early phase, elevated levels of inflammatory cytokines (so-called cytokine storm) induce overwhelming systemic immune response including complement activation, decreased immunoglobulin levels and neutrophilia. This cytokine-induced over-activation can cause coagulation problems, endothelial dysfunction, which promotes pathogen invasion and tissue damage [103–105]. In response to the exhausted inflammation the immune system, begins to counteract with immunosuppression [106,108].

Like in the uncontrolled inflammatory phase, the dysregulated immune response can overshoot this counteraction resulting in a (2) anti-inflammatory, immune-suppressive phase (known as immune paralytic phase). In this phase anti-inflammatory cytokines increase, activating cell surface markers decrease and apoptosis leads to an extensive loss of immune cells. This immunosuppressive phase leads to a dysfunction of the immune response which strongly reduces the ability to eliminate further invading pathogens [67,103–105,109]. The pro- and anti-inflammatory mechanisms in each phase of sepsis occur in

variable courses during disease progression, therefore patients can run through each phase multiple times [106,108].

Low plasma levels of IgG, IgA, IgM are associated with reduced survival of severe sepsis patients. Immunoglobulin levels decrease due to reduced production (by immunosuppression), vascular leakage (by endothelial dysfunction), or increased consumption [67].

Immunoglobulin preparations have therefore been used as adjunctive treatment of sepsis patients for decades [67,74]. Their multiple pro- and anti-inflammatory effector functions (compare chapter 1.2.3 and 1.4.3) can weaken both, inflammatory- and immunosuppressive-phases during sepsis [67,109]. Reduced mortality was shown in systematic meta-analysis by treating patients with IgM- and IgA-enriched immunoglobulins, whereas classical IVIg preparations showed no effects [74,110,111]. The superiority of IgM- and IgA-enriched immunoglobulins in the treatment of sepsis could derive from better neutralization of bacterial toxins like lipopolysaccharides (LPS) or streptococcal superantigen and better opsonization of pathogens [76,78,80].

1.3.3. sCAP

Community-acquired pneumonia (CAP) is defined as an acute infection of the pulmonary parenchyma, whereby symptoms occur in community [112]. CAP is the most common infectious disease and a leading cause of mortality worldwide. CAP can induce severe forms (called severe CAP, sCAP) with systemic inflammation leading to reduced alveolar gas exchange, sepsis and end in organ dysfunction and high mortality (~58 % of ICU patients) [112–114].

The main pathogens associated with sCAP are gram$^+$ *Streptococcus pneumoniae* and *Staphylococcus aureus*. Important pathogens are also gram$^-$ pathogens like *Haemophilus influenza*, *Klebsiella pneumoniae or Pseudomonas aeruginosa* and also viral infections (up to 30 % of infections) like influenza A virus and Middle East respiratory syndrome coronavirus. Furthermore, in ~20 % of patients, bacterial and viral co-infections were observed [112,115–117].

Similar to sepsis a combination of persistent infection and dysregulated immune response causes sCAP. Local infection in the lung causes excessive inflammation with cytokine storm leading to disruption of the alveolar-endothelial barrier and lung injury. This induces systemic inflammation as described in sepsis patients [117].

Crucial for sCAP therapy is the early treatment with appropriate antibiotics, however, problems arise by infections with antibiotic-resistant pathogens like *Haemophilus influenza, Pseudomonas aeruginosa* and methicillin-resistant *Staphylococcus aureus* [115,118]. Due to the high mortality, more common antibiotic resistance, and no progress in CAP therapy, there is a high demand for adjunctive treatments. Previous studies reveal that a combination of antibiotic therapy with adjunctive therapy directed against the host immune response is most promising for the management of sCAP [118]. As adjunctive therapy for sCAP

several anti-inflammatory treatments, like corticosteroids, statins, activated protein C, macrolides and immunoglobulin preparations were tested [115,117].

Intact mucosal immunity is the basis for prevention of pneumonia and sCAP. A crucial player is SIgA that elicits anti-pathogenic defense as well as immunomodulation. As described above, exhausted neutrophils can mediate a detrimental role in sepsis and sCAP by inducing tissue damage. Modulation of exhausted neutrophil inflammation on mucosa can be mediated by SIgA, which was shown *in vitro* [28,29]. In line with this, a recent study showed lower levels of serum IgG, IgA and IgM in ICU compared to non-ICU patients. Lower levels of IgG and IgA were related to disease severity [119]. Therefore, treatment with immunoglobulin preparations is a promising adjunctive therapy, based on the multiple anti-bacterial and immunomodulatory activities of these preparations [115,117,119].

The efficacy of IgM- and IgA-enriched immunoglobulin Pentaglobin® in the treatment of severe acute respiratory syndrome coronavirus (SARS-CoV) induced pneumonia was shown in 2005 [120]. Trimodulin was shown to be effective in ventilated patients with sCAP, high inflammation markers (C-reactive protein (CRP)) and low IgM levels (CIGMA-Study) [82]. Overall, the previous data using immunoglobulin preparations as adjunctive therapy in sCAP reveal that promising results were mainly achieved in subgroups with high inflammation and low immunoglobulin levels. For beneficial effects, the identification of these subgroups has to be further investigated [115,117,119,121].

1.3.4. COVID-19

COVID-19 is a global threat induced by the rapid spread of the newly emerged severe acute respiratory syndrome coronavirus 2 (SARS-CoV-2). From the beginning in December 2019 until June 2021 >179 million confirmed cases and >3.8 million deaths were registered (WHO Coronavirus, https://covid19.who.int/). SARS-CoV-2 is classified into the family of *Coronaviridae*, lineage beta-coronavirus. The virus is an enveloped, single-stranded RNA virus with a genome of ~29,891 bases. Genome sequencing reveals 79.5 % sequence homology with next related SARS-CoV virus and 96 % identity with bat coronavirus strain, therefore SARS-CoV-2 was designated as a new beta-coronavirus [122,123].

Structurally SARS-CoV-2 is similar to other coronaviruses: the virus particles are relatively large with a diameter of 60-140 nm and the typical spike protein occupied surface. Besides spike protein, the nucleocapsid-, membrane-, and envelope-protein define the structure of SARS-CoV-2 [123,124]. The spike protein on the surface of SARS-CoV-2 is critical for virus binding to angiotensin-converting enzyme II (ACE-II) receptor and the fusion of virus and host membrane [123]. Further the spike protein has a central role in mediating the inflammatory immune response against the virus [125].

In comparison to other coronaviruses, the infectivity and virulence of SARS-CoV-2 is higher. Reasons are likely differences in spike protein structure, which lead to higher binding affinity to ACE-II, and enhanced

cell membrane fusion by additional cleavage sites in the spike protein [123,126]. Due to enhanced virulence and easy transmission between humans via droplets or aerosols, SARS-CoV-2 and COVID-19 spread fast across the world [122].

Based on distinct clinical findings COVID-19 can be divided into three major stages with increasing severity [127] (Figure 1-5):

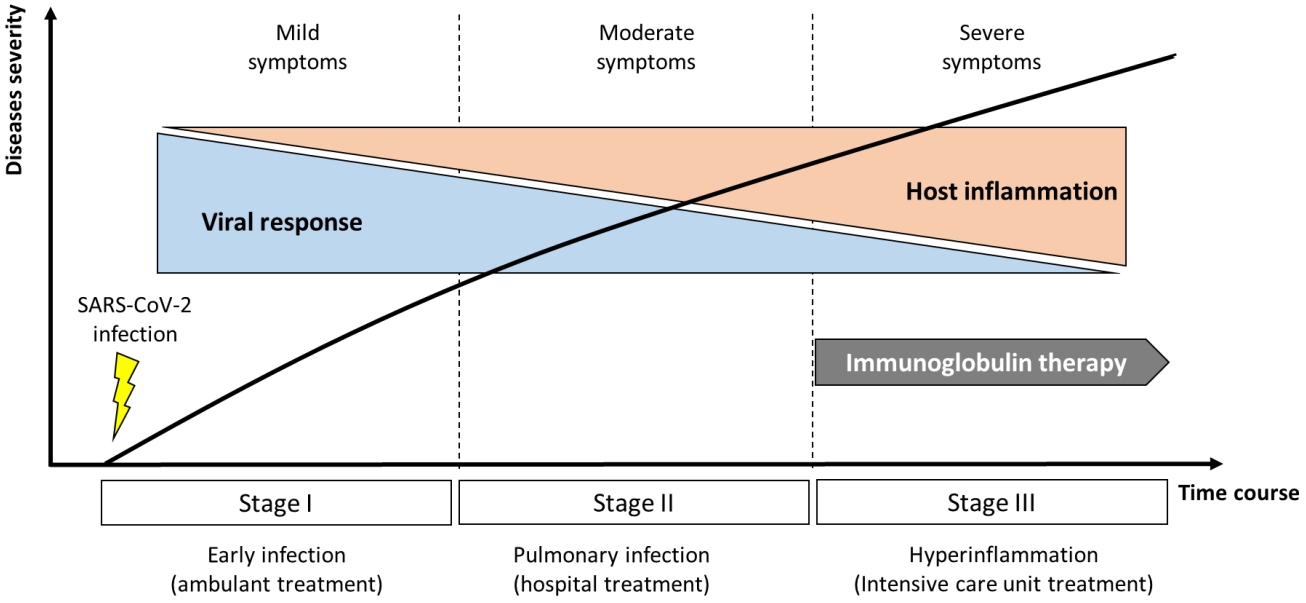

Figure 1-5: Stages of coronavirus-induced diseases 2019 (COVID-19) diseases. Upon infection with severe acute respiratory syndrome coronavirus 2 (SARS-CoV-2) COVID-19 is induced and patients went into stage I with mild symptoms. With the virus, progression patients develop viral pneumonia (stage II), which requires hospitalization. When patients transit into stage III a systemic hyperinflammation develops. Patients require intensive care unit treatment with mechanical ventilation. In the early stages of COVID-19 host response against the virus is dominant, whereas in later stages the exhausted inflammation is of greater importance. In hyperinflammatory stage III, immunoglobulin therapy is promising. Figure based on [127].

The initial stage I of COVID-19 diseases starts with virus infection and replication in the respiratory tract. Most patients (>80%) [128–130] remain in this phase being asymptomatic or developing mild symptoms (like fever and cough). Although most people are asymptomatic, they can transmit the virus, a key point for virus spreading. In stage I the disease severity is dependent on the immune response against the virus [122,127]. When patients cannot defeat the virus, pulmonary disease can develop (stage II). Virus progression leads to local infection of lung tissue. Patients show moderate symptoms (cough, fever, hypoxia) which require hospitalization. Anti-viral therapy can be successful to defeat the diseases in this stage [122,127]. In the most severe stage of COVID-19 (stage III) patients develop a systemic inflammation. These patients are characterized by an exhausted immune system with hyperinflammation related severe ARDS and so-called “cytokine storm” [122,127,131,132].

COVID-19 relevant inflammatory cytokines like IL-6, IL-8, tumor necrosis factor (TNF)-α, monocyte chemoattractant protein (MCP)-1 or IL-1β and anti-inflammatory cytokines like IL-10 or IL-1 receptor

antagonist (IL-1ra) were shown to correlate with disease severity [133–136]. Previous data indicate that excessive immune response (in stage III) by the host is of greater importance for COVID-19 progression than virus-induced damage alone [66]. A key player in this damage seems to be neutrophil infiltration (neutrophilia) which was shown to be associated with poor clinical outcomes of severe cases [137–139]. Therefore, down-modulation of hyperinflammation in severe COVID-19 patients is of major importance [127,132,140–142].

In addition, in COVID-19, antibody-mediated effector functions are crucial for disease outcome and severity. It was shown, that in response to SARS-CoV-2 infection, specific antibodies of IgG, IgA and IgM class were produced. These antibody titers were correlated with disease severity, clearance of virus and for induction of inflammation; highlighting the importance of antibodies for adaptive immunity [136,143, 146]. Despite the urgent need for appropriate therapeutics and the multitude of ongoing studies only Remdesivir (a nucleoside analog inhibiting viral replication) is approved for COVID-19 therapy (https://www.nytimes.com/interactive/2020/science/coronavirus-drugs-treatments.html) [147]. As an alternative, immunoglobulin preparations are fast available immunomodulatory drugs [61,66,70,127,148]. Immunoglobulin preparations have been used for the treatment of inflammatory diseases for decades and the first clinical studies have shown promising results in treatment of COVID-19 patients [149–153]. Because currently available batches of immunoglobulin preparations lack neutralizing antibodies against SARS-CoV-2 ([154] and *in house data*) immunomodulatory activities to fight against dysregulated inflammatory responses are important for severe COVID-19 patients (see chapter 1.4).

In comparison to other available broad immune modulators, immunoglobulin preparations can mediate multiple modes of action [66,125,127]. Besides immunomodulation also anti-pathogenic effects of immunoglobulins against bacterial- and viral co-infections could be beneficial [155–157]. Further, modulation of the complement system and protection of the lung tissue by preventing ARDS could be beneficial effects mediated by immunoglobulin preparations [79,158–160].

In summary, the described diseases show some similarities: A combination of compromised immune system with strong and persistent infection is leading to a dysregulated and exhausted immune system. Characteristics are high levels of pro-and anti-inflammatory cytokines (cytokine storm) leading to over-activated neutrophils and tissue damage. Sepsis, sCAP and COVID-19 are common diseases with high mortality rates and limited treatment opportunities. In these diseases, a multifaceted modulation of the immune response seems to be more beneficial than broad suppression. Polyclonal IgM- and IgA- enriched immunoglobulin preparations are, therefore, a promising therapeutic approach.

1.4. Immunomodulation as a therapeutic approach

As described in the previous chapter, patients with severe infection diseases suffer from an overwhelming immune response, which is associated with cytokine storm and tissue damage. To prevent this, the major goal of therapy is suppression and/or modulation of the exhausted immune response. Generally, there are several therapeutic approaches to achieve this:

(1) Broad immune suppressors, like corticosteroids or janus kinase inhibitors, are widely used in the therapy of inflammatory conditions. Those suppressors target multiple pathways, thereby broadly dampening the immune system. The immune suppression on the other hand has the side effect that anti-pathogenic activities of the immune response are limited [103,130,140,156,161].

(2) The increase of inflammatory cytokines is a major driver for inflammation and is often associated with disease severity [105,141]. Therefore, antagonists of inflammatory cytokines, such as IL-6 receptor inhibitor (tocilizumab), anti-IL-8 antibody (HuMax-IL-8) or IL-1 receptor antagonist (anakinra), are often used in the treatment of inflammatory diseases. Similar to corticosteroids, cytokine antagonists have the disadvantage to dampen the whole immune response [130,140,161,162].

(3) Another approach rather modeling the immune response instead of broad suppression are immunoglobulin preparations. Based on their anti-pathogenic as well as anti-inflammatory and immunomodulatory properties, immunoglobulins do not dampen the whole immune system, resulting in fewer adverse effects [66,70,163]. The complex nature and mechanism behind these beneficial properties will be discussed in the following chapter.

1.4.1. Immunoglobulin-FcR interaction regulates immunity

As a basis for immunoglobulin-mediated immunomodulation, it is important to understand the crucial mechanism of immunoglobulin-FcR regulation. There are several opportunities how the immune response can be modulated in association with FcRs, these ways act in a complex network and, thereby, fine-tune the immune system [44,46]. In the following section, central mechanisms are classified:

(1) FcR expression: Balance between expression of activating and inhibitory FcRs regulates the immune system, by setting a threshold for cell activation [39,42,43,46]. The variation of FcR expression between different cell types depends on different gene copy numbers [46]. However, FcR expression can be modulated by more dynamic parameters like the activation status of the cell. In case of infection, pro-inflammatory cytokines increase expression of activating FcγRI and FcγRIIA, whereas anti-inflammatory cytokines reduce expression. Contrary, inhibitory FcγRIIB expression is increased by anti-inflammatory cytokines [42,164]. Similarly, the exposure to monomeric IgG reduces the expression of FcγRIIA and upregulates the expression of FcγRIIB [42]. Besides cytokines, also like LPS or the anaphylatoxin C5a increase the expression of activating FcRs [43].

(2) Clustering of FcRs: But not the expression of FcRs alone is sufficient for modulating effector function, also the correct arrangement is important [46,165]. Spatial organization of activating FcRs is necessary to activate sufficient intracellular signaling kinases via ITAM or ITIM. Processes like actin-polymerization lead to modification of cellular cytoskeleton, finally promoting the uptake of immune complex [46,165].

(3) Posttranslational modifications: As in many cellular processes, posttranslational modifications of antibodies or FcRs influence immune response. Antibodies are highly glycosylated molecules [39], therefore, it is obvious that such complex structures play a major role in antibody-FcR interaction strength and FcR function [44,46,166].

(4) Multivalent binding on FcRs: Besides the differences in monovalent binding of immunoglobulins on FcRs, the multivalent binding is more important for the immunological response *in vivo* [46]. The high level of IgG molecules in human serum leads to saturation of FcRs on circulating immune cells. Therefore, multivalent binding of immune complex and receptor clustering is essential for an appropriate binding on activating FcR and immune cell activation [39,46]. Therefore, the size and concentration of the immune complex is a critical parameter for the immune response [167].

(5) Antibody-antigen interaction: Basis for immune response is the availability of antibodies with specificity for an antigen. The ratio of antibody to antigen is changing during infection. When the antibody-antigen ratio exceeds a threshold, the immune response increases [39,46]. Modulation of immune response by immune complex is an FcR dependent mechanism influenced by parameters regulating the interaction between antibody and antigen. These parameters are affinity and concentration of antibodies and size of the resulting immune complex [46].

(6) IgG-subclasses: Different affinities of IgG-subclasses to FcγR can modulate the immune response. For example, IgG4 has a relatively high affinity for inhibitory FcγRIIB [168]. The ratio of IgG-subclasses interacting with an antigen on a multivalent immune complex is critical for the resulting immune response [46,50].

(7) Interaction with other proteins: The interaction between FcRs and other proteins on the cell surface was also shown to influence the immune response. For example, CD11b (Mac-1) interacts with FcγRIIA on resting neutrophils lowering the affinity for IgG, whereby in activated neutrophils the interaction between IgG and FcγRIIA is promoted [44]. Acute-phase proteins, like CRP, were shown to bind to FcRs and promote immune complex uptake. IgG immune complex were able to reduce CRP binding on FcγRIIA [169].

(8) FcR-TLR cross-talk: TLR are a class of PRR that recognize microbial membrane components like LPS. It was shown that FcRs and TLRs act together to defeat pathogenic infections [36,37]. Targeting FcγR or FcαRI by immune complex together with TLR strongly enhanced inflammatory responses of immune cells [42,89,170–172].

(9) Inside-out signaling: The concept of inside-out control describes an increase of receptor affinity, valency or function that is induced by an endogenous stimulus [36]. Enhanced binding capacity is known for FcαRI and FcγRII after priming of cells with inflammatory mediators like cytokines or endotoxins [36,52–54].

1.4.2. FcR signaling defines effector outcome

Several extracellular parameters modulate the immune response FcR dependently (chapter 1.4.1). As indicated above, also downstream intracellular signaling is of major importance for effector outcome. Low-affinity FcR like FcαRI, FcγRIIA or FcγRIIIA can act as bi-functional receptors transducing either activating or inhibitory signals based on their interaction partner [56]. The binding of a multimeric immune complex on cell surface activates several FcR leading to activating ITAM signaling. In contrast, binding of monomeric IgG or IgA to these receptors results in inhibitory ITAM-mediated signaling (ITAMi) [173]. As a third way, binding of IGG to FcγRIIB induces inhibitory ITIM signaling [164]. In the following section, the molecular basis of these pathways is described more in detail with an overview in Figure 1-6.

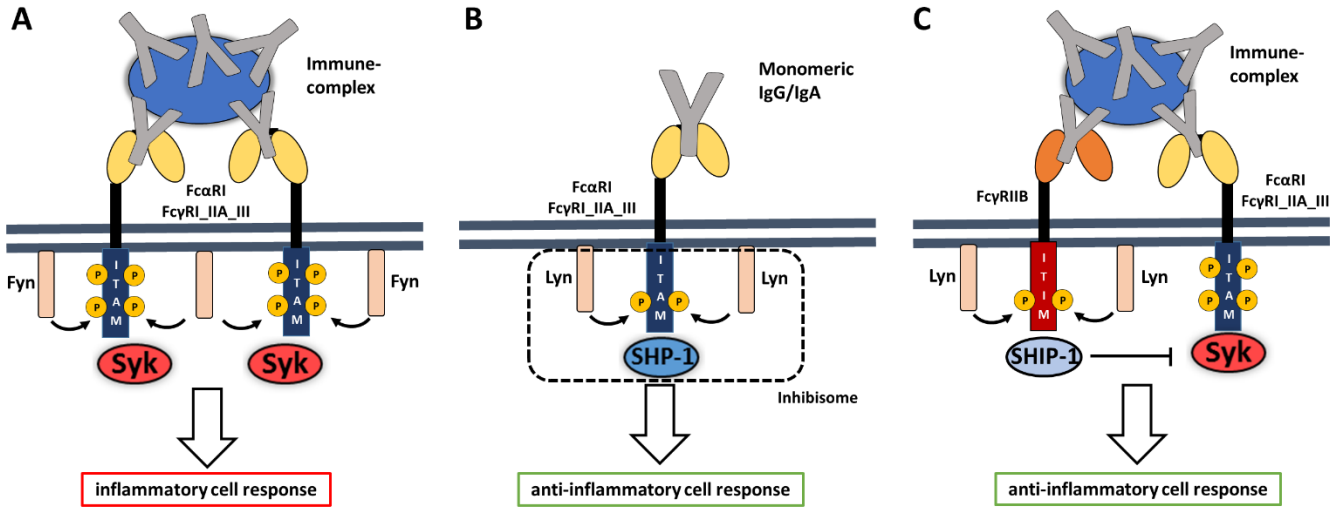

Figure 1-6: Overview of FcR signaling **(A)** Immunoreceptor tyrosine-based activation motif (ITAM) signaling: Binding of immune complex to activating FcαRI or FcγR recruits Fyn kinase. Fyn kinase fully phosphorylates the ITAM motif, resulting in SYK recruitment. SYK activates downstream signaling ending in inflammatory cell response. **(B)** Inhibitory ITAM (ITAMi) signaling: Interaction of monomeric IgA or IgG activates Lyn kinase, Lyn partially phosphorylates ITAM motif resulting in inhibitory ITAMi signaling. SHP-1 is recruited and inhibits activated proteins by inhibisome formation. **(C)** Immunoreceptor tyrosine-based inhibition motif (ITIM) signaling: Co-ligation of the immune complex to inhibitory FcγRIIB and another activating receptor (e.g. FcαRI or FcγRIIA) activates Lyn kinase that phosphorylates ITIM motif. ITIM phosphorylation recruits SHIP-1 phosphatase, SHIP-1 inhibits SYK signaling. Figure based on [56,174,175].

A. ITAM signaling via immune complex binding: Binding of a multimeric immune complex on several FcRs leads to receptor clustering and intracellular cross-linking, thereby, activating Src family kinase Fyn [56,174]. Full phosphorylation of specific tyrosines in the ITAM-motif by Fyn results in the recruitment of tyrosine kinase SYK [175]. Recruitment of SYK activates multiple proteins and kinases, ultimately resulting in activation of pro-inflammatory gene expression and associated effector functions [56,174].

B. ITAMi signaling via monomeric immunoglobulin binding: When low-affinity FcR are targeted by low avidity ligands like monomeric IgA or IgG, Src family kinase Lyn is recruited. Lyn phosphorylates a single tyrosine motif on ITAM, which results in stable recruitment of SHP-1 [175]. The recruitment of SHP-1 initiates the formation of so-called inhibisomes. These clusters inhibit activating receptors like FcRs or TLRs and trap the targeted proteins via actin polymerization [94,176,177]. This process downregulates multiple activating signals resulting in immunomodulation [37].

C. ITIM signaling after binding to FcγRIIB: Inhibition of cell activation is possible by co-ligation of inhibitory FcγRIIB and another activating receptor with IgG immune complex (e.g. B-cell-receptor or FcR) [173]. Binding induces phosphorylation within the ITIM motif by Lyn kinase, resulting in the recruitment of phosphatase SHIP-1 [56]. SHIP-1 phosphatase can efficiently hamper the ITAM mediated effector functions by interacting with the signal cascade proteins [35,42,174].

The modulation of immune response by this fine-tuned network is critical for enabling adequate immune function. Activating and inhibitory pathways are often triggered simultaneously; therefore, the cellular response is a result of both pathways [178]. ITAM dependent activation of immune cells is crucial for clearance of immune complex, but the return to homeostatic conditions is a major concern. Thus, counteracting by ITIM and ITAMi is important. Inhibition of immune response by ITIM is an instant step, whereas ITAMi is a continuous process adapting to the immunoglobulin levels in circulation. ITAMi is, therefore, a critical checkpoint to maintain immune homeostasis, without changing FcR expression [42,174]. In several inflammatory diseases, this balance is disturbed, therefore, modulation of FcR signaling via immunoglobulin preparations is a therapeutic opportunity [42,56,174].

1.4.3. Immunomodulatory activity of immunoglobulin preparations

The immunomodulatory activities of immunoglobulin preparations are beneficial especially in patients with a hyperinflammatory immune system, induced by autoimmune- or inflammatory diseases. Generally, anti-inflammatory effects of IVIg are seen at high dose treatment when the supplemented immunoglobulins compete with present immunoglobulins [63,68,69]. Based on the broad spectrum of functions mediated by immunoglobulin preparations, which are also anti-pathogenic (see chapter 1.2.3), the beneficial effects in inflammatory diseases were attributed as immunomodulatory rather than immunosuppressive [72].

For more clarity, an overview of the multiple immunomodulatory effects is shown in Figure 1-7. The effects are structured into (1) modulation via FcR (Figure 1-7A-C), (2) effects that defeat problems arising in autoimmune disorders (Figure 1-7D-E), and (3) the interaction with soluble mediators of inflammation like complement or cytokines (Figure 1-7F-G).

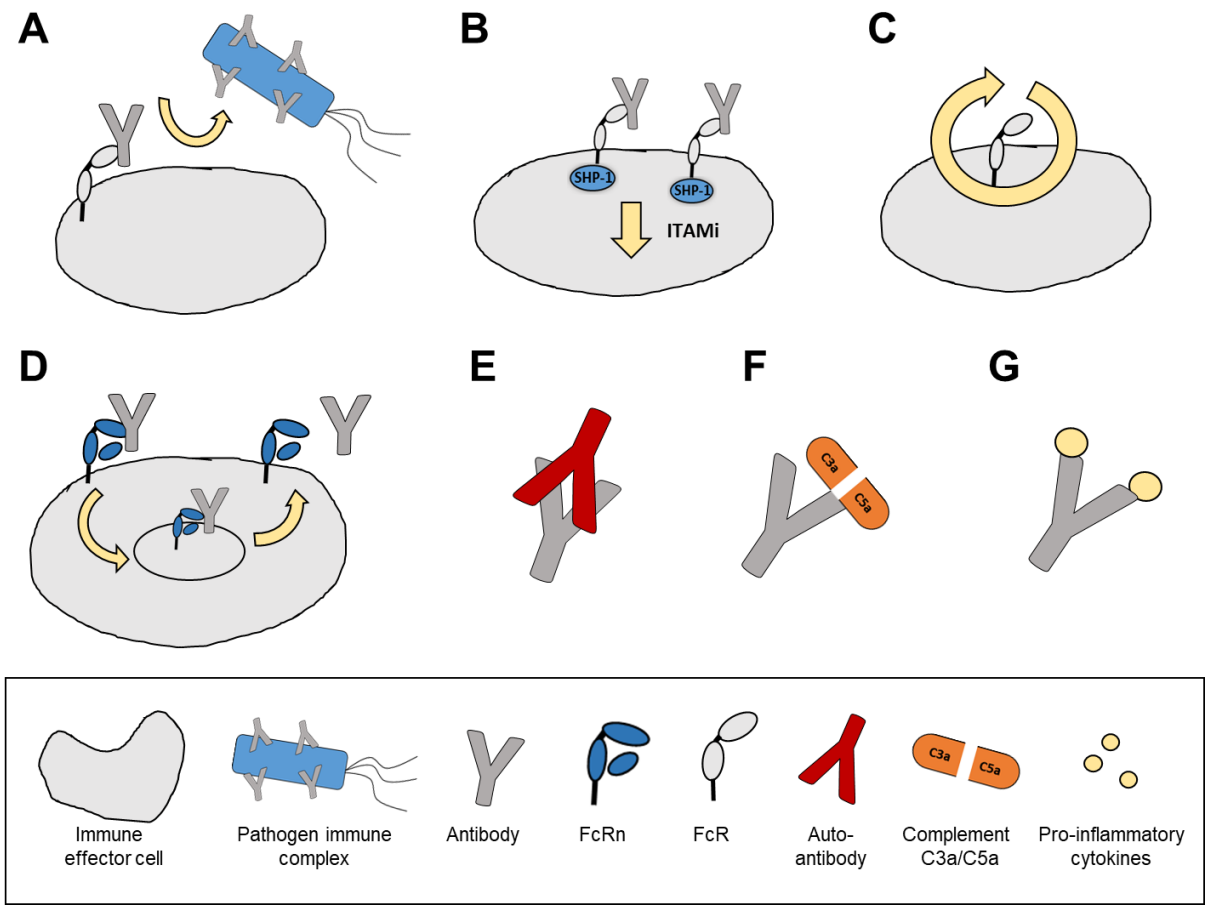

Figure 1-7: Overview of immunomodulatory activities of antibodies and immunoglobulin preparations. **(A)** Antibodies can block activating Fc-receptors (FcR), thereby inhibiting the binding of immune complex. **(B)** Activation of inhibitory immunoreceptor tyrosine-based activation motif (ITAMi) by monomeric antibodies. **(C)** Antibodies modulate the expression of cell surface receptors (like activating and inhibitory FcR) and other surface markers. **(D)** Saturation of FcR neonatal (FcRn) reduces the half-life of pathogenic autoantibodies. **(E)** Binding of autoantibodies by anti-idiotypic antibodies. **(F)** Neutralization of activating complement factors C3a and C5a. **(G)** Reduction of pro-inflammatory cytokines. Figure based on [68,69].

(1) Modulation via FcR

(A) Blockade of activating FcR and limiting the access of immune complex to FcR: Because of the high relevance of activating FcRs in many inflammatory effector functions, blocking of these receptors by IVIg appears to be an important mode of action [63,65,66]. Although competition of monomeric IgG or IgA species against highly valent immune complex seems to be problematic. Therefore, the hypothesis that IgG dimers in IVIg are crucial for blocking is under discussion [63,68,69]. In line with this, beneficial effects of IgM- and IgA- enriched immunoglobulins in the treatment of sepsis can be explained, because the multimeric species compete more efficiently with immune complex than monomeric IgG [62,90].

(B) Targeting inhibitory FcR signaling: While displacement of immune complex from activating FcRs is under discussion, another mechanism of anti-inflammatory cell modulation is described. Monomeric IgA and IgG binding on activating FcαRI or FcγR induce inhibitory ITAMi signaling, leading to cell inhibition [33,173,177]. It was shown that classical IVIg can target ITAMi signaling via FcγRIIA and FcγRIII [176,179,180].

(C) Modulation of cell phenotype: As described in chapter 1.4.1, the balance between activating and inhibitory FcRs is modulating the immune response. Treatment with monomeric IVIg preparations led to an increase in FcγRIIB expression [62,63,69,74] and to a decrease in activating FcR expression [31,69]. Besides FcR modulation, also the influence on the expression of other surface markers on macrophages was shown for trimodulin [84]. Further, other immune cells like dendritic cells and T-cells were modulated by IVIg preparations [69].

(2) Defeat autoimmunity

(D) Modulation of antibody half-life: A potential anti-inflammatory mode of action in IVIg preparations is the saturation or blockade of Fc receptor neonatal (FcRn) in high dose treatment [63,69,181]. This is especially the case in the treatment of autoimmune diseases, where FcRn blockade decreases the half-life of pathological autoantibodies [182]. The results from various studies using animal models are differing relativize the meaning of FcRn saturation [63,69].

(E) Neutralization of autoantibodies: Another way of IVIg modes of action in autoimmune disease is the direct neutralization of autoantibodies through anti-idiotypic antibodies delivered in IVIg [69]. These antibodies bind epitopes (in this special case called idiotopes) on the variable region of another antibody [183]. Several studies showing anti-idiotypic antibodies in IVIg preparations are reviewed in Schwab and Nimmerjahn [69].

(3) Interaction with soluble mediators of inflammation

(F) Inhibition of activating complement factors: On the one side IgG or IgM in immunoglobulin preparations can activate the complement system, but, on the other side immunomodulatory inhibition of complement factors is a mode of action attributed to both components [63,69,75,120]. Neutralization of activated complement factors, like anaphylatoxins C3a and C5a, was demonstrated for IVIg [158,184]. It was shown that IgM- and IgA-enriched preparations are more efficient than IVIg in preventing complement activation *in vitro* and in a rat model of inflammation [79].

(G) Modulating cytokine response: Studies revealed that immunoglobulin preparations modulate the cytokine response either via direct neutralization or indirect by neutralization of toxins [80,84,185]. The neutralization of pro-inflammatory cytokines TNF-α, IL-8 and the macrophage inflammatory protein (MIP)1α by multimeric IgM- and IgA-species was better in comparison to monomeric IgG [90].

Summarized, there is a high medical need for adjunctive therapies in severe infection diseases. The treatment of hyperinflammation in those patients is of major importance. Immunoglobulin preparations are a promising alternative with multifaceted functions; several studies indicate how immunoglobulin preparations could modulate the inflammatory immune response. IgM- and IgA-enriched immunoglobulins seem to have beneficial properties in some of those mechanisms. Nevertheless, open questions regarding immunomodulation and the functional role of each immunoglobulin component (IgM, IgA and IgG) remain.

2. Aim of the thesis

In this PhD thesis, the aim is to analyze the immunomodulatory functions of the IgM- and IgA-enriched immunoglobulin preparation trimodulin. In the course of this, four main questions arise:

1. Can trimodulin induce immune modulation on neutrophils?
2. If so, which pathways induce immune modulation?
3. Has trimodulin superior immunomodulatory effects in comparison to standard IVIg?
4. What is the functional relevance of IgA in immune modulation?

IgM- and IgA enriched immunoglobulins are polyvalent mixtures containing IgG, IgA and IgM. Due to the complexity of this product class, it is challenging to define distinct modes of action. Instead, multiple modes of action work synergistically to fulfill their clinical benefits [62,63]. These can be divided into anti-pathogenic effects (promoting pathogen clearance and inflammation) and immunomodulatory effects (dampening the inflammatory response and mediate anti-inflammatory effects). Because treatment of patients with severe infection diseases like sepsis, sCAP or COVID-19 requires regulation of the immune system [67,125,141], the focus of this work is immunomodulation.

As a basis to show immunomodulatory effects, a model system, which can be inflammatory activated, has to be established. Because of their elementary role in innate and adaptive immunity, as well as in important inflammatory diseases [5,6,101], primary human neutrophils and the neutrophil-like HL-60 cell line were established as immune effector cells in this work. This establishment has to include phenotypical identification of surface markers as well as functional relevant FcRs for IgG and IgA. By using a complement-free system and IgM-FcμR negative neutrophils, FcR dependent effects of trimodulin IgM component are of minor importance. As immunoglobulin preparations can modulate the immune response via several modes of action, different cellular parameters have to be investigated. Here the immunomodulatory capacity of trimodulin in comparison to IVIg was tested by facilitating an anti-inflammatory phenotype on resting neutrophils, modulating the inflammatory responses induced by bacterial stimuli (endotoxin/LPS and *S.aureus*) and modulation of SARS-CoV-2-virus-like inflammation in a COVID-19 model. Within these models, the activation of following modes of action should be tested: (1) interaction with soluble cytokines and modulation of cytokine release, (2) activation of ITAMi signaling, (3) targeting of FcγRIIB and ITIM signaling, (4) Modulation of FcR expression and (5) displacement of immune complex from activating FcR.

Based on challenging research, the functions of serum IgA are in relation to IgG not well investigated [31,51]. In line with this, the functional role of IgA in immunoglobulin preparations was underrated [64,73]. Therefore, a goal of this thesis is to shed light on the IgA component of trimodulin. By including the central IgA-FcαRI in phenotype modulation and blocking experiments, as well as the comparison between IgA-containing and classical IVIg preparations the role of this component will be highlighted.

3. Materials

3.1. Chemicals

Name	Manufacturer	Order number
Aqua dest.	B. Braun	0082479E
BSA	Sigma-Aldrich	A9647-50G
Calcein-AM	BioLegend	425201
Carbonate-Bicarbonate Buffer	Sigma-Aldrich	C3041-50CAP
D-PBS	Thermo-Fisher-Scientific	14190-094
EDAC	Sigma-Aldrich	E7750
Glycine	Merck KGaA	1042010100
MES	Sigma-Aldrich	M3671
NaOH 1 N	Merck KGaA	1.09137.1000

3.2. Reagents

Name	Manufacturer	Order number
AbC™ total antibody compensation beads	Thermo-Fisher-Scientific	A10497
Alexa Fluor™ 647 NHS Ester	Thermo-Fisher-Scientific	A37573
Anti-Mouse Ig, κ Compensation Particles Set	BD Biosciences	552843
ArC™-amine reactive beads	Thermo-Fisher-Scientific	A10346
BD Cytofix™ Buffer	BD Biosciences	554655
BD FACSFlow™	Becton Dickinson	342003
BD FACS™ Clean	Becton Dickinson	340345
BD FACS™ Shutdown solution	Becton Dickinson	334224
BD Phosflow™ Perm Buffer III	BD Biosciences	558050
CST-Research-Beads	Becton Dickinson	655051
Full-length COVID-19 spike protein, His-Tag	Acro Biosystems	SPN-C52H4
Latex beads [0.9 μm]	Sigma Aldrich	CLB9-1ML
Latex beads, fluorescent yellow-green [1μm]	Sigma Aldrich	L4655-1ML
LPS (*Escherichia coli* O111:B4)	Sigma-Aldrich	L2630-25MG
S.aureus BioParticles™, Alexa Fluor™ 488	Thermo-Fisher-Scientific	S23371
S.aureus BioParticles™, unlabeled	Thermo-Fisher-Scientific	S2859
SARS-CoV-2 Spike antibody, Chimeric Mab	SinoBiological	40150-D001-50
Zombie Aqua™ Viability Stain	BioLegend	423102

3.3. Cell culture material

Name	Manufacturer	Order number
0,4 % Trypane blue	Corning	25-900-CI
12-Well plate (non-treated)	Eppendorf AG	0030721012
24-Well plate (non-treated)	VWR	10861-558
48-Well plate (non-treated)	Eppendorf AG	0030723015
6-Well plate (non-treated)	Eppendorf AG	0030720016
96-Well plate (non-treated)	Eppendorf AG	0030730011
Cryotubes	Nunc	363401
Cyro freezing container	Nalgene	5100-0001
DMSO for cell culture	Sigma Aldrich	D2650-100ML
eBioscience™ 1x RBC lysis solution	Thermo-Fisher-Scientific	00-4333-57
FBS	Life technologies	10270-106
HL60 (ATCC® CCL-240™)	ATCC	CCL-240
IMDM	Life technologies	12440-053
Neubauer improved counting chamber	En-Tek	DHC-N01
Penicillin-Streptomycin	Sigma Aldrich	P0781-100ML
RPMI-1640	Life technologies	21875-034
T175 flask (non-treated)	Eppendorf AG	0030712013
T25 flask (non-treated)	Eppendorf AG	0030710010
T75 flask (non-treated)	Eppendorf AG	0030711017

3.4. Consumables

Name	Manufacturer	Order number
0,2 μm Filters (Minisart®)	Sartorius	16534
96-Well Nunc MaxiSorp™, flat-bottom	Thermo Scientific	44-2404-21
96-Well, deep-well plates	VWR	732-3323
96-Well, U-bottom	Greiner Bio-one	650101
96-Well, V-bottom	Greiner Bio-one	651161
Aluminium foil	VWR	291-0044
Amicon Ultra, Centrifugal filter unit	Merck Millipore	UFC505096
Bacillol®	Paul Hartmann AG	973380
Cannula	B. Braun	4665120
Cloves	Kimberly-Clark	90628
Combitips advanced® (sterilized)	Eppendorf AG	0030089618 (0.1 mL) 0030089650 (2.5 mL) 0030089669 (5 mL) 0030089677 (10 mL)
Coverfilm, 96-Well	VWR	60941-062
Disposabal bags	Brand AG	759705
FACS tubes	Corning Science	352052
Parafilm®	Bemis	WI 54956
Pipette tips (sterilized)	Eppendorf AG	0030075005 (10 μL) 0030075331 (200 μL) 0030073444 (300 μL) 0030075358 (1000 μL)
Profix® tissues	TEMCA GmbH	005099
Reaction tubes	Eppendorf AG	0030121023 (0.5 mL) 0030120086 (1.5 mL) 0030120094 (2 mL)
Reaction tubes (sterilized)	Greiner Bio-one	188261 (15 mL) 352070 (50 mL)
Serological pipettes (sterilized)	VWR	612-3702 (5 mL) 612-5541 (10 mL) 612-5544 (25 mL) 612-5546 (50 mL)
Single use weighting pan	VWR	613-1174
Vacuum bottles (1 l)	Medipack AG	50112100

3.5. Equipment

Name	Type / Modell	Manufacturer
Centrifuge	Multifuge X3R	Thermo Scientific
Flow Cytometer	FACSCanto™ II	BD Biosciences
Fluorescence-reader	Odyssey CLx	LI-COR
Freezer -150 °C	UltraLow	Sanyo
Freezer -20 °C/Fridge	LCv4010	Liebherr
Freezer -80 °C	Hera Freeze basic	Thermo Scientific
Incubator	HeraCell 240	Thermo Electron Corporation
Laminar Flow	Hera Safe HS18	Thermo Electron Corporation
MACSmix Tube Rotator	130-090-753	Miltenyi Biotec
MACSxpress Separator	130-098-308	Miltenyi Biotec
Magnet stirrer	RH Basic 2	IKA
Microplate reader	Infinite F200	Tecan
Microplate reader	Infinite M200 Pro	Tecan
Microplate shaker	ThermoStar	BMG Labtech
Microplate washer	405 Select	Tecan
Microscope	Visiscope IT405H	VWR International GmbH
Multipette	E3	Eppendorf AG
pH-meter	Seven Excellence	Mettler Toledo
Pipettes	Research Plus	Eppendorf AG
Pipetting aid	Integra Pipetboy	VWR International GmbH
Precision balance	XPE 205	Mettler Toledo
Rotator	SB3	Stuart
Table top rocker	Polymax 1040	Heidolph
Tabletop centrifuge	Centrifuge 5424R	Eppendorf AG
Thermomix	Thermomixer Comfort	Eppendorf AG
Ultrasonic Cleaner	USC6000TH	VWR International GmbH
Vortexer	RS-VA 10	Tecan
Water bath	Sub Aqua 18	Grant

3.6. Software

Name of software	Version	Manufacturer
DIVA™	6	Becton Dickinson
FlowJo™	10.6.2	FlowJo LLC
GraphPad Prism™	6.1	GraphPad Software, Inc
Image Quant™	TL 8.1	GE-Healthcare
Image Studio™	2.1	LI-COR
Office (Word, PowerPoint, Excel)	2010	Microsoft

3.7. Kits

Name	Manufacturer	Order number
Human Cytokine Array-Kit	R&D-Systems	ARY005B
Human IL-10 simple step ELISA Kit	Abcam	ab185986
Human IL-1ra simple step ELISA Kit	Abcam	ab211650
Human IL-8 simple step ELISA-Kit	Abcam	ab46032
Human MCP-1 simple step ELISA Kit	Abcam	ab179886
Human MIP1α simple step ELISA Kit	Abcam	ab214569
Kinetic Chromogenic LAL-test kit	Charles River	R1708K
MACSxpress® Whole Blood Neutrophil Isolation Kit, human	Miltenyi Biotec	130-104-434
Quantum™ Simply Cellular® anti-Mouse IgG	Bangs Laboratories Ltd.	BLI815B-5

3.8. Antibodies

Name	Clone	Isotype	Manufacturer	Order number
Antibodies for flow cytometry				
ACE-II-PE	E-11	Mouse IgG1	SantaCruz Biotech	sc390851-PE
CD11b-AF488	ICRF44	Mouse IgG1	Stemcell	60040AD
CD15-PE	W6D3	Mouse IgG1	BD Biosciences	562371
CD193-BV421	5E8	Mouse IgG2b	BD Biosciences	562570
CD35-BB700	E11	Mouse IgG1	BD Biosciences	745950
CD71-APC-H7	M-A712	Mouse IgG2a	BD Biosciences	563671
FcμR-BV421	HM14-1	Mouse IgG1	BD Biosciences	564714
FcαRI-PerCP Cy5.5	A59	Mouse IgG1	BioLegend	354110
FcγRIIA-FITC	IV.3	Mouse IgG2b	Stemcell	60012FI
FcγRIIB-AF647	2B6	Mouse IgG1	Creative BioLabs	TAB-036WM
FcγRIII-APC-Cy7	3G8	Mouse IgG1	BD Biosciences	557758
FγRI-PE-Cy7	10.1	Mouse IgG1	BD Biosciences	561191
IgA-VioBlue	IS11-8E10	Mouse IgG1	Miltenyi-Biotec	CBL114F
IgG-APC-H7	561297	G18-145	BD Biosciences	561297
IgM-PE-Cy5	551079	G20-127	BD Biosciences	551079
SHP-1 pY536-FITC	2A7	Rabbit IgG	Abwitz Bio	2353
SYK-pY348-APC	REA681	Mouse IgG1	Miltenyi-Biotec	130-110-300
SYK-pY352-PE-Cy7	17A	Mouse IgG1	BD Biosciences	561458
SYK-pY525/26-PE	C87C1	Rabbit IgG	Cell Signaling	6485S
TLR2-PE	TL2.1	Mouse IgG2a	BioLegend	309708
TLR4-BV421	HTA125	Mouse IgG2a	BioLegend	312811
Isotype controls for flow cytometry				
IgG1-AF488	MOPC-21	Mouse IgG1	Stemcell	60070AD.1
IgG1-AF647	MOPC-21	Mouse IgG1	BioLegend	400130
IgG1-APC-Cy7	MOPC-21	Mouse IgG1	BD Biosciences	557873
IgG1-BB700	X40	Mouse IgG1	BD Biosciences	566404
IgG1-PE	MOPC-21	Mouse IgG1	BioLegend	555749
IgG1-PE	MOPC-21	Mouse IgG1	SantaCruz Biotech	sc-2866
IgG1-PE-Cy7	MOPC-21	Mouse IgG1	BD Biosciences	557872
IgG1-PerCP Cy5.5	MOPC-21	Mouse IgG1	BioLegend	400150
IgG2a-APC-H7	MOPC-21	Mouse IgG2a	BD Biosciences	560167

Name	Clone	Isotype	Manufacturer	Order number
IgG2a-BV421	MOPC-173	Mouse IgG2a	BioLegend	400260
IgG2a-PE	MOPC-173	Mouse IgG2a	BioLegend	400214
IgG2b-BV421	X40	Mouse IgG2b	BD Biosciences	562438
IgG2b-FITC	MPC-1	Mouse IgG2b	Stemcell	60072FI.1
Blocking antibodies				
FcαRI	MIP8α	Mouse IgG1	Bio-Rad	MCA1824
FcγRIIA	IV.3	Mouse IgG2b	Stemcell	60012
FcγRIIB	2B6	Mouse IgG1	Creative BioLabs	TAB-036WM
FcγRIII	3G8	Mouse IgG1	BioLegend	302002
FγRI	10.1	Mouse IgG1	BioLegend	305002
Antibodies for cytokine array				
Streptavidin IRDye® 800CW	-	-	LI-COR	926-32230

3.9. Inhibitors

Name	Target	Manufacturer	Order number
3AC	SHIP-1	Sigma-Aldrich	565835
C29	TLR2	MedChemExpress	HY-100461-5mg
CLI-095	TLR4	Invivogen	tlrl-cli95
NSC-87877	SHP-1	Sigma-Aldrich	565851
Piceatannol	SYK	Sigma-Aldrich	P0453
ST2825	MyD88	MedChemExpress	HY-50937-1MG

3.10. Plasma products

Name	Manufacturer	Order number / lot
IgA from human serum	Sigma-Aldrich	I4036
IgM from human serum	Sigma-Aldrich	I8260
IVIg (*IgG Next Generation* (BT595))	Biotest AG	B595086
Plasma from COVID-19 recovered patients	Plasma Service Europe	-
Trimodulin (*IgM Concentrate* (BT588))	Biotest AG	B588027

3.11. Buffer protocols

Formulation buffer (300 mM glycine)

Referred as “buffer” throughout the document.

24 g	Glycine
1000 mL	Aqua dest.

Dissolve glycine in 1000 mL Aqua. Adjust pH to 4.3.

0,1 % BSA

0.5 g	BSA
500 mL	D-PBS

Dissolve 0.5 g BSA in 500 mL D-PBS. Filtrate through a 0.2 μM filter. Store at 2-8 °C.

1 % BSA

5 g	BSA
500 mL	D-PBS

Dissolve 5 g BSA in 500 mL D-PBS. Filtrate through a 0.2 μM filter. Store at 2-8 °C.

2 % BSA

10 g	BSA
500 mL	D-PBS

Dissolve 10 g BSA in 500 mL D-PBS. Filtrate through a 0.2 μM filter. Store at 2-8 °C.

Carbonate-bicarbonate-buffer

1 capsule	Carbonate-bicarbonate-buffer
100 mL	Aqua dest.

Dissolve capsule in 100 mL Aqua dest. Mix on magnet stirrer and remove capsule shell. Store at 2-8 °C.

4. Methods

4.1. Cell culture

4.1.1. General techniques

General procedures

All cells were cultivated under a humidified atmosphere at 37 °C and 5 % CO_2. All steps for cultivation, preparation of medium, and other reagents were performed under sterile conditions under a laminar flow bench. Centrifugation steps were performed at 350 x g for 5 min, if not otherwise indicated.

Determination of cell numbers

Cell numbers and viability were determined by a disposable Neubauer improved counting chamber. Therefore, 50 μL of cell suspension was diluted 1:2 with 0.2 % trypane blue solution and the cell number counted under the microscope. Blue cells were counted as dead cells. If necessary the cell suspension was further diluted with Dulbeccosphosphate-buffered-saline (D-PBS). From the cell count of the four squares, the total cell concentration and the cell viability were calculated with the following formulas:

$$\text{Cell concentration (cells/mL)} = \frac{\text{Number of viable cells} \cdot \text{Dilution factor} \cdot 10^4}{\text{Number of squares counted}}$$

$$\text{Viability (\%)} = \frac{\text{Number of viable cells}}{\text{Number of total cells}} \cdot 100$$

Cryopreservation

Before cryopreservation, the cells should have a viability ≥ 95 %. After determination of the cell number, the needed amount of cells was centrifuged. The cell pellet was re-suspended in cold cryomedium (90 % fetal bovine serum (FBS) with 10 % Dimethyl sulfoxide (DMSO)), to a cell number of $1x10^7$ cells/mL. After resuspending, the cell suspension was divided into aliquots of 1 mL into cryovials. The freezing was performed by placing the vials into a pre-cooled freezing container, which ensures a cooling rate of 1 °C per minute and placing it into a -70 °C freezer. After 24 h to four days, the cells were transferred into a < -150 °C freezer for long-term storage.

Thawing of cells

The frozen aliquot of cells was thawed in a 37 °C water bath. Immediately after the cell suspension was fluid, the cells were pipetted into a tube with 9 mL pre-warmed medium. After centrifugation, the pellet was resuspended in 10 mL pre-warmed medium and the cells were seeded in a T-75-flask.

4.1.2. Isolation of primary human neutrophils

Isolation of primary human neutrophils was performed by using the MACSxpress® Whole Blood Neutrophil Isolation Kit. Isolation was performed according to the manufacturer's instructions. 8 mL of fresh blood donation were mixed with 4 mL isolation mix-cocktail and incubated for 5 min on a tube rotator, then the tube was transferred into the magnetic field of MACSxpress® separator for 15 min. Magnetic labeled (non-target) cells were separated from neutrophils. Red blood cells (RBC) sediment to the bottom of the tube (compare Figure 4-1).

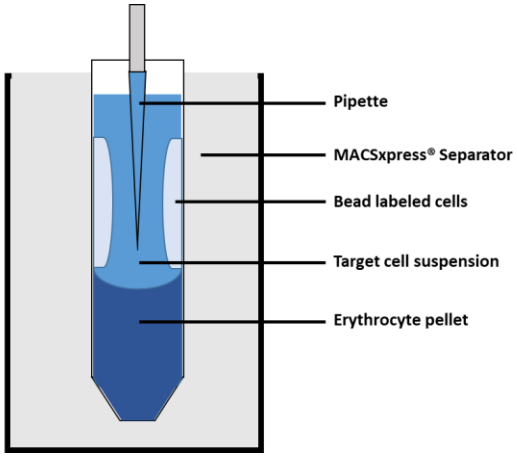

Figure 4-1: Schematic drawing for isolation of primary neutrophils. The mix of magnetic beads and blood was separated in a tube by MACSxpress® separator. Target cells (primary neutrophils) remain in suspension and can be removed by pipette.

The untouched primary neutrophils were centrifuged for 5 min at 350 x g. RBCs were lysed by resuspending the cell pellet in 10 mL 1x RBC lysis solution for 10 min. The reaction was stopped by the addition of 25 mL D-PBS. After centrifugation, the cells were re-suspended in RPMI-1640 medium and the cell number were determined (chapter 4.1.1). To verify the purity and the success of isolation, cells were analyzed using flow-cytometry (chapter 4.4.1). The isolated neutrophils were rest in RPMI-1640 supplemented with 5 % FBS for 1-2 h and were directly used in phagocytosis assays (chapter 4.4.5).

4.1.3. Cultivation and differentiation of HL-60 cell line

HL-60 cells were cultivated in IMDM medium supplemented with 20 % FBS and 1 % Penicillin (10.000 U/mL)/ Streptomycin (10.000 μg/mL). After seeding, cells were cultivated for 3-4 days at 37 °C in the incubator. For sub-culturing, cells were counted and seeded with a density of $2x10^5$ cells/mL in fresh medium into a new flask. When cells reached passage 4-5 with a viability $\geq$ 95 %, assays were started. Cultivation was resumed until cells reach passage 25; then a new aliquot was thawed.
Differentiation of HL-60 cells was performed by resuspending a cell pellet in complete culture medium supplemented with 1.3 % (v/v) DMSO to a cell density of $6x10^5$ cells/mL. These cells were incubated for 3-5 days at 37 °C in the incubator to reach a neutrophil-like phenotype needed for assays. Successful differentiation was verified by flow cytometry.

4.2. Cell-binding-assay

The initial step of antibody-mediated effector functions is the interaction of cell surface receptors for immunoglobulins (e.g. FcRs) with the immunoglobulin molecule. To examine the binding of different IgG-, IgA- and IgM-species on FcR bearing human immune cells or the binding of immune cells to immunoglobulin species, a binding assay was performed.
The cell-binding assay compares the relative binding of immune cells to immunoglobulin-coated plastic surfaces. The assay was performed related to Brandsma *et al.* [98] (compare Figure 4-2).

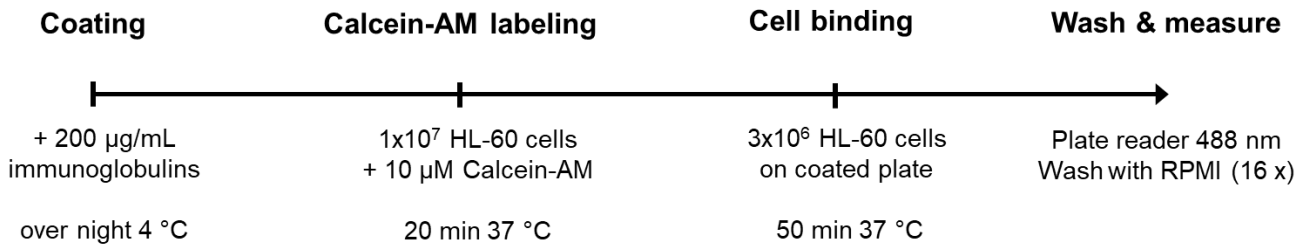

Figure 4-2: Procedure of cell binding assay. Immunoglobulin coated wells were incubated with Calcein-AM labeled neutrophil-like HL-60 cells and fluorescence was measured after every second washing step. Fluorescence of cells before washing was set as 100 % and results were calculated as relative binding in [%].

First 96-Well Maxisorp plates were coated with 100 μL of 200 μg/mL immunoglobulin preparations diluted in Carbonate-bicarbonate-buffer. Coating was performed overnight at 4 °C. The following day plates were washed with 100 μL/well RPMI-1640 medium and blocked with 100 μL 1 % Bovine serum albumin (BSA) in D-PBS for 1-2 h. Meanwhile, cells were counted and washed with D-PBS. 1 mM Calcein-acetoxymethylester (Calcein-AM) solution was prepared by reconstitution with 50 μL DMSO. 10 μM working dilution was prepared in D-PBS. Cells were centrifuged (350 x g, 5 min) and resuspended in 10 μM Calcein-AM solution with a cell density of $1x10^7$ cells/mL. Cells were incubated 20 min at 37 °C. After staining, cells were washed three times with RPMI- 1640 medium without supplements, after the last washing steps cells were resuspended to a density of $3x10^6$ cells/mL and let rest for 30 min at 37 °C. After Calcein-AM staining, the 96-Well plate was washed with RPMI-1640 and 100 μL of cell suspension was added. Following short centrifugation (40 x g, 3 min), cells were left for 50 min at 37 °C in the incubator to bind to immunoglobulins. Calcein fluorescence was measured on a plate reader with 488 nm and 520 nm reference wavelength to get 100 % binding value. In the following washing steps, the plate was washed with 100 μL RPMI-1640 and the fluorescence was measured after every second wash up to wash 16. The relative fluorescence intensity was normalized to the first measurement (before washing), which was set as 100 % binding, to compare the relative binding kinetics of different coatings.

4.3. Cell treatments

To investigate possible effects and modes of action immunoglobulins exert on neutrophil-like immune cells, cells had to be treated with various combinations of inflammatory stimuli, inhibitors, blocking antibodies and immunoglobulin preparations. In this work, the effects of trimodulin and IVIg on resting or inflammatory activated neutrophil-like HL-60 cells was analyzed. In the following section basic cell treatments by LPS, immunoglobulins or signaling inhibitors are described, as effector outcomes modifications of cell phenotype (chapter 4.4.3) and influence on the cytokine release (chapter 4.5) were measured.

4.3.1. LPS stimulation

Bacterial endotoxins, like LPS, are commonly used inflammatory stimuli. In this work LPS from *Escherichia coli* O111:B4 was incubated with neutrophil-like HL-60 cells to induce an inflammatory cell phenotype.

To test optimal concentration and time for cell activation, dose- and time-kinetics were performed. Doses of 1, 10, 100, 500 and 1000 ng/mL LPS were added to cells for 24 h. Further, 500 ng/mL LPS was added for 1, 2, 4, 6, 24 and 48 h to cells. Inflammation was assessed by the release of various inflammatory cytokines by cytokine array (chapter 4.5.1) and quantified by IL-8-ELISA as a marker for neutrophil activation. Additionally, modulation of cell phenotype was monitored (chapter 4.4.3).

LPS bind and activate immune cells mainly via TLR 4 and 2, central for subsequent signaling is MyD88 [186,187]. To prove this for the used HL-60 cell line indicated concentrations of inhibitors for TLR4 (CLI-095), TLR2 (C29) and MyD88 (ST2825) were incubated for 30 min at 37 °C before the addition of 500 ng/mL LPS. Cells were incubated for 4 h and the influence of inhibitors on IL-8 release was measured.

Immunoglobulins can directly bind and neutralize LPS via anti-LPS antibodies [80]. To examine the capacity of trimodulin and IVIg to bind LPS directly, varying concentrations of immunoglobulin preparations were added to 7.5 ng/mL LPS (corresponds to 50 EU/mL) for 1 h at 37 °C. The remaining endotoxin level in the solution was determined by LAL method according to manufacturer's instructions.

4.3.2. Immunoglobulins on resting cells

Direct effects of immunoglobulin preparations (trimodulin or IVIg) on neutrophil-like HL-60 cells were investigated by monitoring cytokine release and cell phenotype (FcR expression). For cytokine readout cells were incubated for 4 h with 0.005 - 20 g/L IVIg or trimodulin at 37 °C. All samples (wells) were filled up to the same end volume with formulation buffer. After incubation, cells were centrifuged and the supernatant was analyzed for IL-8 release as described (chapter 4.5).

To examine activation of intracellular immunoglobulin receptor signaling, inhibitors of central ITIM phosphatase SHIP-1 (3AC) and ITAMi phosphatase SHP-1 (NSC-87877) were used. Inhibitors were dissolved in DMSO and diluted 1:10 in supplemental free IMDM. Inhibitors (10 μM 3AC or 200 μM NSC-87877) were added 30 min before the 4 h incubation at 37 °C with immunoglobulin preparations.

The direct neutralization of cytokines by immunoglobulin preparations is known in literature [78,185]. To test if this mode of action is relevant for the here used model system 300 pg/mL recombinant IL-8 (standard from Abcam ELISA-Kit) was dissolved in D-PBS and trimodulin or IVIg added as described above. IL-8-immunoglobulin mixture was incubated for 1 h at 37 °C before storing at -20 °C. The remaining, soluble IL-8 was measured by ELISA.

Modulation of FcR expression was measured after incubating 0.005 – 20 g/L trimodulin or IVIg for 24 h with neutrophil-like HL-60 cells as described in chapter 4.4.1 IL-8 release was measured additionally after 24 h.

4.4. Flow cytometry assays

The analysis of cells with flow cytometry is a common technic in cell biology. One of the biggest advantages is the analysis on a single-cell level; this is possible due to the separation in a flow cell, where every cell passes the detector one after another. Typically, cells were analyzed based on their forward-scatter (FSC) and side-ward-scatter (SSC) properties, which are indicators for the size and granularity of the cell. Additionally, cells can be stained with various dyes and fluorophore-labeled antibodies to analyze specific surface- or intracellular proteins. With different emitting lasers and detection filters, it is possible to analyze multiple fluorophores on one cell simultaneously.

In this work, the BD FACSCanto™ II Cytometer with a 3-laser option was used. The 3 lasers can be used with different filters to analyze combinations of up to 8 fluorophores simultaneously:

Blue laser (488 nm): Fluorescein isothiocyanate (FITC), Alexa Fluor® 488 (AF488), BD Horizon Brilliant™ Blue 515 (BB515), Phycoerythrin (PE), Peridinin-chlorophyll-protein complex (PerCP), PerCP-cyanine 5.5 (PerCP-Cy5.5), PE-cyanine® 5 (PE-Cy5), PE-cyanine® 7 (PE-Cy7)

Red laser (633 nm): Allophycocyanin (APC), Alexa Fluor® 647 (AF647), APC-cyanine® 7 (APC-Cy7), APC-Histidine® 7 (APC-H7)

Violet laser (405 nm): Brilliant Violet™ 421 (BV421), *Anemonia majano* Cyan (AmCyan)

For analysis of cell population the collected events were evaluated as followed (compare Figure 4-3): Cell debris with low FSC-Area was excluded. Single cells were gated based on the relation between FSH-height and FSC-area. Dead cells were excluded by life-death staining with Zombie-Aqua™ viability stain. This dye can pass the membrane of dead cells and attach to primary amines inside the cell, whereas the dye is non-permeant for intact cells [188]. Histogram gates for every tested surface marker or FcR were set according to the corresponding isotype- and FMO-controls.

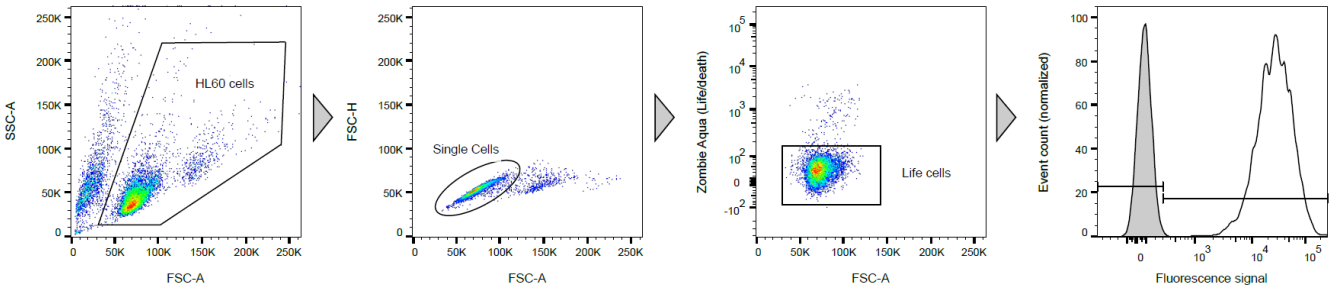

Figure 4-3: Exemplary gating strategy of HL-60 cells and primary neutrophils for surface marker staining. Cell population was gated based on SSC/FSC to exclude debris, followed by single-cell gating. To exclude death cells viability staining using Zombie-Aqua™ was performed. The threshold gate for each fluorescence channel was set using isotype controls. Isotype controls are shown as gray-filled histograms, stained cells are shown as black histograms, respectively. Data show representative values from different experiments.

4.4.1. Analysis of cell surface markers and FcR

For flow cytometry analysis the cells were counted, the required amount of cell suspension transferred in falcon tubes and centrifuged at 350 x g for 5 min. Afterwards, the pellet was washed with D-PBS and resuspended in the required volume D-PBS to yield $1x10^7$ cells/mL. For the staining 100 μL cell suspension was transferred into each well of 96-V-bottom plate to get $1x10^6$ cells/well. Unspecific binding of detection antibodies to FcRs was blocked by incubation with 100 μg/mL IVIg (*IgG Next Generation*) for 15 min at 4 °C [189].

Meanwhile, detection antibody mixes were prepared according to Table 4-1 and Table 4-2. Compensation of multicolor panels was done using Anti-Mouse Ig, κ compensation particles according to manufacturer's instructions. For accurate results fluorescence minus one (FMO), fluorescence minus two (FMT) and isotype controls were added. The antibody mix was added to each well and mixed briefly. Besides multicolor panels, detection of FcμR and ACE-II receptor on cells was performed by single color staining using 5 μL FcμR and 5 μL of ACE-II detection antibody per 10^6 cells/test. The staining was performed for 30 min at 4 °C in the dark.

After incubation, cells were mixed and centrifuged as described. The supernatant was discarded and the pellets were washed twice with 100 μL of D-PBS. Finally, pellets were resuspended in 100 μL D-PBS and analyzed using FACSCanto™ II Cytometer with high throughput sampler.

Panel 1: Neutrophil surface markers

Table 4-1: Multicolor staining panel 1. Fluorophore labeled antibody combinations and required volumes for staining of neutrophil surface markers on neutrophil-like HL-60 cells or primary neutrophils.

Excitation laser	Fluorophore	Antibody target	Volume/test
Blue laser (488 nm)	AF488	CD11b	5 µL
	PE	CD15	5 µL
	BB700	CD35	5 µL
Red laser (633 nm)	APC-H7	CD71	5 µL
Violet laser (405 nm)	AmCyan	Zombie-Aqua™	5 µL (1:10)
	BV421	CD193	5 µL

Panel 2: FcR and TLR

Table 4-2: Multicolor staining panel 2. Fluorophore labeled antibody combinations and required volumes for staining of FcR and TLR expression on neutrophil-like HL-60 cells or primary neutrophils.

Excitation laser	Fluorophore-channel	Antibody target	Volume/test
Blue laser (488 nm)	PerCP Cy5.5	FcαRI	5 µL
	PE-Cy7	FcγRI	5 µL
	PE	TLR2	5 µL
	FITC	FcγRIIA	20 µL
Red laser (633 nm)	AF647	FcγRIIB	2.5 µL
	APC-Cy7	FcγRIII	5 µL
Violet laser (405 nm)	AmCyan	Zombie-Aqua™	5 µL (1:10)
	BV421	TLR4	5 µL

4.4.2. Quantification of cell surface FcR

Quantification of FcR on HL-60 neutrophil-like cells and primary neutrophils was performed as described previously [41] using Quantum™ Simply Cellular® Beads. FcR number per cell was determined by calculating the antibody binding capacity (ABC) based on a reference curve with beads of known antibody binding capacity. In short, 4 bead populations with increasing binding capacity and one blank population were stained with the volumes of FcR detection antibodies described in Table 4-2. Before detection, antibody titration was performed to verify that the used amount detection antibody is sufficient to saturate all binding sites. Beads were washed and analyzed using FACSCanto™ II cytometer. The median fluorescence intensity (MFI) of each bead population was filled into the Quickcal® template to calculate standard curve. The ABC-value (or number of FcR per cell) was calculated by inserting the median fluorescence values of each FcR staining of the cell population into the Quickcal® template.

4.4.3. Change in cell phenotype

The modulation of cells by various stimuli can be measured at different levels. Besides the change in intracellular signaling and gene expression, the modulation of cell surface proteins can be used for monitoring the immunological status of the cell. FcR for IgG and IgA were chosen as an indicator for cell phenotype modulation. HL-60 cells were differentiated to a neutrophil-like phenotype and treated with different stimuli of LPS, immunoglobulins and combinations of those (compare chapter 4.3). Figure 4-4 summarizes the experimental design. Importantly cells were pre-treated for 24 h with LPS before adding immunoglobulins for further 24 h.

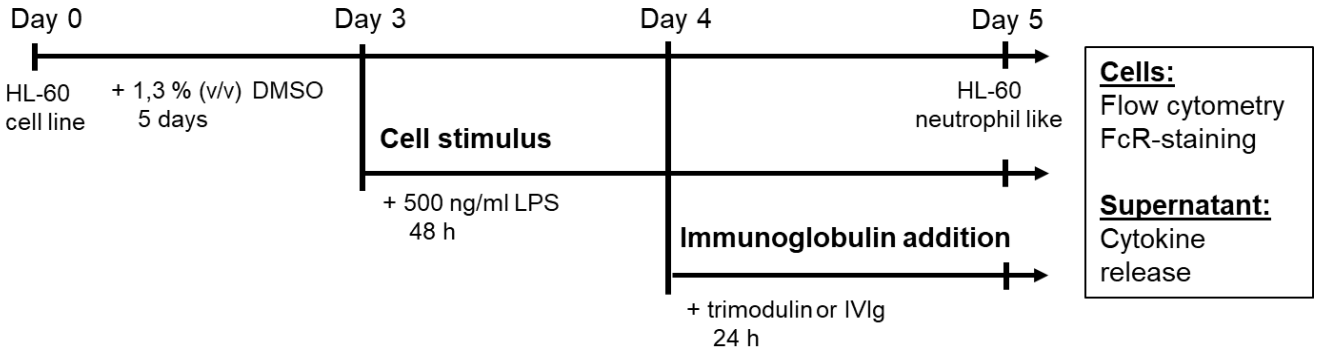

Figure 4-4: Overview of experimental procedure. Differentiation of HL-60 cells to neutrophil-like phenotype is started by adding 1.3 % (v/v) dimethylsulfoxide (DMSO) into the culture medium. On day 3, cells were stimulated with 500 ng/mL lipopolysaccharide (LPS) followed by the addition of immunoglobulins 24 h afterwards. On day 5 after differentiation start, neutrophil-like HL-60 cells were harvested, cell culture supernatant analyzed for cytokine secretion and cells stained for modifications in Fc-receptor (FcR) expression.

After treatment of cells, cell culture supernatant was collected and stored for IL-8 analysis at -20 °C. Cells were stained for FcR expression as described in chapter 4.4.1. The used antibody volumes for multicolor staining are shown in Table 4-3. For comparison of FcR expression, the MFI of each fluorophore was compared with either the MFI of untreated or LPS treated cells. The value was depicted as x- fold change in comparison to untreated cells or LPS treated cells.

Panel 3: FcRs modulation

Table 4-3: Multicolor staining panel 3: Fluorophore labeled antibody combinations and required volumes for the comparison of FcR expression on neutrophil-like HL-60 cells.

Excitation laser	Fluorophore-channel	Antibody target	Volume/test
Blue laser (488 nm)	PerCP Cy5.5	FcαRI	5 µL
	PE-Cy7	FcγRI	5 µL
	FITC	FcγRIIA	20 µL
Red laser (633 nm)	AF647	FcγRIIB	2.5 µL
	APC-Cy7	FcγRIII	5 µL

4.4.4. *S.aureus* phagocytosis assay

Phagocytosis of pathogenic particles is a crucial mechanism of the immune system to neutralize pathogens like bacteria. Opsonization of pathogens with antibodies increases the level of phagocytosis. To investigate the role of trimodulin in promoting phagocytosis, an ADCP assay was established.
Heat inactivated *S.aureus* wood strain without protein A was used as a gram$^+$ model microorganism. For monitoring the level of phagocytosis an AF488 conjugated variant was chosen. HL-60 neutrophil-like cells were used as phagocytic cells. Figure 4-5 gives an overview of the main experimental steps and the evaluation procedure.

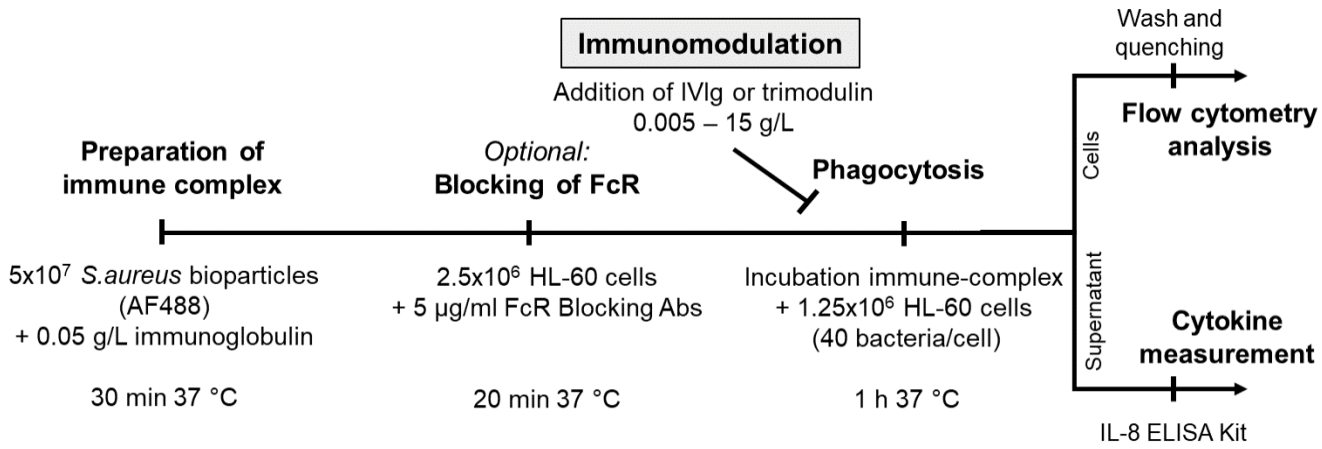

Figure 4-5: Experimental steps of *S.aureus* phagocytosis assay. *S.aureus* AF488 bioparticles were incubated with immunoglobulins to generate an immune complex. Fc-receptors (FcR) on neutrophil-like HL-60 cells were optionally blocked and phagocytosis was performed by addition of immune complex to cells. Phagocytosis and resultant cell activation were modulated by the addition of IVIg or trimodulin. After incubation, cells were harvested and analyzed by flow cytometry, culture supernatant was measured for IL-8 release.

Preparation of immune complex

On the day of experiment *S.aureus* particles were reconstituted in 500 μL D-PBS, vortexed and sonicated for 1 min in an ultrasonic cleaner to dissolve bacterial particles. The number of bacteria particles per mL was determined by Neubauer improved counting chamber, as described for cell culture in chapter 4.1.1. Next, immune complex were generated by incubating 50 μg/mL immunoglobulin preparations with 5x10^7 *S.aureus* particles/mL, for 30 min at 37 °C. In the meantime, neutrophil-like HL-60 cells were prepared: Therefore, cell number was determined and an appropriate volume cell suspension centrifuged (350 x g, 5 min). Cells were resuspended in IMDM medium without FBS to a cell number of 2.5x10^6 cells/mL. 500 μL cell suspension per well was transferred into 24-Well plates. After incubation of the immune complex, the suspension was vortexed and centrifuged for 18 min at 1,100 x g. Supernatant was discarded and the pellet was resuspended in D-PBS, subsequent to a second centrifugation step. At least immune complex were resuspended in 100 μL IMDM medium without FBS.

Characterization of immune complex

Additional analysis of coated and opsonized beads was performed by detecting IgG, IgA and IgM on the surface of *S.aureus* bioparticles by flow cytometry. Staining and measurement procedures were performed as described above (chapter 4.4.1). Centrifugation steps were performed with 1,100 x g for 18 min. Used anti-IgG, IgA or IgM detection antibody volumes are shown in Table 4-4. Isotype controls were used to set gates as shown in Figure 4-6.

Table 4-4: Multicolor staining panel 4: Fluorophore labeled antibody combinations and required volumes for staining IgG, IgA and IgM on the surface of *S.aureus* bioparticles.

Excitation laser	Fluorophore-channel	Antibody target	Volume/test
Blue laser (488 nm)	PE-Cy5	IgM	20 µL
Red laser (633 nm)	APC-H7	IgG	10 µL
Violet laser (405 nm)	VioBlue	IgA	2 µL (1:10)

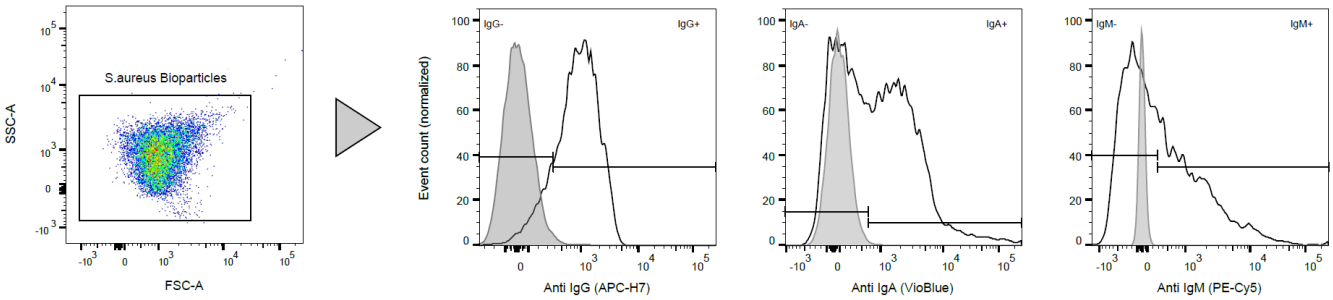

Figure 4-6: Gating strategy for the detection of IgG, IgA and IgM on the surface of *S.aureus* bioparticles. SSC-FSC values were set as logarithmic scale and the main population was gated. Histogram gates were set based on isotype controls to show the percentage of positive particles for each detection antibody.

Phagocytosis assay

For the phagocytosis assay, neutrophil-like HL-60 cells were used. The generated immune complex were added to the cell suspension and the wells were filled up to 1 mL with IMDM medium without FBS. For phagocytosis step, cells were transferred into the incubator at 37 °C for 1 hour. After incubation, the cell suspension was transferred into a 96-well deep-well plate and centrifuged for 5 min at 350 x g. Culture supernatants were stored at -20 °C for subsequent cytokine measurement. Pellets were washed twice with D-PBS and resuspended in 100 µL D-PBS and 25 µL of 0.2 % trypane-blue solution. 10 min incubation at 4 °C with trypane blue quenches the extracellular fluorescence of remaining *S.aureus* particles on the cell surface, leading to signals only from ingested bacteria. Cells were analyzed in duplicates by FACSCanto™ II cytometer.

For data evaluation, HL-60 cells and single cells were gated as shown in Figure 4-7. Untreated cells were used as a control for setting the gate of AF488 positive cells. To include parameters of percentage positive cells and median fluorescence intensity a phagocytic index was calculated. Therefore, the number of percentage positive cells was multiplied by the median fluorescence intensity.

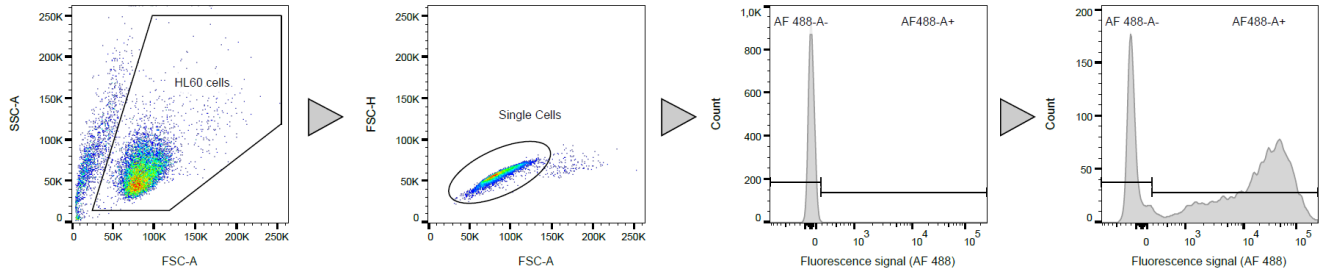

Figure 4-7: Gating strategy for *S.aureus* phagocytosis assay. For evaluation, the cell population was gated based on SSC/FSC to exclude debris, and gate single cells, followed by setting a threshold gate for AF488 positive cells based on untreated cells. The percentage and MFI of AF488 positive cells were analyzed and multiplied to calculate the phagocytic index

FcR-Blocking

For experiments with specific FcR blocking, an additional blocking step was performed. Specific blocking antibodies bind to the corresponding FcR and inhibit further interactions in the assay. To block binding of immunoglobulins on FcγRI, -IIA, -IIB, -III or FcαRI, cells were pre-incubated with 5 μg/mL specific blocking antibodies for 20 min at 37 °C in the incubator. All blocking antibodies are shown in chapter 3.8.

Immune modulation by trimodulin and IVIg

The effect on *S.aureus* phagocytosis by a different dosage of trimodulin or IVIg was tested. Therefore, dosages from 0.05 – 20 g/L of both preparations were mixed directly with $5x10^7$ *S.aureus* particles into cell suspension. Alternatively, prepared immune complex were added to HL-60 cells and 0.05 – 15 g/L trimodulin or IVIg were added to the mixture. Each well was filled up with formulation buffer to equal volume. Phagocytosis and IL-8 release were measured as described above.

Signaling inhibitor experiments

To test if ITAM signaling is activated by phagocytosis the central kinase, SYK was inhibited by the addition of chemical inhibitor Piceatannol. Therefore, cells were pre-incubated 30 min with 0.1-20 μM Piceatannol (1:10 diluted in IMDM) as indicated before adding *S.aureus* immune complex. Immune modulation by ITAMi signaling pathway was investigated by inhibition of central ITAMi phosphatase SHP-1 with chemical inhibitor NSC-87877. 200 μM (1:10 diluted in IMDM) of the inhibitor was added 30 min before addition of immune complex and indicated concentrations of immunoglobulin preparations. DMSO (1:10 diluted in IMDM) served as buffer control.

4.4.5. COVID-19 phagocytosis assay

Similar to bacteria, antibodies can opsonize viral particles and generate an immune complex, which can be phagocytosed by neutrophils or macrophages. Because of their biological safety class, many viruses cannot be analyzed easily. Therefore, a virus-like particle (based on latex beads) was developed and tested for phagocytosis:

Recombinant spike protein of the novel SARS-CoV-2 virus was coated on fluorescent latex beads to yield virus-like particles. The assay setup is based on the above-described *S.aureus* phagocytosis assay. The central experimental steps are shown in Figure 4-8.

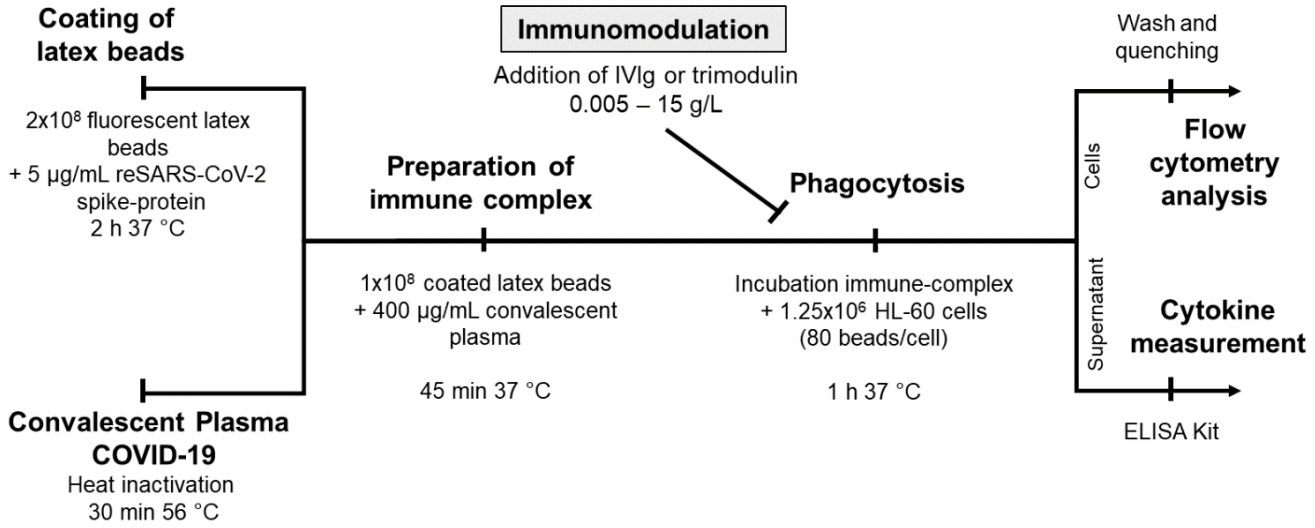

Figure 4-8: Experimental steps of SARS-CoV-2-like particles phagocytosis assay. Fluorescent latex beads were coated with recombinant SARS-CoV-2 spike protein. Convalescent plasma was heat-inactivated. Next coated and blocked latex beads were incubated with antibodies from convalescent plasma to generate SARS-CoV-2-like immune complex. Immune complex were added to HL-60 neutrophil-like cells to get phagocytosed and activate the cells. Phagocytosis and resultant cell activation were modulated optionally by the addition of IVIg or trimodulin. After incubation, cells were harvested and analyzed in flow cytometer, culture supernatant was measured for cytokine release.

Preparation of SARS-CoV-2-like particles and immune complex

For the preparation of virus-like particles, fluorescent latex beads were coated with recombinant SARS-CoV-2 spike protein. Coated carboxylate-modified polystyrene yellow fluorescent latex beads can be stored for several weeks at 2-8 °C. First beads were washed twice with a buffer consisting of 50 mM 2-(N-Morpholino) ethanesulfonic acid (MES) and 1.3 mM N-Ethyl-N′-(3-dimethylaminopropyl) carbodiimide hydrochloride (EDAC) in Aqua dest. at pH 6.1. MES/EDAC-Buffer has to be prepared fresh because of the low stability of EDAC.

Bead suspension was transferred into 15 mL falcon tube and centrifuged at 4,700 x g for 20 min. The supernatant was discarded and beads were resuspended in 7 mL MES/EDAC-Buffer. To dissolve beads completely, sonication in ultrasonic cleaner was done for 1:30 min. Because centrifugation led to loss of

beads, the number of beads per mL was determined with Neubauer improved counting chamber. Coating of latex beads was performed by adding 5 μg/mL reSARS-CoV-2 full-length spike protein to 2x10^8 beads/mL in 1 mL MES/EDAC-Buffer. The mixture was incubated for 2 h at 37 °C at 350 rpm on a heat block in the dark.

To block the remaining binding sites the double volume of 2 % (w/v) BSA/D-PBS was added to the bead/spike-protein mixture after incubation. Followed centrifugation at 4,700 x g, 15 min pellet was resuspended in 2 % (w/v) BSA/D-PBS and centrifuged again. Finally, the pellet was resuspended in 0.1 % (w/v) BSA/D-PBS to 1x10^8 beads/mL.

Manufacturing of immune complex with SARS-CoV-2 virus-like particles was done, by adding either 5 μg/mL specific anti-SARS-CoV-2 chimeric antibody (as positive control), 400 μg/mL heat-inactivated convalescent COVID-19 plasma or further immunoglobulin preparations to the coated and blocked beads. Heat inactivation of plasma was done by incubation for 30 min at 56 °C, followed centrifugation at 4,000 x g for 10 min. The precipitate was discarded and the supernatant was used for opsonization.

Immune complex formation was done by incubating SARS-CoV-2 specific antibodies (recombinant or plasma source) with the blocked beads for 45 min at 37 °C. As negative controls immunoglobulins (negative for SARS-CoV-2) or BSA were mixed with blocked beads and incubated as described above.

Characterization of immune complex

Analysis of coated and opsonized beads was performed by detecting IgG, IgA and IgM on the surface of beads by flow cytometry. Staining, measurement and gating procedures were performed as described (chapter 4.4.4). Divergently centrifugation steps were performed with 4,700 x g for 15 min.

Phagocytosis assay

Phagocytosis assay was performed based on the described *S.aureus* phagocytosis protocol (see chapter 4.4.4). The following modifications were made:

Immune complex were washed with D-PBS by centrifugation with 4,700 x g for 15 min. SARS-CoV-2-like immune complex were added to the cells and incubated for 1 h at 37 °C in the incubator. Fluorescent bead uptake was monitored with BB515 channel on FACSCanto™ II cytometer.

FcR blocking

FcR blocking was done as described in chapter 4.4.4.

Immune modulation by trimodulin and IVIg

To show immunomodulatory effects of trimodulin and IVIg in this COVID-19-like setup SARS-CoV-2-like immune complexes were prepared and the phagocytosis assay performed as described. Following the addition of immunoglobulin opsonized immune complex 0.005 – 15 g/L, trimodulin or IVIg was added to the cell-bead mixture. Each well was filled up with formulation buffer to equal volume. Cells were incubated for 1 h, phagocytosis and cytokine release were measured as described above.

Signaling inhibitor experiments

To test if SARS-CoV-2-like immune complex phagocytosis activates ITAM signaling, SYK kinase was inhibited by Piceatannol as described for *S.aureus* phagocytosis assay. Immune modulation due to ITAMi signaling was investigated by the addition of SHP-1 inhibitor NSC-87877 (compare chapter 4.4.4). Inhibitors were added 30 min before the addition of immune complex and indicated concentrations of immunoglobulin preparations.

Adaptions with primary neutrophils

Primary human neutrophils were isolated according to chapter 4.1.2. Followed by a resting phase of 1-2 h in RPMI-1640 supplemented with 5 % FBS. COVID-19 phagocytosis assay was performed as described above, except cells were treated in RPMI-1640 medium with 5 % FBS and centrifuged with 250 x g for 5 min.

4.4.6. Intracellular phosphorylation

Intracellular signaling cascades can be investigated by several methods. Besides inhibiting key proteins of intracellular signaling cascades by chemical inhibitors, the direct measurement of the activation status of these key proteins is possible. This activation status can be detected by the phosphorylation of specific amino acid residues like serine, threonine or tyrosine with specific detection antibodies [190]. Here the activation of SYK and SHP-1 was analyzed by detecting tyrosine phosphorylation via intracellular flow cytometry staining. In comparison to western-blot analysis, this method has the advantage to measure on a single-cell level in comparison to the whole population. An overview of experimental steps is shown in Figure 4-9.

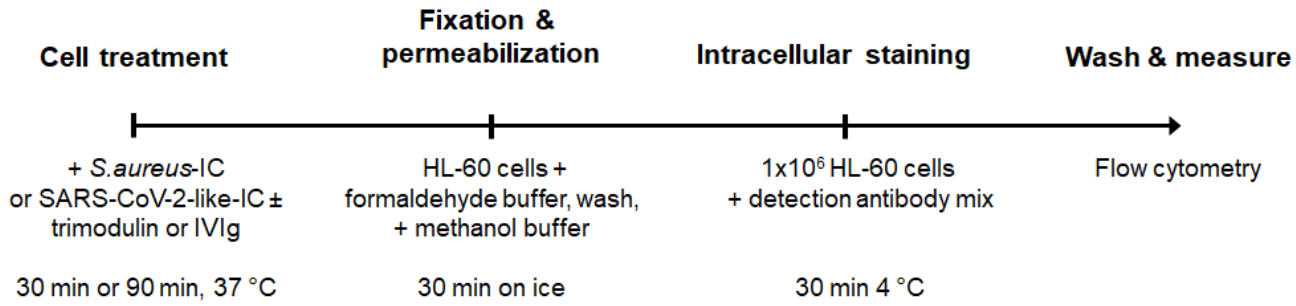

Figure 4-9: Overview experimental steps intracellular phosphorylation assay. Cells were treated as described with immune complex and trimodulin or IVIg, after 30 min (SYK phosphorylation) or 90 min (SHP-1 phosphorylation) reaction was stopped by fixation and permeabilization of cells. Permeabilzed cells were now able to be stained intracellularly with antibody mixes specific for SYK and SHP-1 phosphorylation. After washing steps cells were analyzed by flow cytometry.

Cell stimulation

Before phosphorylation measurements, neutrophil-like HL-60 cells have to be treated as described above. Activation of SYK by *S.aureus*- or SARS-CoV-2-like immune complex and the activation of SHP-1 by combined treatment of immune complex and immunoglobulin preparations was analyzed (compare chapter 4.4.4 and 4.4.5). Cell number was determined and a volume containing $1x10^6$ cells/mL was transferred into 96-well deep-well plates. Cells were treated 30 min for SYK or 90 min for SHP-1 phosphorylation at 37 °C. Importantly cell treatment was performed in the same medium as cultivation was performed. No centrifugation or wash steps were performed, to maintain the phosphorylation status.

Fixation and permeabilization

After stimulating cellular signaling cascades, the phosphorylation status of the cells has to be fixed. Therefore, cells were incubated with an equal volume of pre-warmed formaldehyde containing fixation buffer for 10 min at 37 °C. Cells were centrifuged and washed two times with 0.1 % D-PBS/BSA. Followed fixation cells were permeabilized to enable intracellular staining. Therefore, the cell pellet was resuspended in 100 μL methanol containing permeabilization buffer, transferred to a 96-well V-bottom plate and incubated for 30 min on ice.

Intracellular antibody staining

During the permeabilization step antibody mixes were prepared as shown in Table 4-5. Fixed and permeabilized cells were washed again and resuspended in 0.1 % D-PBS/BSA. The required volume of detection antibody mix was added to the cell suspension and incubated for 30 min at 4 °C in the dark.

Table 4-5: Multicolor staining panel 5: Fluorophore labeled antibody combinations and required volumes for intracellular staining of SHP-1 and SYK phosphorylation on neutrophil-like HL-60 cells.

Excitation laser	Fluorophore	Antibody target	Volume/test
Blue laser (488 nm)	FITC	SHP-1 pY536	6 μL
	PE	SYK pY525/26	5 μL
	PE-Cy7	SYK pY352	2.5 μL
Red laser (633 nm)	APC	SYK pY348	10 μL

After two washing steps, cells were resuspended in D-PBS and analyzed by FACSCanto™ II cytometer. Multicolor panels were compensated by AbC total antibody compensation kit according to the manufacturer's instruction. Gating was performed as described for surface marker staining (chapter 4.4.1 and Figure 4-3). The signals from SYK kinase phosphorylation at tyrosine 525/526, 348 and 352 of untreated cells were normalized to 100 % and percentage change during immune complex treatment was calculated. For SHP-1 phosphorylation signal at tyrosine 536 of immune complex treated cells were normalized to 100 % and percentage change due to trimodulin or IVIg addition was calculated.

4.5. Determination of cytokine release

For measurement of the cytokine release, cell culture supernatant was analyzed by different techniques. To get an overview of expressed cytokines semi-quantitative cytokine arrays were performed. Quantification of selected cytokines was done with commercial human cytokine ELISA-Kits.

4.5.1. Cytokine arrays

Cytokine arrays are a semi-quantitative opportunity to detect 36 different human cytokines in a sample. The technique provides no quantification of the single cytokine levels but enables a comparison between different samples and gives an overview of the secreted cytokines.
Capture antibodies against different cytokines are coated in duplicate on a nitrocellulose membrane in defined positions (compare Table 4-6). After sample application, a mixture of streptavidin coupled detection antibodies, specific for each of the cytokines, is added. Finally, the signal is detected via a fluorophore-labeled streptavidin.

Table 4-6: Overview of the detectable cytokines with cytokine array membrane.

	1_2	3_4	5_6	7_8	9_10	11_12	13_14	15_16	17_18	19_20
A	Pos. control	CCL1	MCP-1	MIP1α MIP1β	RANTES	CD40L	C5a	GROα	CXCL10	Pos. control
B		CXCL11	CXCL12	G-CSF	GM-CSF	ICAM-1	IFN-γ	IL1-α	IL-1β	
C		IL-1ra	IL-2	IL-4	IL-5	IL-6	IL-8	IL-10	IL-12	
D		IL-13	IL-16	IL-17A	IL-17E	IL-18	IL-21	IL-27	IL-32a	
E	Pos. control	MIF	Serpin E1	TNF-α	TREM-1					Neg. control

Before starting the array all reagents were pre-warmed to room temperature. The detection antibody cocktail war was reconstituted with 100 μL Aqua dest. Membranes were blocked for 1 h at RT in the provided dishes with 3 mL of array buffer 4 on a rocking platform shaker. After thawing, the samples were prepared by addition of 0.5 mL array buffer 4 to 1 mL sample to generate a final volume of 1.5 mL. 15 μL of reconstituted detection antibody mix was added and mixed with the samples for 1 h at RT.
After incubation, the array buffer 4 from the membranes was aspirated and every sample was added to a prepared membrane. The followed incubation was performed at 2-8 °C on a rocking platform shaker overnight. The next day membranes were washed 3-times with 20 mL wash buffer for 10 min. For detection, IRDye® 800CW streptavidin was diluted 1:2000 in array buffer 5. The membranes were

transferred back into provided dishes and 3 mL of diluted streptavidin was added to each well. The membranes were incubated for 30 min on a shaker, followed by 3-times washing as described.
The membranes were scanned with an Odyssey® CLx imager. For analysis, the signal intensities were exported into an excel-template where the percentage of the measurement spots in relation to the positive control spots was calculated. The relative percentage of each cytokine was compared between untreated and treated cells. Signals from untreated cells were set to 1 and relative induction (values >1) or reduction (values <1) were calculated and imaged in a heat map.

4.5.2. Simple step ELISA

Quantification of IL-6, IL-8, IL-10, MCP-1, MIP1-α and IL-1ra levels in cell culture supernatants were performed via Abcam human SimpleStep ELISA® Kit. The kits contain a classical sandwich ELISA. The assay was performed according to the manufacturer's instructions. Samples were thawed and reagents were equilibrated to room temperature for 1 hour.

4.6. Statistical analysis

All data are expressed as [mean ± standard deviation] of the indicated number of measurements. Statistics were calculated using GraphPad Prism 6.1. Software. Two-way analysis of variance (ANOVA) with Turkeys or Dunnett's multiple comparisons test and one-way ANOVA with Dunnett's multiple comparison test were performed as indicated. Significance was quantified as p-values with asterisks: * $p \leq 0.05$, ** $p \leq 0.01$, *** $p \leq 0.001$, **** $p \leq 0.0001$; with 95 % confidence interval.

5. Results

The immunomodulatory modes of action of IgM- and IgA-enriched immunoglobulins like trimodulin are complex and especially the role of IgA in these preparations was not identified yet. This work will unravel the effects of trimodulin in comparison to a classical IVIg in the context of neutrophil inflammation. By head-to-head comparison between IgM-, IgA-, IgG-containing trimodulin and IgG-containing IVIg differential effects can be explored. Immune modulation was analyzed at different levels: First, the here used neutrophil-like HL-60 cell line was characterized and compared to primary neutrophils (chapter 5.1), followed by observing effects of immunoglobulin preparations on resting neutrophils (chapter 5.2). Immunomodulatory effects on inflammatory activated neutrophils were investigated in bacterial context (Endotoxin model and *S.aureus* phagocytosis model; chapter 5.3 and 5.4) and viral context (COVID-19 model; chapter 5.5).

5.1. Comparison of neutrophil-like HL-60 cells and primary neutrophils

Investigations regarding the cellular modes of action of immunoglobulin preparations require a defined and comparable cell system. Primary cells are heterogenic and distinguish between different donors, further, the laboratory handling is more complicated [191]. In many cases, investigations can be done with immortalized cell lines. The basis for studies with cell lines is the comparison to their native counterpart. Here the HL-60 cell line was used and differentiated to a neutrophil-like phenotype. The comparability with primary neutrophils isolated from fresh blood was done by comparison of cytokine secretion profile and cellular phenotype.

Neutrophil markers (CD15, CD35, CD11b, CD71, CD193) and FcR expression (FcγRI, -IIA, -IIB, III, FcαRI, FcμR) were detected and quantified (Figure 5-1). The cytokine profile was semi-quantitative compared with LPS stimulated cells (Figure 5-2).

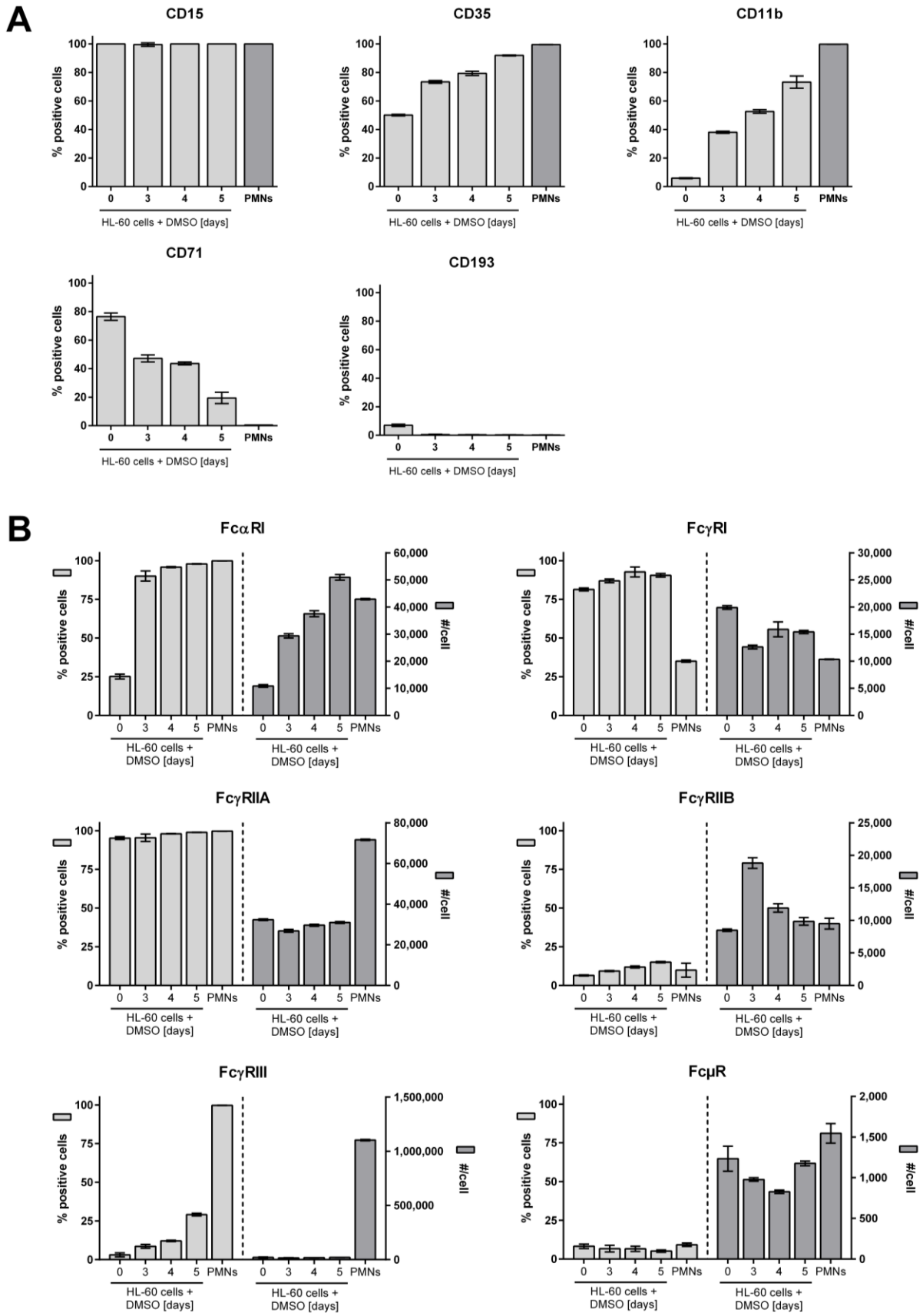

Figure 5-1: Comparison of HL-60 cells and primary neutrophils. HL-60 cells were differentiated by adding 1.3 % (v/v) dimethylsulfoxide (DMSO) into cell culture medium for indicated times, primary neutrophils were isolated from six human blood donations. Cells were washed, stained with corresponding detection antibodies, and analyzed by flow cytometry. **(A)** Comparison of neutrophil cell marker expression (CD15, CD35, CD11b, CD71 and CD193). The percentage of positive cells from

the cell population is shown for HL-60 cells (light gray) and primary neutrophils (PMNs, dark gray). **(B)** Comparison of Fc-receptor (FcR) expression (FcαRI, FcγRI. FcγRIIA. FcγRIIB. FcγRIII and FcμR). Percentage of positive cells (light gray bars, left axis) and number of FcR per cell (dark gray, right axis) were compared for indicated cells. FcR quantification was measured as antibody binding capacity using Quantum™ Simply Cellular® beads. Data represent the mean of 6 independent experiments or from 6 different donors.

Figure 5-1 compares primary neutrophils with the neutrophil-like HL-60 cell line. As seen in Figure 5-1A neutrophil-markers show greater comparability with the ongoing differentiation process. CD15 is continuously detected on the HL-60 cell population and primary cells. CD35 and CD11b expression is increasing during differentiation days and reaches a similar level as on primary cells. CD71 and CD193 expression is decreasing during differentiation; primary cells show no expression of those markers.

The FcR expression seen in Figure 5-1B shows that FcαRI expression increases after 3 days differentiation on HL-60 cell line to a similar level (~99 % of cells) and number of FcR per cell (~40,000) than primary cells. FcγRI expression slightly increases during differentiation and is higher as on primary cells (85 % vs. 30 %), whereby the FcγRI number per cell is comparable (10- 15,000). FcγRIIA is expressed continuously on almost all HL-60 and primary cells (~99 % of cell population). The FcR number per cell is about 35,000 on HL-60 cells whereas primary cells show the double number of FcγRIIA per cell (~70,000). FcγRIIB expression aligned during differentiation to primary cells and FcR number per cell is similar (~10,000). FcγRIII expression differs between primary cells and cell line. Primary cells express on ~99 % of cells ~1.000.000 copies of this receptor, whereas FcγRIII expression increases during HL-60 cell differentiation to 30 % of cell population with ~20,000 receptors per cell.

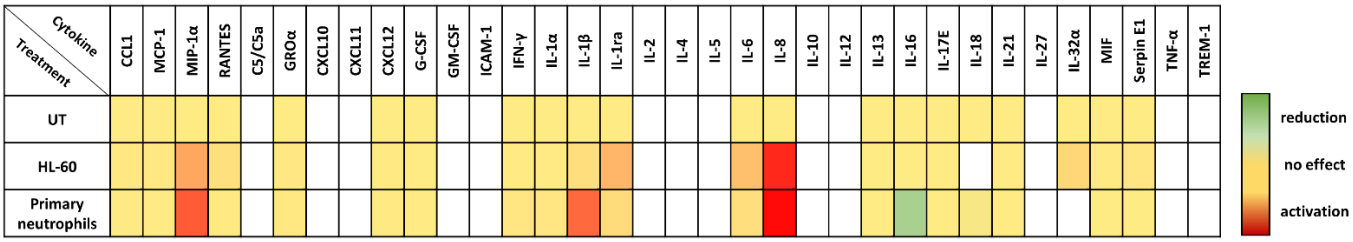

Figure 5-2: Comparison of the cytokine profile of LPS stimulated HL-60 cells and primary neutrophils. Heat map of chemokines and cytokines secreted by HL-60 cells (4 days differentiated) and primary neutrophils. Both cell types were stimulated for 18 h with 500 ng/mL LPS. Semi-quantitative cytokine secretion was measured by using human cytokine arrays. Relative signal intensities for every detected cytokine of untreated (UT) cells of each cell type were set as 1 (yellow). The x-fold induction (red) or reduction (green) in comparison to untreated cells (HL-60 or primary neutrophils) was calculated. Not detected cytokines are shown in white. Results represent the mean of three independent experiments.

The pattern of secreted cytokines and chemokines after stimulation with LPS is comparable between the HL-60 cell line and primary cells. The same cytokines were detectable (yellow boxes) or not (white boxes). LPS treatment led to induction of MIP-1α, IL-1β, IL-1ra, IL-6 and IL-8 on both cell types. A semi-quantitative comparison of signal intensities shows small differences between primary neutrophils and neutrophil-like HL-60 cells.

As additional parameters cell viability, quantitative cytokine release (IL-8) and cell number during HL-60 differentiation process were analyzed (appendix, Figure 8-1). Cell number and IL-8 release increased, whereas cell viability decreased during differentiation.
Summarized, the data clearly show that neutrophil-like HL-60 cells were comparable to primary human neutrophils. Cell markers, FcR-expression and secreted cytokines clarify the suitability of the cell line as a model system for antibody-mediated immune modulation.

5.2. Influence of immunoglobulins on resting neutrophils

Immunoglobulins are circulating molecules constitutively expressed and detectable in our bloodstream. Therefore, immunoglobulins can interact with immune cells in their resting state and maintain an anti-inflammatory status of the immune system. If and how immunoglobulin preparations can facilitate an anti-inflammatory phenotype of the here used neutrophil-like HL-60 cells is investigated in this chapter.

5.2.1. HL-60 cells interact with immunoglobulin preparations

The basis for immunoglobulin-mediated effects is the interaction between cells and immunoglobulins. Enhanced antibody binding is known to mediate stronger effector outcomes [47]. Thus, the binding of different immunoglobulin preparations to neutrophil-like HL-60 cells was tested. Immunoglobulins were coated on a plastic surface and Calcein-AM labeled cells were incubated for binding. Differences in binding strength were detected by measuring the remaining cellular fluorescence after subsequent washing steps (Figure 5-3).

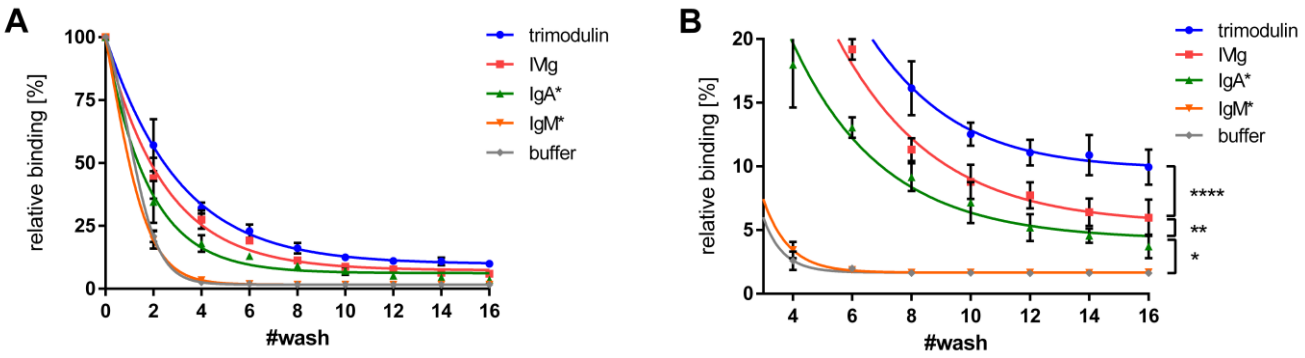

Figure 5-3: Binding of neutrophil-like HL-60 cells on immunoglobulin coated surface. **(A)** Relative binding of HL-60 cells on immunoglobulin coated surface during 16 wash steps. 96-Well plate was coated with indicated immunoglobulin preparations or formulation buffer. Calcein-AM labeled HL-60 cells were added and incubated for 50 min, afterwards cells were washed and remaining Calcein-AM fluorescence was measured. Fluorescence before first wash was referenced as 100 % and relative binding [%] calculated. *Purified IgA- and IgM- from human serum were used for coating (Sigma-Aldrich) **(B)** Expansion of (A), relative binding between wash 4 and 16 is shown. Data represent mean values of 8 independent experiments. Statistics: Two-way ANOVA, Tukey's multiple comparison test, 95 % confidence interval.

The binding strength of cells to the tested immunoglobulin preparations is varying (Buffer=purified IgM<purified monomeric IgA<IVIg<trimodulin). Cellular fluorescence is strongly decreasing during wash step 2-4. On the surface, without immunoglobulin coating (buffer = negative control) only baseline fluorescence remains after 6 washing steps. Binding similar to buffer control was observed for purified IgM coated surface. On (purified monomeric) IgA, (purified monomeric IgG) IVIg and trimodulin coated surface cells show stronger binding. Cells elicit the strongest binding to the trimodulin-coated surface.

5.2.2. Trimodulin and IVIg facilitate anti-inflammatory phenotype

Immunoglobulin preparations may induce anti-inflammatory phenotype by several modes of action. The effect of trimodulin and IVIg on resting neutrophil-like HL-60 cells was investigated by adding different concentrations to not stimulated (resting) cells. Anti-inflammatory phenotype was observed by modulation of inflammatory cytokine release (Figure 5-4A) and changes in FcR expression (Figure 5-6B). Underlying modes of action were further addressed by studying the direct binding of cytokines by immunoglobulins (Figure 5-4B), as well as activation of inhibitory ITIM and ITAMi signaling (Figure 5-5).

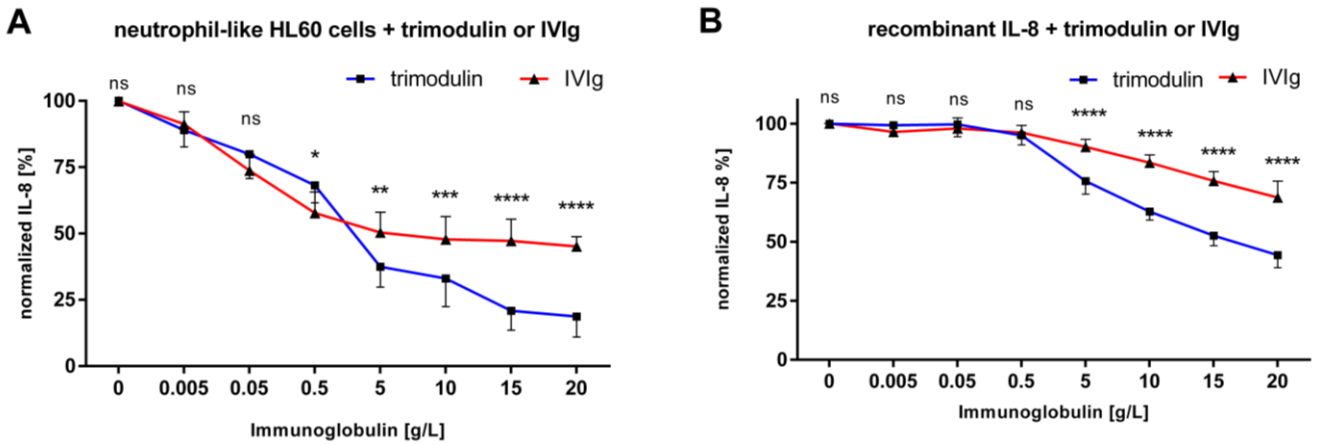

Figure 5-4: Immunoglobulin preparations modulate cytokine release of neutrophil-like HL-60 cells and directly interact with IL-8 **(A)** IL-8 release is reduced by the addition of trimodulin and IVIg to resting neutrophil-like HL-60 cells. Cells were incubated for 4 h at 37 °C with indicated concentrations of trimodulin (square, blue line) or IVIg (triangle, red line). Cell culture supernatant was analyzed for IL-8 release using ELISA-Kit, cells incubated with buffer were referenced as 100 % and remaining IL-8 [%] was calculated. **(B)** Immunoglobulins directly interact with IL-8. 300 pg/mL recombinant IL-8 was dissolved in D-PBS and indicated concentrations trimodulin (square, blue line) or IVIg (triangle, red line) were added for 1 h at 37 °C. The remaining accessible IL-8 in suspension was measured via IL-8 ELISA Kit. All data represent the mean of 6 independent experiments. Statistics: Two-way ANOVA; Tukey's multiple comparisons test.

As seen in Figure 5-4A, incubation of HL-60 cells with trimodulin or IVIg decreased the IL-8 release dose-dependently. No significant differences between both preparations were observed in low doses (<0.5 g/L), whereas in high doses (>5 g/L) the effects differ significantly. IVIg led to a reduction of 50 %, whereas trimodulin was able to reduce IL-8 up to 80 % of buffer control. Similar results were observed for the direct binding of IL-8 (Figure 5-4B). IVIg reduced IL-8 detection up to 30 % of control, trimodulin reduced IL-8 level up to 50 %.

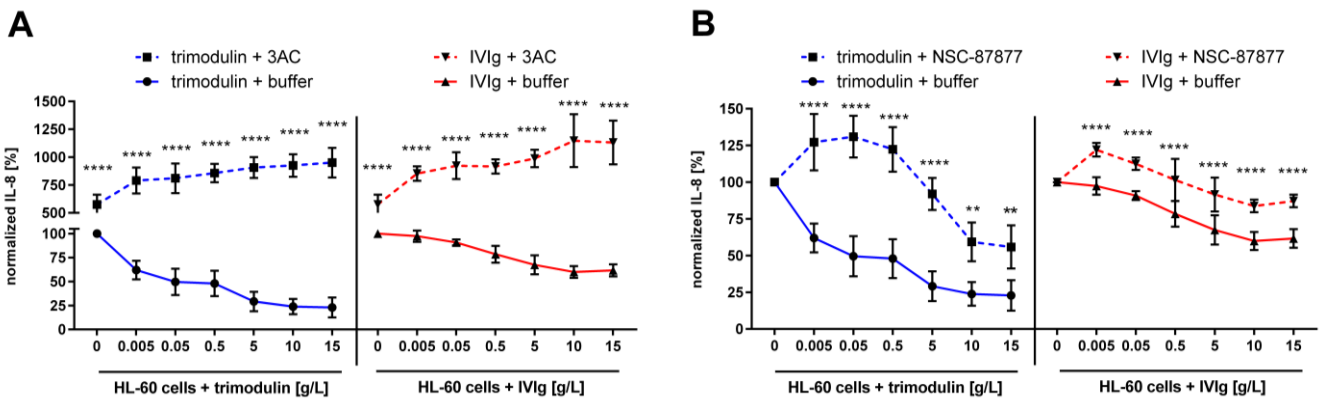

Figure 5-5: Inhibitory FcR-signaling responsible for immunomodulation. **(A)** Blocking of ITIM-signaling potently activates IL-8 release. Cells were pre-incubated for 30 min with 10 µM SHIP-1 inhibitor 3AC and incubated for 4 h at 37 °C with indicated concentrations of trimodulin or IVIg. IL-8 release of cells treated with indicated concentrations trimodulin (blue solid lines) or IVIg (red solid lines) is compared with 3AC pre-incubation (dotted lines). **(B)** ITAMi signaling induced by immunoglobulins reduces IL-8 release. Same as in (A), but SHP-1 Inhibitor 200 µM NSC-87877 was pre-incubated with HL-60 cells. All data represent the mean of 6 independent experiments. Statistics: Two-way ANOVA; Tukey's multiple comparisons test.

To test the importance of ITIM signaling in this assay setup, SHIP-1 phosphatase was inhibited using 3AC. Inhibition of SHIP-1 and relating ITIM signaling lead to a strong increase of IL-8 release (up to 10-fold induction) by trimodulin and IVIg treatment (Figure 5-5A). As seen in Figure 5-5B, inhibition of SHP-1 phosphatase by NSC-87877 affects cytokine release. Inhibiting the central ITAMi phosphatase results in increased IL-8 release compared to non-inhibited cells. Trimodulin treated cells were more affected by SHP-1 inhibition, as seen by greater differences between treated and not treated cells compared to IVIg. This indicates a stronger induction of ITAMi signaling by trimodulin.

Modulation of cellular phenotype, here measured by changed FcR detection, requires a 24 h incubation step to detect differences between the treatments. In Figure 5-6 the influence of 24 h immunoglobulin treatment on cytokine release and FcR expression is shown.

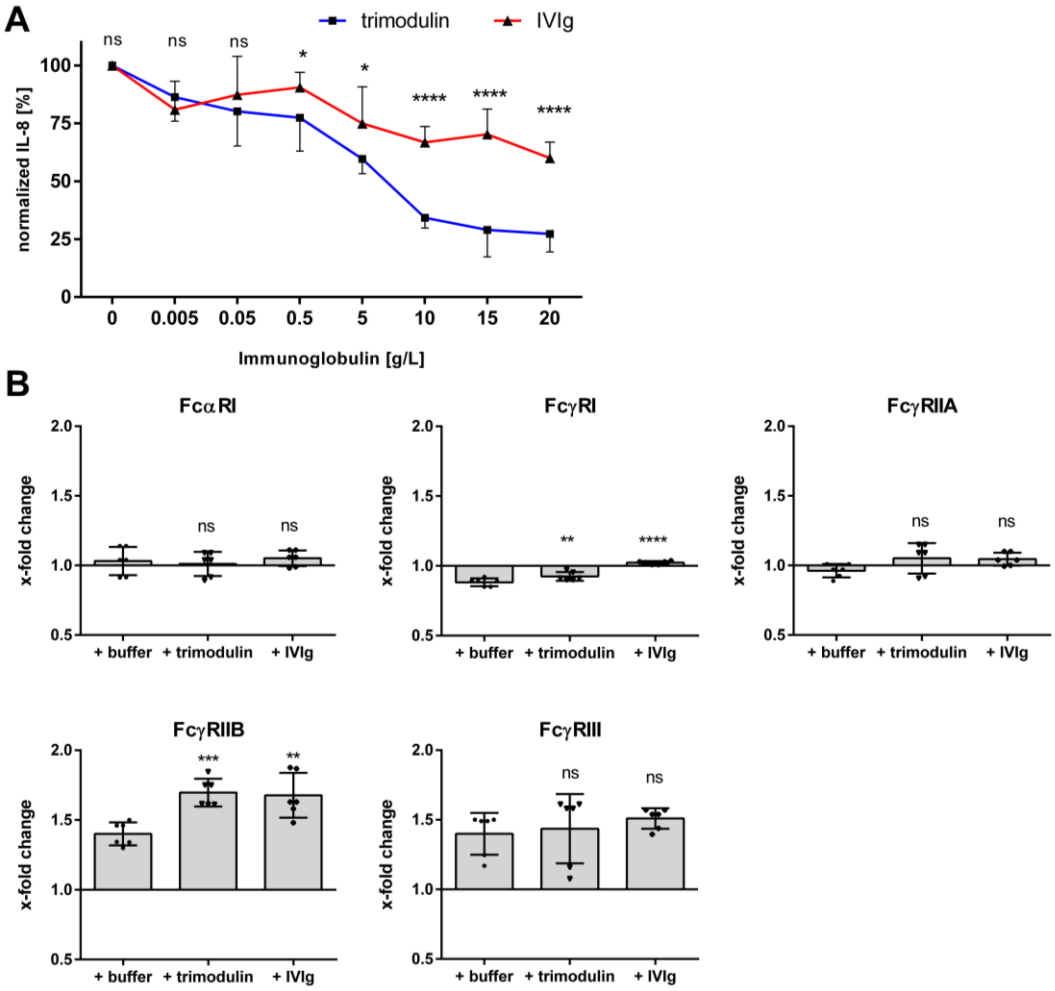

Figure 5-6: Immunoglobulin preparations modulate cell phenotype by altered FcR expression. **(A)** IL-8 release is reduced by the addition of trimodulin and IVIg to resting neutrophil-like HL-60 cells. Cells were incubated for 24 h at 37 °C with indicated concentrations of trimodulin (square, blue line) or IVIg (triangle, red line). Cell culture supernatant was analyzed for IL-8 release, buffer control was referenced as 100 % and remaining IL-8 [%] was calculated. **(B)** Modulation of FcR expression. Neutrophil-like HL-60 cells were incubated for 24 h with 5 g/L trimodulin, IVIg or buffer. FcR expression was analyzed via flow cytometry. The fluorescence value of untreated cells was set as 1 and x-fold change during treatment was calculated. Values represent the mean of 6 independent experiments. Statistics: One way ANOVA; Dunnett's multiple comparisons test (between buffer and immunoglobulin), 95 % confidence interval.

The release of pro-inflammatory IL-8 is reduced after 24 h trimodulin or IVIg treatment, as observed after 4 h (compare Figure 5-6A). Trimodulin elicited a stronger downregulation compared to IVIg. Cell phenotype is slightly modulated by both preparations (see Figure 5-6B). Detection of FcαRI, FcγRIIA and FcγRIII was not affected. FcγRI detection was slightly decreased by trimodulin and increased by IVIg treatment. FcγRIIB detection was significantly upregulated by trimodulin and IVIg. To summarize, immunoglobulin preparations interact on various levels with immune cells. Trimodulin and IVIg facilitate an anti-inflammatory phenotype as shown by reduction of inflammatory cytokines and upregulation of inhibitory FcγRIIB. The central role of inhibitory FcR signaling was clarified by blocking central ITIM and ITAMi phosphatases. Superior immune modulation by trimodulin in comparison to IVIg was shown to be due to the direct binding of cytokines and stronger ITAMi signaling in high doses.

5.3. Immunomodulation in an endotoxin model

In the previous experiments, the immunomodulatory effect of trimodulin and IVIg on resting neutrophil-like cells was shown. Most patients treated with these preparations suffer from systemic inflammation (compare chapter 1.3). Therefore, the immunomodulatory properties in an inflammatory context are of great importance. Bacterial endotoxins are well-known inducers of inflammation in various *in vitro* models. Here, LPS from *Escherichia coli* O111:B4 was used as a pro-inflammatory stimulus for cell activation, because the influence on neutrophils and FcR expression is well studied [43,192].

5.3.1. LPS induce inflammation via TLR-pathways

Before investigating the effects of immunoglobulins on inflammatory cell phenotype, the LPS induced effects themselves were analyzed in detail. Therefore, cells were stimulated with LPS and the induced changes in cytokine release and cell phenotype were measured. LPS induced cytokine release was assessed by semi-quantitative detection, as well as dose- and time-dependent measurements of IL-8. Furthermore, the dependency on TLR-signaling was tested by inhibitor experiments (Figure 5-7). LPS induced modulation of cell phenotype was investigated by monitoring time-dependent FcR and TLR expression on the cell surface (Figure 5-8).

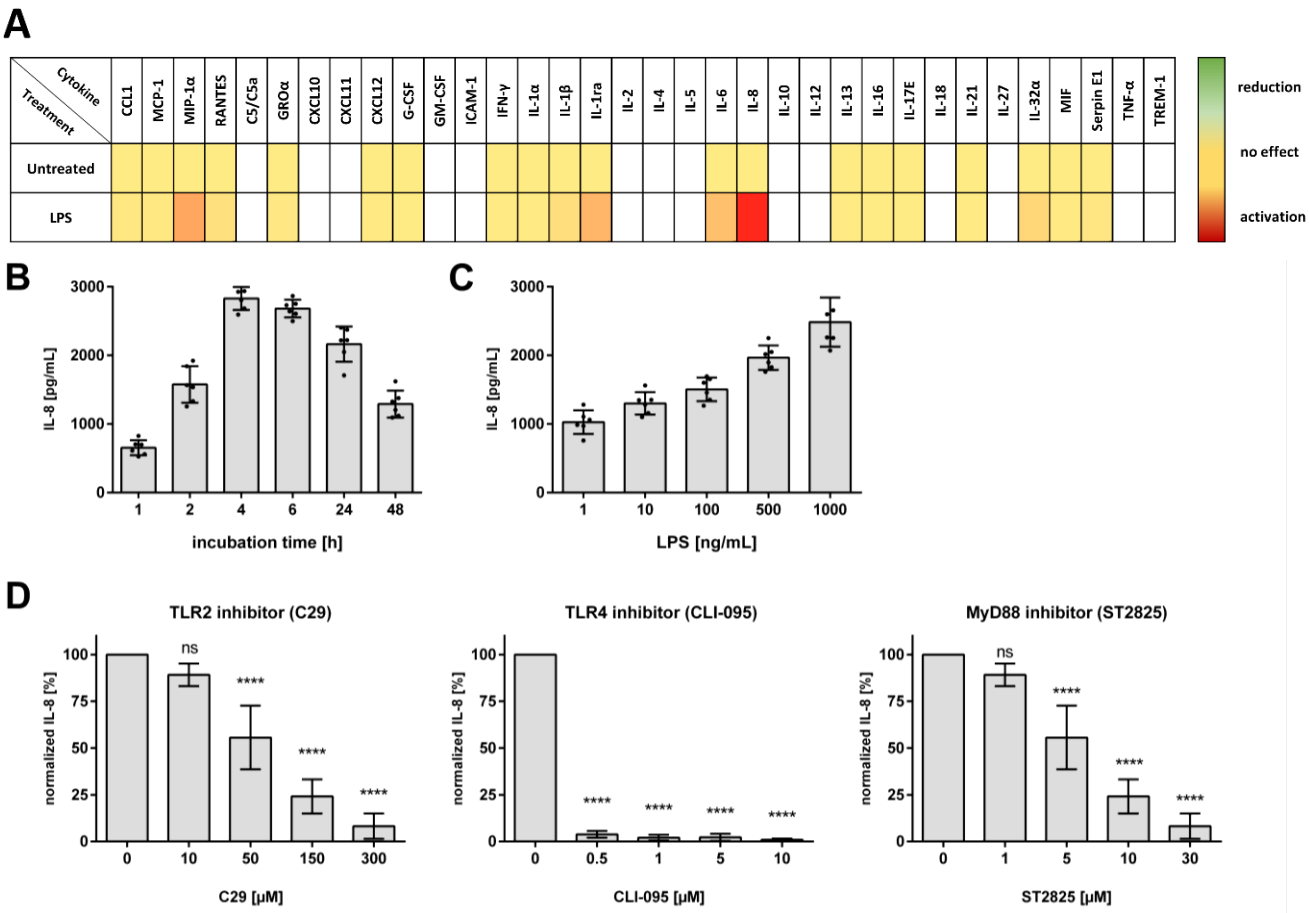

Figure 5-7: Effects induced by lipopolysaccharide (LPS) treatment of neutrophil-like HL-60 cells. **(A)** Cytokine and chemokine secretion induced by treatment with LPS. HL-60 cells were treated for 18 h with 500 ng/mL LPS; cell culture supernatant was semi-quantitative analyzed by cytokine arrays. Data represent the x-fold change in comparison to untreated cells, results represent the mean of 3 independent experiments. **(B)** LPS induces time-dependent IL-8 release. HL-60 cells were treated for indicated times with 500 ng/mL LPS, cells were centrifuged and supernatant analyzed for IL-8 release by ELISA. **(C)** LPS induces dose-dependent IL-8 release. HL-60 cells were stimulated with indicated concentrations of LPS and harvested after 24 h. Cell culture supernatant was analyzed by IL-8 ELISA kit. **(D)** LPS induced cytokine release is dependent on TLR-signaling. HL-60 cells were pre-incubated with indicated concentrations of TLR-2 inhibitor C29, TLR-4 inhibitor CLI-095 or MyD88 inhibitor ST2825 for 30 min. 500 ng/mL LPS was added and IL-8 release was measured after 4 h. IL-8 release of cells treated with buffer and DMSO (= 0 µM) was set as 100 % control and the percentage of remaining IL-8 release was calculated. Data represent mean values of 6 independent experiments. Statistics: Two-way ANOVA; Dunnett's multiple comparisons test, 95 % confidence interval.

Figure 5-7A shows a pattern of cytokines and chemokines released after LPS treatment. Enhanced release of inflammatory cytokines like MIP1-α, IL1-β, IL-6, IL-8 or IL32a was detected. The strongly induced chemokine IL-8 was used exemplary for further investigations. Figure 5-7B and C show dose- and time-dependent IL-8 release after LPS stimulus. Cytokine release peaked after 4-6 h, whereas tested LPS doses increase up to the highest dose. Treatment of cells with TLR inhibitors reveals that LPS induced inflammation is dependent on TLR4, TLR2, as well as signaling protein myeloid differentiation primary response 88 (MyD88) (Figure 5-7D). Inhibition of TLR2 by C29 reduced LPS induced IL-8 release with dosages $>50\,\mu$M. The strongest reduction was observed by blocking TLR4 with CLI-095, a dosage above

0.5 μM reduced IL-8 release completely. The inhibition of MyD88 signaling protein by ST2825 exhibits effects similar to TLR2 inhibitor C29.

Furthermore, LPS induced activation of SYK kinase was investigated (appendix, Figure 8-2). LPS induced significant phosphorylation of SYK at pY348 and pY525/26 in comparison to negative control (buffer).

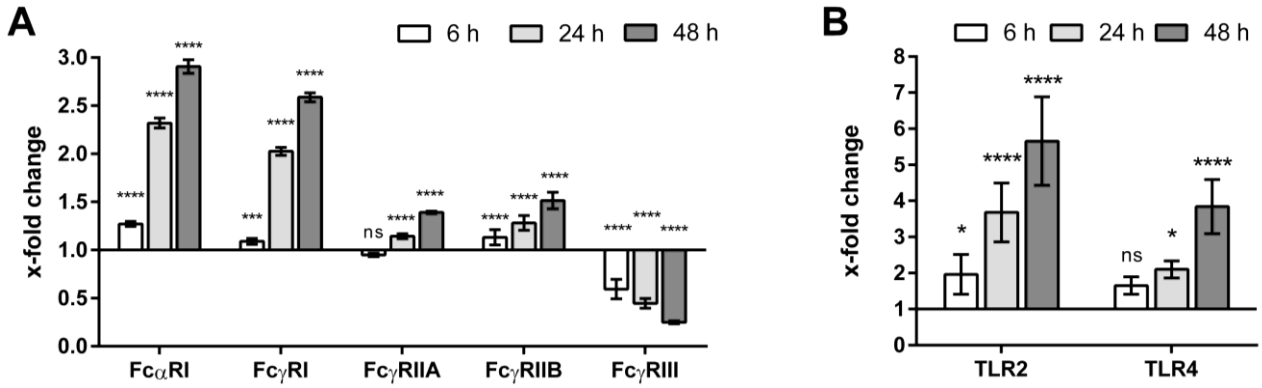

Figure 5-8: LPS modulate Fc-receptor (FcR) and toll-like receptor (TLR) expression. **(A)** FcR expression is modulated by lipopolysaccharide (LPS) treatment. Cells were treated with 500 ng/mL LPS for 6 h (white bars), 24 h (light gray bars) or 48 h (dark gray bars). FcR expression was analyzed with immunological staining using flow cytometry. The fluorescence value of untreated cells was set as 1 and x-fold change during treatment was calculated. **(B)** TLR expression is modulated by LPS treatment. Same as in (A), except TLR modulation was investigated. Data represent mean values of 6 independent experiments. Statistics: Two-way ANOVA; Dunnett's multiple comparisons test, 95 % confidence interval.

Besides cytokine release, LPS also modulated the cellular phenotype. LPS significantly affected FcR expression (Figure 5-8A) and TLR expression (Figure 5-8B). Increased levels of FcαRI (3-fold), FcγRI (2.5-fold), FcγRIIA (1.5-fold), FcγRIIB (1.5-fold) were detected upon LPS treatment. FcγRIII showed contrary effects, here LPS leads to decreased detection (0.5-fold). TLR2 and TLR4 were upregulated (5.5-fold and 4-fold) by LPS treatment. The effects on FcR- and TLR-expression time-dependent increase from 6 h < 24 h < 48 h. The here observed correlation between LPS stimulation and expression of cell surface proteins indicates a connection between cellular signaling pathways.

5.3.2. Immunoglobulins reduce LPS induced inflammation

The effect of immunoglobulin treatment on LPS stimulated neutrophil-like HL-60 cells was analyzed next. To simulate an inflammatory environment cells were stimulated with LPS before the addition of immunoglobulin preparations. With this setup, it is possible to mimic *in vitro* the treatment conditions and the immunomodulatory effects as they are expected in inflammatory patients (e.g. sepsis patients). Immunomodulation was monitored by IL-8 release and modulation of FcR expression (Figure 5-9).

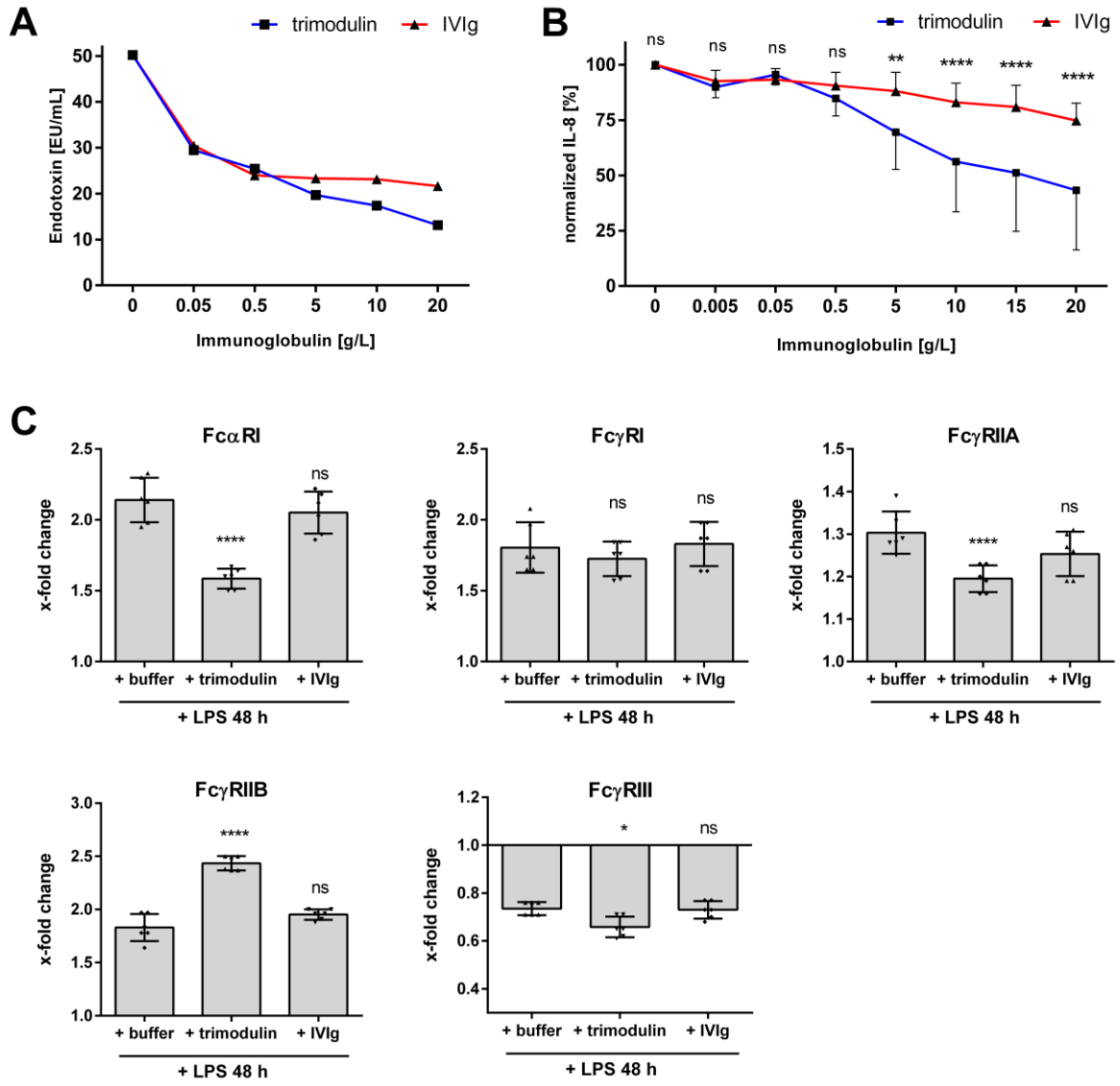

Figure 5-9: LPS induced inflammation is modulated by immunoglobulin preparations. **(A)** Immunoglobulins directly interact with LPS. 50 EU/mL LPS (=7.5 ng/mL LPS) in D-PBS was incubated with indicated concentrations of trimodulin (square, blue line) or IVIg (triangle, red line) for 1 h. The remaining LPS was determined by LAL method, data show the mean of one experiment. **(B)** LPS induced IL-8 release is reduced by the addition of trimodulin and IVIg. HL-60 cells were incubated for 48 h at 37 °C with 500 ng/mL LPS and subsequently, 24 h with indicated concentrations of trimodulin (square, blue line) or IVIg (triangle, red line). Cell culture supernatant was analyzed for IL-8 release by ELISA-kit, cells incubated with buffer were referenced as 100 % control and remaining IL-8 [%] was calculated. **(C)** Modulation of LPS induced FcR expression. Neutrophil-like HL-60 cells were incubated for 48 h with 500 ng/mL LPS and subsequently, 24 h with 15 g/L trimodulin, IVIg or buffer as a negative control. FcR expression was analyzed with immunological staining via flow cytometry. The fluorescence value of LPS treated cells was set as 1 and x-fold change during immunoglobulin treatment was calculated. Values represent the mean of 6 independent experiments. Statistics: One way ANOVA; Dunnett's multiple comparisons test, 95 % confidence interval.

The direct influence of trimodulin and IVIg on LPS was investigated first. Figure 5-9A shows that 20- 30 EU/mL LPS in D-PBS buffer can directly be bound by trimodulin and IVIg. Next, the cytokine release of LPS pre-stimulated cells treated with trimodulin or IVIg was measured (Figure 5-9B). Both preparations reduced IL-8 secretion dose-dependent, whereas trimodulin shows significant stronger down-modulation at high dosages (>5 g/L).
LPS induced phenotype was also affected by immunoglobulin treatment when comparing with buffer treatment as negative control (Figure 5-9C). Trimodulin significantly reduced FcαRI and FcγRIIA detection, whereas IVIg did not. FcγRI was not modulated by both preparations. Inhibitory FcγRIIB detection was significantly increased by trimodulin and not by IVIg. The detection of FcγRIII was slightly reduced by trimodulin, IVIg mediates no significant effect.

In this chapter, the inflammatory activation of neutrophil-like HL-60 cells by LPS treatment was characterized and immunomodulatory properties of trimodulin and IVIg illustrated. It was shown that LPS induced cytokine release and FcR modulation by TLR signaling. The LPS induced phenotype and cytokine release were reduced by both preparations, whereby trimodulin could elicit stronger immune modulation which is probably due to stronger interaction with cellular FcαRI and FcγRIIB.

5.4. Immunomodulation in bacterial inflammation

In the previous experiments, bacterial endotoxin LPS was used to induce inflammation. In the following chapter, the antibody-mediated effector functions come into focus. ADCP is one mechanism for the clearance of pathogens, but also a potent inducer of inflammation [39]. Here a phagocytosis model was established to show (1) the anti-pathogenic activity of immunoglobulin preparations and (2) the modulation of immune complex induced inflammation by high dose trimodulin or IVIg treatment.

5.4.1. Immunoglobulins promote phagocytosis via ITAM-signaling

ADCP was investigated by analyzing opsonization and phagocytosis of heat-inactivated and fluorophore-labeled *S.aureus* by neutrophil-like HL-60 cells. First *S.aureus* was opsonized with different immunoglobulin preparations to generate an immune complex. Phagocytosis and subsequent inflammatory activation of cells by these immune complexes were measured (Figure 5-10).

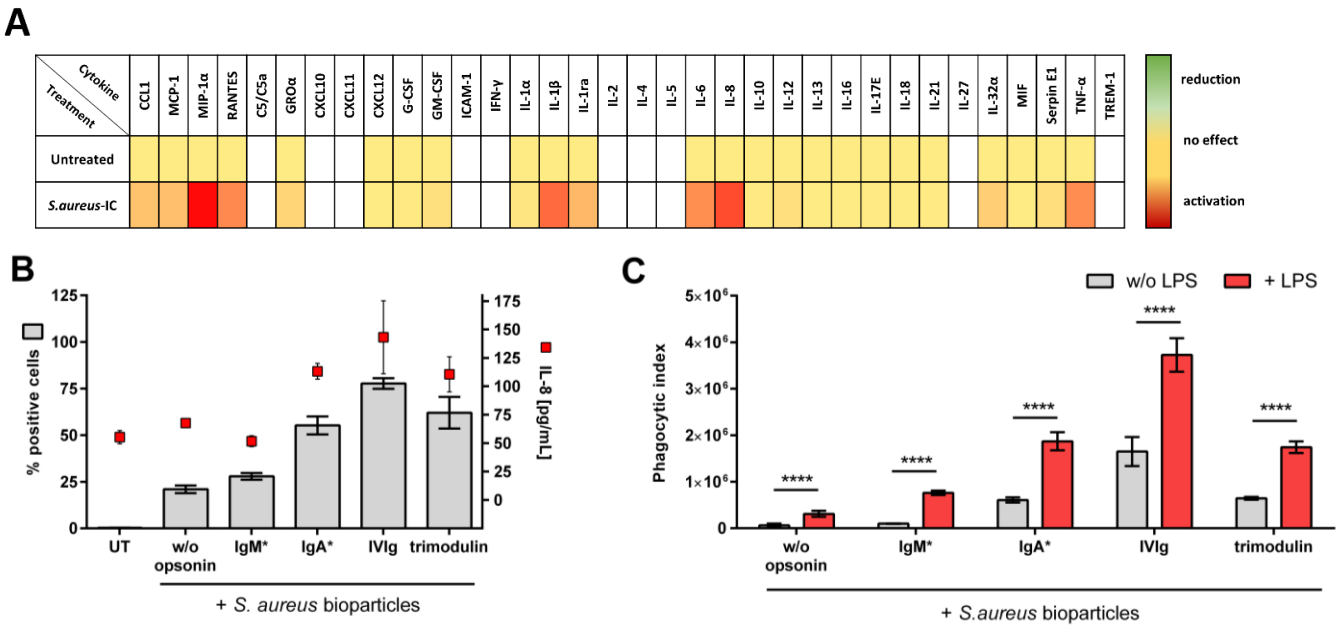

Figure 5-10: Immunoglobulin preparations promote *S.aureus* phagocytosis and inflammatory activation **(A)** Heat map of cytokines secreted by HL-60 cells after stimulation with *S.aureus*-IVIg immune complex (IC). HL-60 cells were stimulated for 18 h at 37 °C with *S.aureus*-IVIg-IC. Semi-quantitative cytokine secretion was measured with human cytokine arrays. Relative signal intensities for every measured cytokine of untreated cells were set as 1 (yellow). The x-fold induction (red) or reduction (green) in comparison to untreated cells was calculated. Not detected cytokines are shown in white. Results represent the mean of 3 independent experiments. **(B)** *S.aureus* AF488 fluorescent bioparticles were opsonized with 50 µg/mL of indicated immunoglobulin preparations or buffer. Immune complex were added to neutrophil-like HL-60 cells for 1 h. Phagocytosis (gray bars) was measured as a percentage of AF488 positive cells. Cell culture supernatant was analyzed for IL-8 release (red dots). *Purified IgA and IgM from human serum (Sigma-Aldrich) were used for opsonization. **(C)** LPS pre-stimulation leads to increased phagocytosis. Same as in (B), not stimulated cells (gray bars) were compared with cells pre-stimulated for 24 h with 500 ng/mL LPS (red bars) before phagocytosis assay. Phagocytosis is shown as a phagocytic index (percentage positive cells multiplied with median fluorescence intensity). Values show the mean of 6 independent experiments. Statistics: Two-way ANOVA; Tukey's multiple comparisons test.

The inflammatory activation of neutrophil-like cells by immune complex was elucidated by a semi-quantitative comparison of cytokine and chemokine secretion (Figure 5-10A). Increased levels of pro-inflammatory cytokines like MCP-1, MIP-1α, RANTES, IL-1β, IL-6, IL-8, IL32a and TNFα were observed in comparison to untreated cells.

As shown in Figure 5-10B, the opsonization of *S.aureus* with most immunoglobulin preparations enhance phagocytosis and IL-8 release. Solely opsonization with purified IgM preparation did not affect phagocytosis compared to *S.aureus* without opsonin. Purified monomeric IgA, IgG (IVIg) and IgM, IgA, IgG containing trimodulin enhance phagocytosis and inflammation (IgA = trimodulin < IVIg).

LPS leads to an inflammatory cell phenotype with increased FcR expression (compare Figure 5-8A). To prove if LPS and increased FcR levels enhance the observed phagocytosis, HL-60 cells were stimulated with LPS 24 h before phagocytosis. LPS stimulated cells exhibit significantly enhanced phagocytic activity of all tested immune complex (Figure 5-10C).

To get a more detailed view on immune complex-mediated inflammation the role of ITAM signaling was tested by inhibiting SYK kinase. Phagocytosis and corresponding IL-8 release of trimodulin- and IVIg-IC was measured in presence of different concentrations of SYK inhibitor Piceatannol (Figure 5-11).

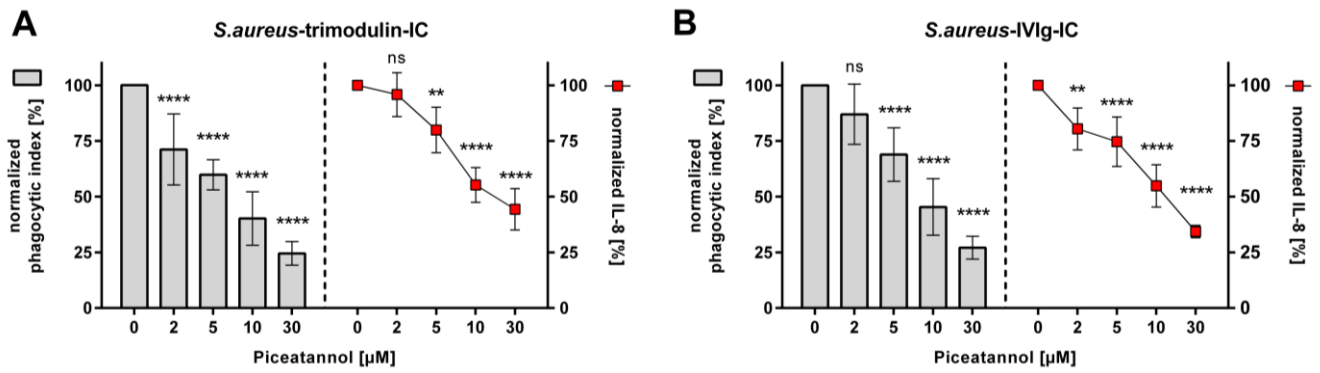

Figure 5-11: ITAM signaling via SYK kinase is induced by immune complex phagocytosis. **(A)** Cells were treated with *S.aureus*-trimodulin-IC or **(B)** *S.aureus*-IVIg-IC. Before immune complex addition cells were pre-incubated for 30 min with indicated concentrations of SYK inhibitor Piceatannol. DMSO-treated cells were normalized as 100 % control and remaining phagocytosis (gray bars) and IL-8 release (red dots) was calculated for inhibitor-treated cells. Values show the mean of 6 independent experiments. Statistics: Two-way ANOVA; Tukey's multiple comparisons test.

As seen in Figure 5-11, phagocytosis and IL-8 secretion decreased dose-dependently, proving SYK and hence ITAM mediated mechanism. Further, the activation of SYK by specific phosphorylation was shown (Appendix Figure 8-3).

5.4.2. Phagocytosis of *S.aureus* is mediated via FcαRI and FcγR

Trimodulin is a complex mixture of monomeric and multimeric IgA-, IgM- and IgG-species; making it challenging to unravel which component is relevant for distinct modes of action. The role of IgA, IgM and IgG of trimodulin in *S.aureus* phagocytosis was investigated by detecting each immunoglobulin class on the surface of *S.aureus* particles, as well as by blocking FcαRI and FcγR (Figure 5-12).

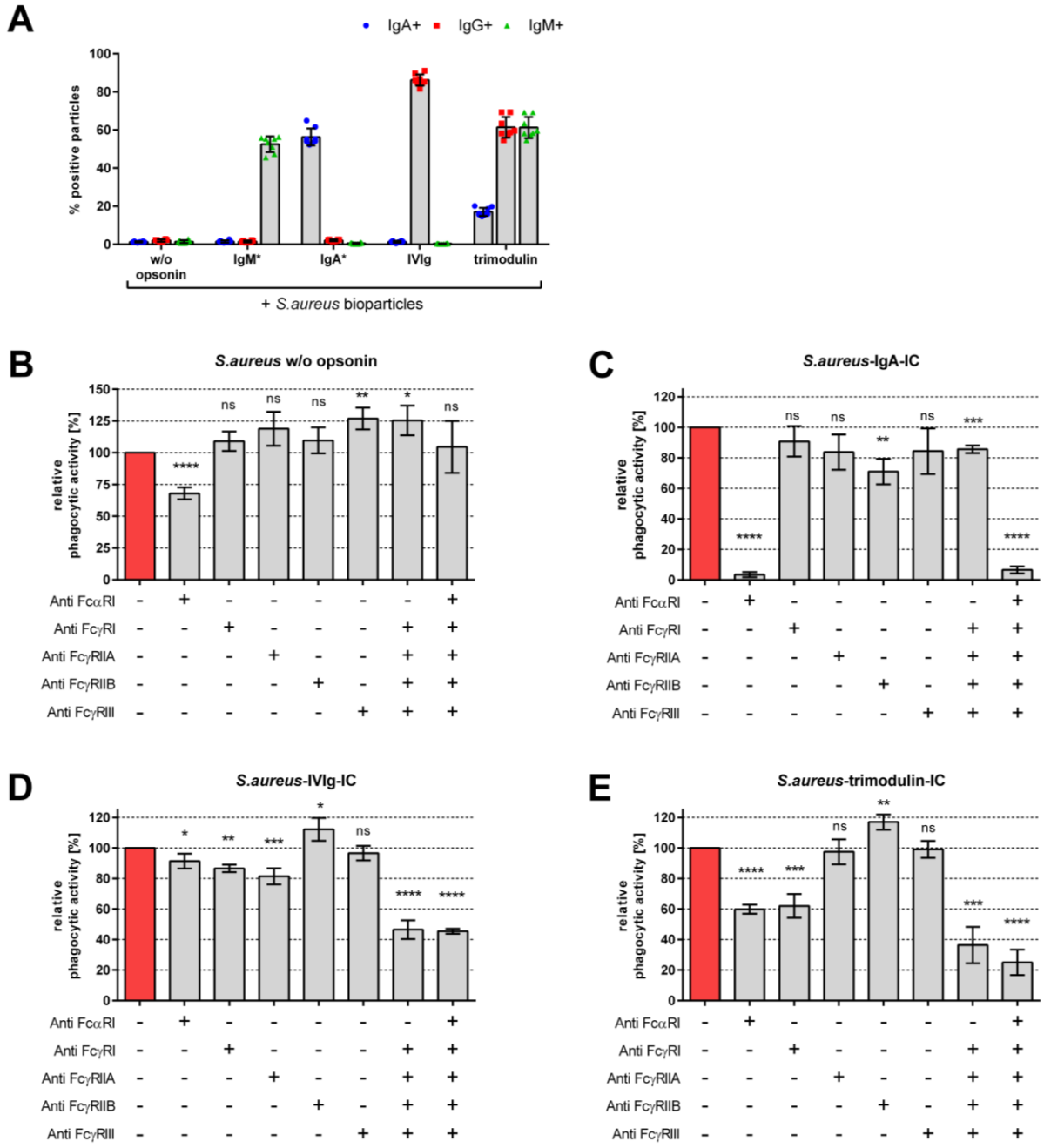

Figure 5-12: IgG and IgA promote phagocytosis of *S.aureus* via FcγR and FcαRI. **(A)** IgA, IgG and IgM bind on the surface of *S.aureus* particles. *S.aureus* bioparticles were opsonized with indicated immunoglobulin preparations for 30 min. After washing steps IgG, IgA and IgM were detected with specific detection antibodies by flow cytometry. Percentage of IgA (blue dots), IgG (red square) or IgM (green triangle) positive *S.aureus* particles is shown. *Purified IgA- and IgM- from human serum (Sigma-Aldrich). **(B)** FcR blocking experiments with *S.aureus* particles. Neutrophil-like HL-60 cells were pre-incubated with 5 µg/mL of indicated blocking antibodies 20 min before the addition of *S.aureus*. Phagocytic index (percentage positive cells multiplied with

median fluorescence intensity) of not blocked cells were referred to as 100 % phagocytic activity and the remaining phagocytic activity is shown. **(C-E)** FcR blocking experiments with *S.aureus*-IgA-IC (C), *S.aureus*-IVIg-IC (D) and *S.aureus*-trimodulin-IC (E). *S.aureus* particles were opsonized with indicated immunoglobulins and FcR blocking was performed as described in (B). Data show a mean of 6 independent experiments. Statistics: One way ANOVA; Dunnett's multiple comparisons test.

IgA, IgM and IgG opsonize *S.aureus* particles as seen by detecting these antibody species on the immune complex (Figure 5-12A). IgM- and IgA-control opsonized *S.aureus* were 50 % positive for respective antibodies. IgG opsonized particles were <80 % positive for IgG. 60 % of trimodulin opsonized *S.aureus* particles were positive for IgM and IgG, whereas ~20 % were IgA positive.

FcR blocking reveals which immunoglobulin species and FcR are functionally relevant for phagocytosis (Figure 5-12B-E). FcRs were blocked by pre-incubation with specific antibody clones impeding the binding of immunoglobulins to FcαRI (clone MIP8α), FcγRI (clone 10.1), FcγRIIA (IV.3), FcγRIIB (clone 2B6) and FcγRIII (clone 3G8). As seen in Figure 5-12B phagocytosis of not opsonized *S.aureus* is reduced by blocking FcαRI. IgA-IC phagocytosis is strongly reduced by blocking FcαRI (Figure 5-12C), whereas IVIg-IC phagocytosis (Figure 5-12D) is significantly reduced by blocking FcγRI, FcγRIIA, slightly FcαRI and combinations of those. Similar trimodulin-IC phagocytosis (Figure 5-12E) is strongly reduced by blocking FcαRI, FcγRI and combinations of those. In comparison phagocytosis of IVIg- and trimodulin-IC is enhanced by blocking FcγRIIB.

5.4.3. Immunoglobulins mediate dual function via ITAMi

Dose-dependent modes of action were reported in IVIg therapy: anti-pathogenic effects were rather observed in low doses, whereas immunomodulatory activities became prevalent in high doses [63]. To investigate these dose-dependent effects in the HL-60 neutrophil-like cell model different concentrations of trimodulin and IVIg, ranging between 0.05 - 20 g/L, were used to opsonize *S.aureus* (Figure 5-13). Phagocytic index and IL-8 release were monitored as effector outcomes.

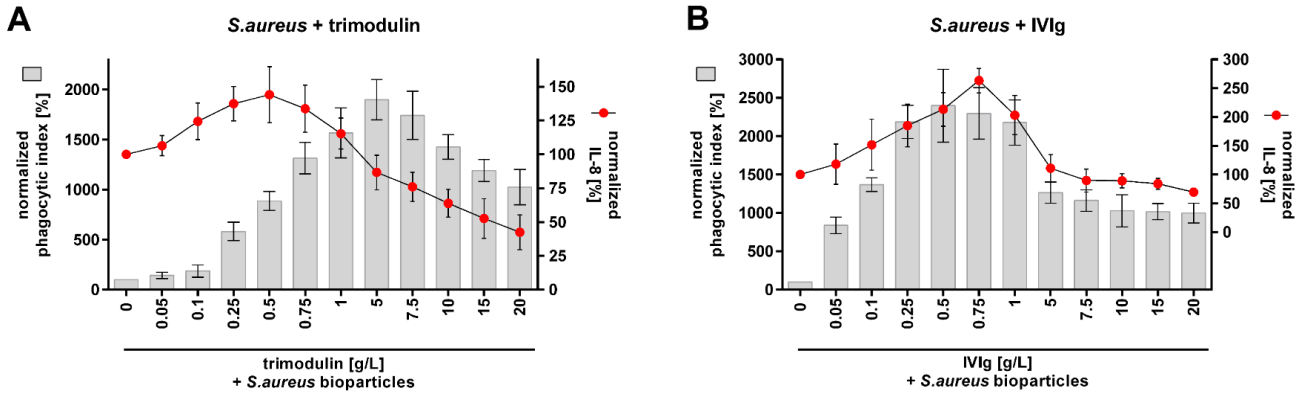

Figure 5-13: Low doses of trimodulin or IVIg promote phagocytosis, high doses mediate immunomodulation **(A)** Dual function of trimodulin on *S.aureus* phagocytosis. Neutrophil-like HL-60 cells were incubated for 1 h with *S.aureus* bioparticles and indicated concentrations of trimodulin. Phagocytosis (gray bars) and corresponding IL-8 release (red dots) is shown. **(B)** Dual function of IVIg on *S.aureus* phagocytosis. Cells were treated as described in (A) with *S.aureus* and IVIg. Values represent the mean of 6 independent experiments.

As expected, dose-dependent effects of trimodulin (Figure 5-13A) and IVIg (Figure 5-13B) on *S.aureus* phagocytosis were observed. Lower doses (up to 5 g/L) trimodulin enhance phagocytosis (up to 0.5 g/L enhance IL-8 release), whereas higher doses (>5 g/L) reduce phagocytosis and IL-8 release. Similar effects were observed for IVIg mediated phagocytosis; divergent phagocytosis and IL-8 release peak at lower dose IVIg (0.75 g/L). To demonstrate the influence of inhibitory ITAMi signaling on the immune modulation, SHP-1 was inhibited and SHP-1 phosphorylation was measured (Figure 5-14).

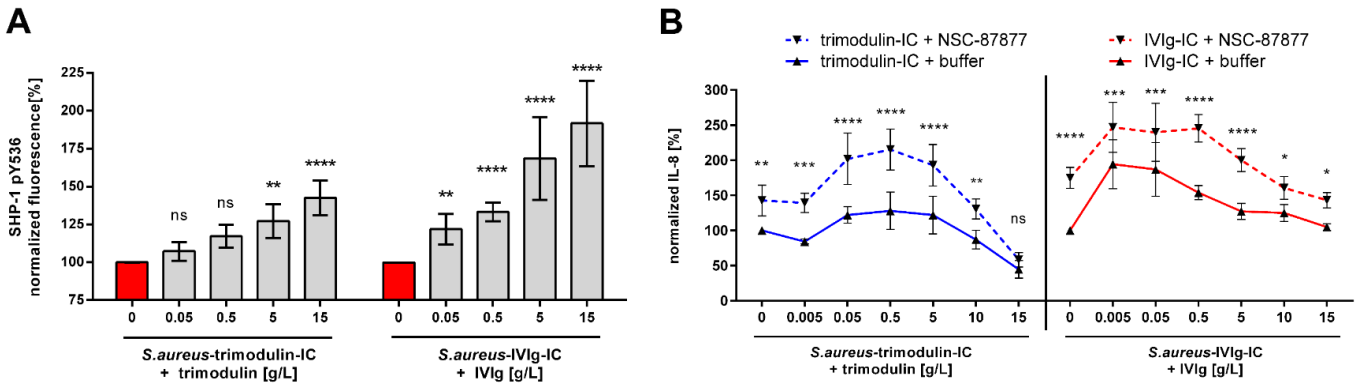

Figure 5-14: Inhibitory ITAMi signaling is activated by high doses immunoglobulins for phagocytosis **(A)** High doses trimodulin or IVIg induce ITAMi signaling. Phosphorylation of SHP-1 at tyrosine 536 (pY536). Cells were treated for 1 h with *S.aureus*-IC and indicated trimodulin or IVIg concentrations for 90 min. Cells were fixed, permeabilized and stained with an anti-phospho-SHP-1 pY536 antibody. The fluorescence signal was measured by flow cytometry and normalized to buffer control. **(B)** Blocking of SHP-1 phosphatase reduces immunomodulatory effects. Cells were treated as in (A), but additional pre-incubation with 200 µM SHP-1 inhibitor NSC-87877 for 30 min. IL-8 release was normalized and compared between NSC-87877 (dotted lines) or buffer treatment (solid lines). Incubation of cells with trimodulin (blue lines) or IVIg (red lines) is shown with or without SHP-1 inhibitor. Values represent mean of 6 independent experiments. Statistics: Two-way ANOVA; Tukey's multiple comparisons test.

The addition of high doses of trimodulin (>5 g/L) and lower doses IVIg (>0.05 g/L) to *S.aureus* immune complex significantly induce phosphorylation of SHP-1. IVIg induces stronger phosphorylation than trimodulin. In addition, inhibition of central ITAMi phosphatase SHP-1 showed the influence of ITAMi on immune modulation. Inhibition of SHP-1 led to a significantly increased cytokine release by both preparations, which implies the immunomodulation via ITAMi signaling.

To summarize, IgA- and IgG-containing immunoglobulin preparations promote phagocytosis of *S.aureus* in this experimental setup. IgM, IgA and IgG of trimodulin bound on the surface of *S.aureus* particles whereas IgA and IgG species are functionally relevant for phagocytosis. Immune complex bind FcαRI, as well as FcγR and induce inflammation via ITAM signaling. Therefore, a mode of action of IgA in trimodulin was shown. Besides the anti-pathogenic activity, leading to ADCP, especially in high doses immunomodulatory effects of trimodulin and IVIg were observed. This leads to the conclusion of a dose-dependent dual function in the context of bacterial inflammation.

5.5. Immunomodulation in a COVID-19 model

Previous experiments showed the immunomodulatory capacity of trimodulin and IVIg on resting neutrophils and in the context of bacterial inflammation.
In contrast to bacterial-induced severe infection diseases like sepsis or sCAP, viral-induced infection diseases were of minor importance until SARS-CoV-2 emerged and COVID-19 became a global threat.
Anti-viral activity of IVIg against common viruses is reported [63,64]. However, there are yet no specific antibodies against SARS-CoV-2 in commercially available immunoglobulin preparations (*in house data* and [154]). Therefore, treatment of severe COVID-19 induced inflammation and dysregulated host immune response is of great importance [61,193,194]. To test the immunomodulatory effects of immunoglobulin preparations in the context of COVID-19, inflammation was triggered by SARS-CoV-2-like immune complex.

5.5.1. Establishment of SARS-CoV-2-like immune complex

Establishing a COVID-19 inflammation model requires a solution that is both simple and workable under standard laboratory conditions as a feasible alternative to the native SARS-CoV-2 virus. As a basis for SARS-CoV-2-like immune complex fluorescent latex beads were used. Beads were coated with recombinant SARS-CoV-2 spike protein to generate SARS-CoV-2-like particles. Immune complex generation was performed by adding SARS-CoV-2 spike protein-specific IgG, IgA and IgM antibodies from convalescent COVID-19 source plasma (Figure 5-15A). As a positive control, an anti-SARS-CoV-2-spike-protein specific antibody (recombinant, humanized IgG) was used.

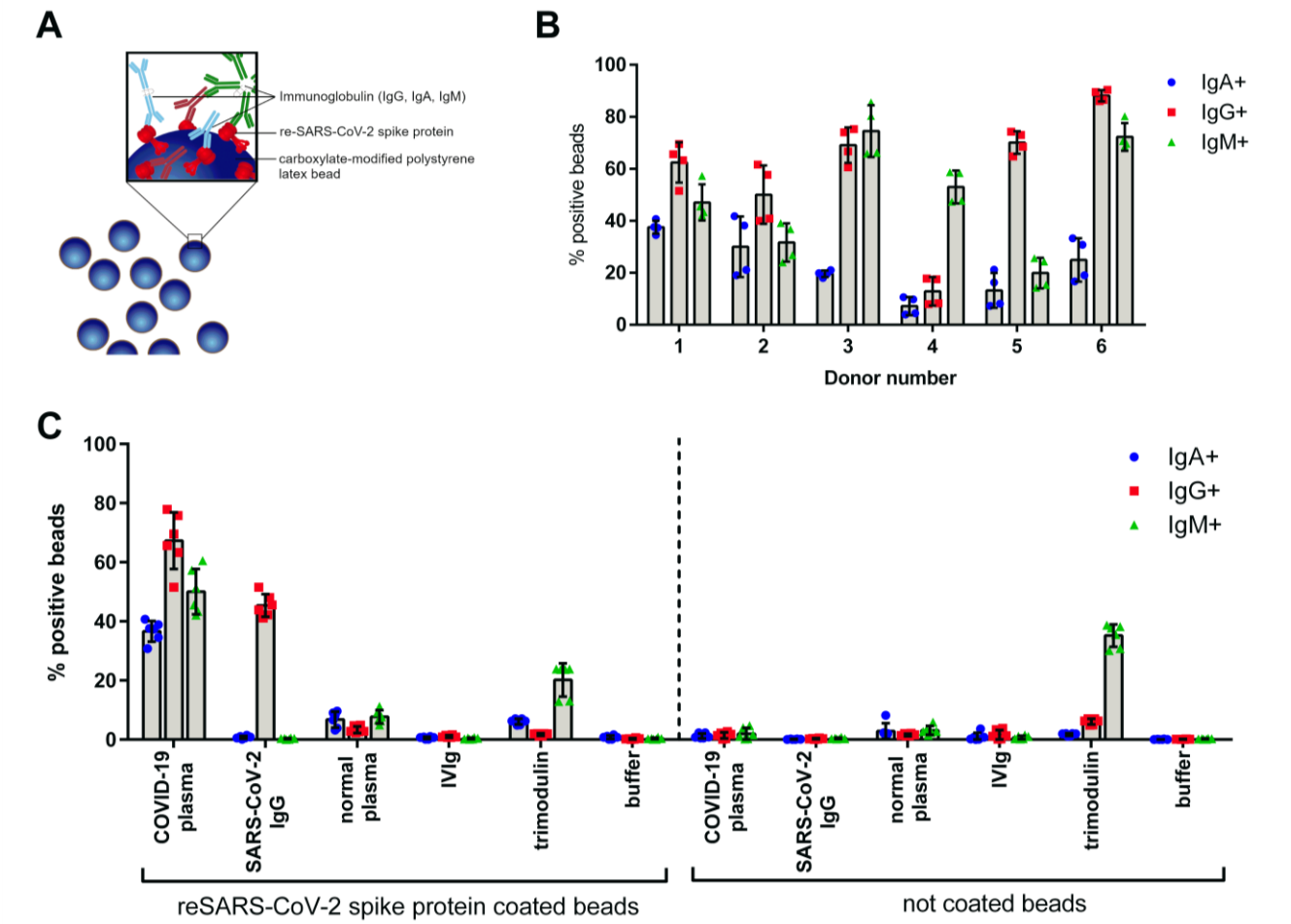

Figure 5-15: Characterization of SARS-CoV-2-like particles **(A)** schematic overview of fluorescent latex beads coated with recombinant (re-) SARS-CoV-2 spike protein, specific immunoglobulins of IgG (red), IgA (blue) and IgM (green) class bound to the spike protein is shown. **(B)** IgG, IgA and IgM bound on the surface of SARS-CoV-2-like latex beads opsonized with different convalescent COVID-19 plasma donations (donor number 1-6). Coated beads were incubated with indicated donors for 45 min at 37 °C. After washing, beads were stained with anti-IgG, anti-IgA and anti-IgM detection antibodies and analyzed by flow cytometry. Percentage of positive beads for IgG (red square), IgA (blue dots) and IgM (green triangle) are shown, data represent the mean of 4 independent experiments. **(C)** Control experiments show specific binding of anti-SARS-CoV-2 antibodies to spike protein. Coated or non-coated beads were incubated with indicated plasma, immunoglobulins, or buffer for 45 min at 37 °C and were stained as described in (B). Data represent the mean of 6 independent experiments.

Plasma from six convalescent donors was characterized for binding of IgG, IgA and IgM to the bead surface (Figure 5-15B). The data indicate that all used COVID-19 plasma donations have IgG, IgA and IgM antibodies against the SARS-CoV-2 spike protein. The levels of IgG, IgA and IgM antibodies vary between the donors.

To exclude non-specific antibody binding to the beads, control experiments were performed. As depicted in Figure 5-15C, neither IgG, IgA nor IgM were detected on SARS-CoV-2 spike protein-coated beads by addition of normal plasma, IVIg or buffer. Trimodulin opsonized beads exhibit small percentage IgM (~20 %) positive beads. Beads incubated with recombinant anti-SARS-CoV-2 IgG positive control showed 45 % IgG positive beads, however, no IgA or IgM. Supporting the data from coated beads, no

antibodies were found on uncoated (but blocked) latex beads. An exception is the unspecific binding of the trimodulin IgM component. For further experiments plasma donation 1 was used (hereafter named COVID-19 plasma), as this donation was available at a sufficient amount and exhibits an equal binding of IgG, IgA and IgM antibodies on the SARS-CoV-2 spike protein-coated beads.

5.5.2. COVID-19-like inflammation via IgG and IgA

For induction of COVID-19-like inflammation, the manufactured immune complex had to be phagocytosed by neutrophil-like HL-60 cells. Based on the bead characterization data (Figure 5-15) and *S.aureus* phagocytosis experiments (chapter 5.4.2) antibody-FcR-dependent phagocytosis of SARS-CoV-2-like immune complex and release of several pro-inflammatory cytokines and chemokines was expected. Phagocytosis was measured by uptake of fluorescent beads while cellular inflammation was detected by cytokine and chemokine release into cell culture supernatant (Figure 5-16).

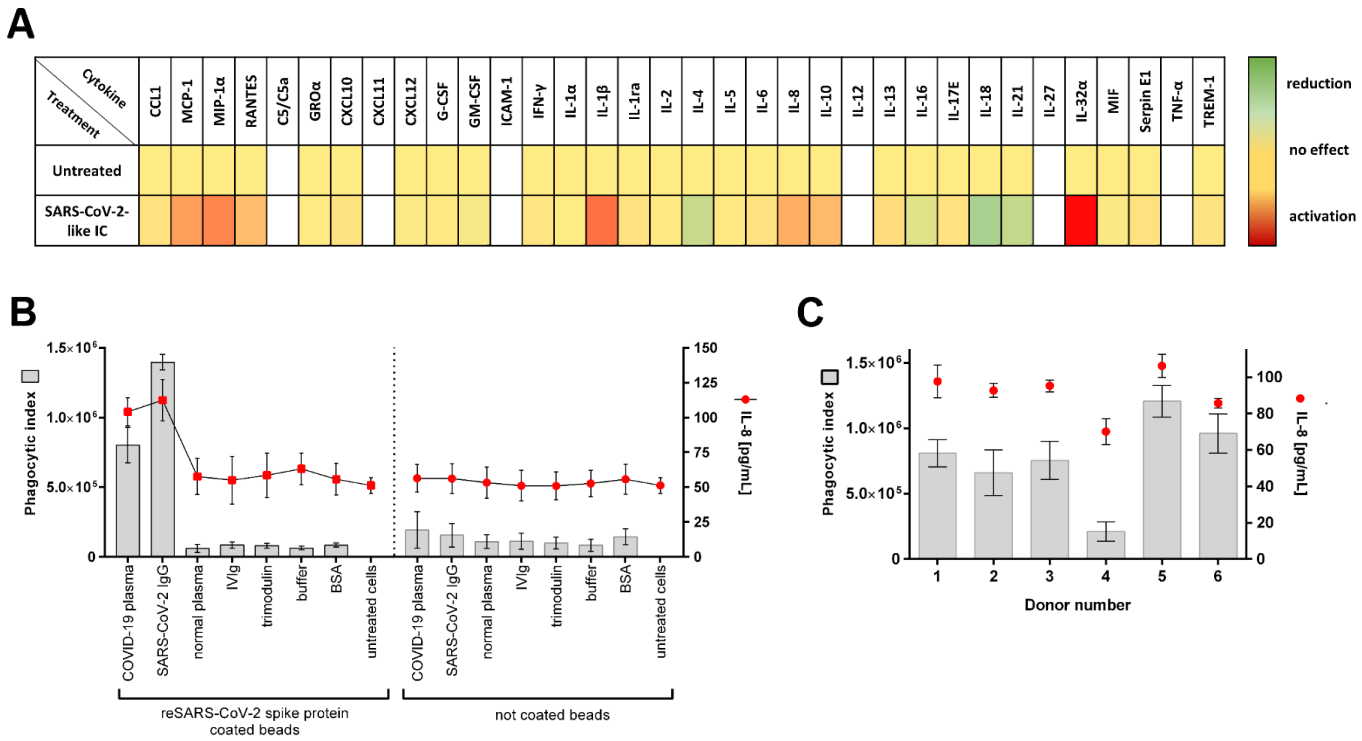

Figure 5-16: Establishment of COVID-19 like inflammation model **(A)** Heat map of chemokines and cytokines secreted by neutrophil-like HL-60 cells after stimulation with anti-SARS-CoV-2 IgG-IC. HL-60 cells were stimulated for 18 h at 37 °C with SARS-CoV-2-IgG immune complex. Semi-quantitative cytokine secretion was measured using human cytokine arrays. Relative signal intensities for every measured cytokine of untreated cells were set as 1 (yellow). The x-fold induction (red) or reduction (green) in comparison to untreated cells was calculated. Not detected cytokines are shown in white. Results represent the mean of 3 independent experiments. **(B)** Evaluation of COVID-19-like inflammation model. Cells were incubated for 1 h with SARS-CoV-2 spike protein-coated or not coated beads opsonized with different immunoglobulins, BSA or D-PBS controls. Phagocytic index (gray bars, left y-axis) for bead uptake and corresponding IL-8 release (red dots, right y-axis) in the cell culture supernatant was measured. Data represent the mean of 8 independent experiments. **(C)** Analysis of phagocytic activity and IL-8 release with different COVID-19 convalescent plasma donors (experimental procedure as in (B)).

First, it was tested if the SARS-CoV-2-like immune complex can induce inflammation similar to severe COVID-19. The pattern of secreted cytokines and chemokines was semi-quantitative assessed using cytokine arrays. SARS-CoV-2-IgG immune complex stimulated cell supernatant was tested. The results demonstrate the induction of multiple pro-inflammatory cytokines (Figure 5-16A). For the establishment of the experimental system, the quantitative detection of IL-8 was focused, a key player in COVID-19 and neutrophil activation [6,100,135,195].

For characterization of our COVID-19 model, phagocytosis and IL-8 release were measured by treating neutrophil-like HL-60 cells with different immune complexes (Figure 5-16B). The data show, that phagocytosis and IL-8 release are induced by the immune complex of SARS-CoV-2 spike protein-coated beads with specific antibodies against mentioned spike protein. In negative controls, the cells display only a very low bead uptake whereas IL-8 release is not affected. In accordance with the immune complex characterization data (Figure 5-15C), cellular inflammation shows no activation with other immunoglobulins. Immunoglobulin independent bead uptake was minimal because neutrophil-like HL-60 cells and primary neutrophils show low expression of ACE-II receptor (Appendix Figure 8-5).

Next, the previously characterized COVID-19 plasma donations (compare Figure 5-15B) were tested. Phagocytosis of SARS-CoV-2-like immune complex opsonized with plasma from different COVID-19 donors results in varying activation of the cell system (Donor 4 < Donor 1-3 < Donor 6 < Donor 5) (Figure 5-16C). Importantly, phagocytic activity and IL-8 release correlate with each other. Higher levels of immune complex uptake also induce higher levels of IL-8 release.

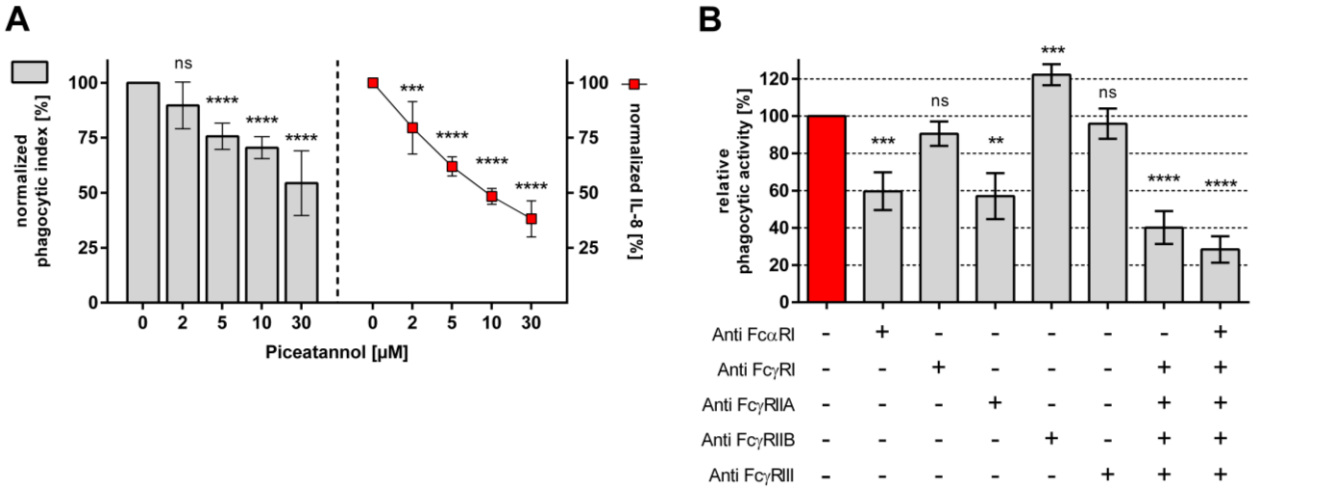

Figure 5-17: Phagocytosis of SARS-CoV-2-like immune complex via FcαRI- and FcγRIIA-ITAM signaling. **(A)** SYK kinase induces SARS-CoV-2-like immune complex phagocytosis. HL-60 cells were treated with indicated concentrations of SYK inhibitor Piceatannol 30 min before the addition of immune complex. Phagocytosis (gray bars) and corresponding IL-8 release (red dots) were measured. DMSO negative control was normalized to 100 % and remaining phagocytosis and IL-8 release was calculated for inhibitor-treated cells. Values show the mean of 6 independent experiments. Statistics: Two-way ANOVA; Tukey's multiple comparisons test. **(B)** FcR blocking experiments with COVID-19 plasma opsonized SARS-CoV-2-like particles. Cells were pre-incubated with 5 µg/mL of indicated blocking antibodies or combinations of those, 20 min before addition of immune complex. The phagocytic index of not blocked cells was referred to as 100 % phagocytic activity and the remaining phagocytic activity is shown as the mean of 6 independent experiments. Statistics: One way ANOVA; Dunnett's multiple comparisons test.

Activation of ITAM signaling by immune complex phagocytosis was tested by inhibition of SYK kinase. Figure 5-17A shows SYK inhibitor Piceatannol-dependent decrease of phagocytosis and corresponding IL-8 release, indicating activation of ITAM by SARS-CoV-2-like immune complex.

To directly show which immunoglobulin classes are functionally relevant for immune complex uptake, phagocytosis after pre-incubation with FcR blocking antibodies was investigated (Figure 5-17B). SARS-CoV-2 like particles opsonized with COVID-19 plasma immunoglobulin IgG, IgA and IgM (compare Figure 5-15B/C) exhibited significantly decreased particle uptake when FcαRI, FcγRIIA and combinations of those were blocked. Blocking of FcγRI and FcγRIII did not affect particle phagocytosis. In comparison to blocking of activating FcR, blocking of inhibitory FcγRIIB increases phagocytosis of COVID-19 plasma opsonized particles significantly (Figure 5-17B). Although IgM binding and opsonization of SARS-CoV-2 like particles was detectable (Figure 5-15B), no IgM FcμR was detectable on HL-60 cells (Figure 5-1B) suggesting no participation in bead phagocytosis.

5.5.3. Trimodulin as potent immune modulator in COVID-19

In patients with severe COVID-19, modulation of the hyper-inflammatory immune response is a major goal of therapy [132]. IVIg preparations are a fast available therapeutic option in the treatment of these severely ill patients [66]. The functions of IgA in immunotherapy and especially in IgM- and IgA- enriched immunoglobulin preparations are in comparison to IgG less studied [87]. Therefore, immune modulation in the COVID-19 cell model was investigated by the addition of various concentrations of trimodulin or IVIg. Used lots were tested negative for anti-SARS-CoV-2 neutralizing antibodies. Concerning the characterization data (compare Figure 5-16A) phagocytosis of beads, IL-1ra, IL-10, MCP-1, MIP1α and IL-8 release were measured as marker of inflammation (Figure 5-18).

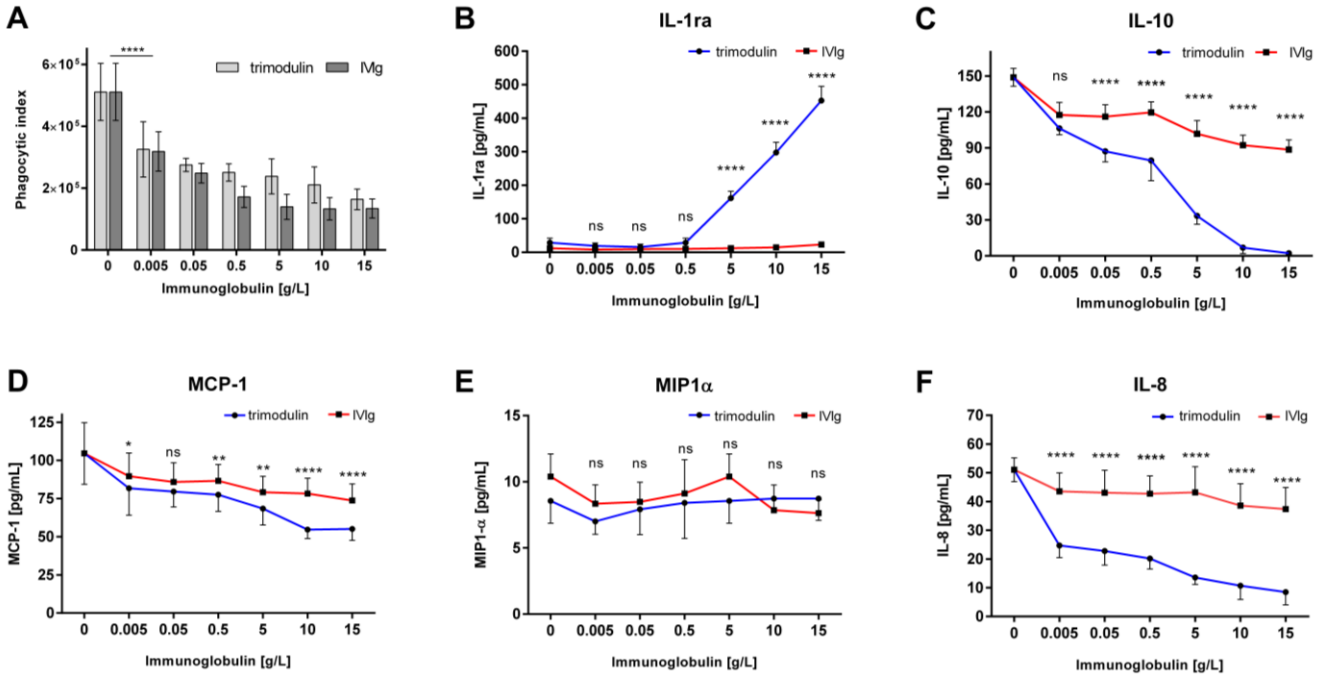

Figure 5-18: Immune modulation in COVID-19-like model by trimodulin and IVIg preparation. **(A)** HL-60 cells were incubated for 1 h with SARS-CoV-2 spike protein-coated beads opsonized with COVID-19 plasma. Trimodulin or IVIg was added in the indicated concentrations to the cell immune complex mixture. Phagocytosis of the SARS-CoV-2-like immune complex was measured with trimodulin (light gray bars) or IVIg (dark gray bars) addition. **(B-F)** Same experimental setup as in (A) instead phagocytosis cytokine release into the cell culture supernatant was measured with trimodulin (dots, blue line) or IVIg (square, red line) addition. IL-1ra (B), IL-10 (C), MCP-1 (D), MIP-1α (E) and IL-8 (F) were measured. Values represent the mean of 6 independent experiments. Statistics: Two-way ANOVA; Tukey's multiple comparisons test.

The addition of IVIg or trimodulin to HL-60 cells significantly and equally decreased bead uptake of SARS-CoV-2-like particles opsonized with COVID-19 plasma (Figure 5-18A). The corresponding cytokine release is also affected: IL-1ra is strongly induced by trimodulin and not by IVIg addition (Figure 5-18B), IL-10, MCP-1 and IL-8 level are reduced by IVIg and significantly more by trimodulin addition (Figure 5-18C/D/F). MIP-1α secretion is low and not affected by both preparations (figure 5-12E). The observed effects were dose-dependent.

The immunomodulatory effects of immunoglobulin preparations are complex and several modes of action work synergistically [62,174]. The dependency on inhibitory ITAMi signaling was tested to gain a better understanding of the molecular mechanism of immune modulation. The mechanism of ITAMi dependent immune modulation was initially explored for IgA-FcαRI interaction [174,177] and is a known mode of action for classical IVIg [94,176]. The importance of ITAMi for trimodulin- and IVIg-induced immunomodulation was shown on resting (chapter 5.2.2) and *S.aureus* immune complex activated neutrophil-like HL-60 cells (chapter 5.4.3). The importance of ITAMi in the COVID-19 model was investigated next (Figure 5-19).

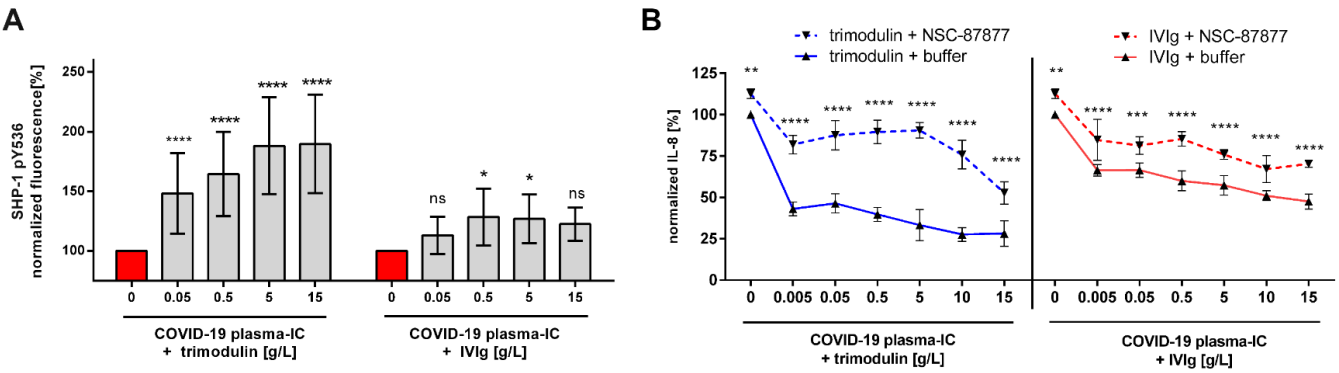

Figure 5-19: Stronger immune modulation by trimodulin due to more potent ITAMi signaling. **(A)** Phosphorylation of SHP-1 at tyrosine 536 (pY536). Cells were treated for 1 h with COVID-19 plasma-IC and indicated trimodulin or IVIg concentrations for 90 min. Cells were fixed, permeabilized and stained with anti-phospho SHP-1 pY536 antibody. The fluorescence signal was measured by flow cytometry and normalized to buffer treated cells. **(B)** Blocking of SHP-1 phosphatase reduces immune-modulatory effects. Cells were treated as in (A), but additional pre-incubation with 200 µM SHP-1 inhibitor NSC-87877. IL-8 release was normalized and, afterwards, IL-8 release was compared between NSC-87877 (dotted lines) and buffer treatment (solid lines). Incubation of cells with trimodulin (blue lines) or IVIg (red lines) is shown with or without SHP-1 inhibitor. Values represent the mean of 6 independent experiments. Statistics: Two-way ANOVA; Tukey's multiple comparisons test.

To directly demonstrate ITAMi activation due to trimodulin or IVIg addition phosphorylation level of SHP-1 was measured. As seen in Figure 5-19A trimodulin induces significantly stronger phosphorylation of SHP-1 than IVIg. Further, inhibition of SHP-1 phosphatase reduced significantly the strong immunomodulatory effects of trimodulin, which were observed on IL-8 release. Similar effects but to a lower extend were seen by IVIg addition (Figure 5-19B).

5.5.4. Transfer to primary neutrophils

In this work, the HL-60 cell line was differentiated to a neutrophil-like phenotype and used for investigations regarding immunomodulation. Although cell line and primary cells were compared based on cell surface markers (compare chapter 5.1) differences in complex cellular effector outcomes, like phagocytosis, could be possible. Therefore, exemplary for the here used test systems, the COVID-19-like model was transferred to fresh isolated primary human neutrophils. The experimental setup had to be slightly adapted concerning centrifugation speed and incubation times.

Figure 5-20 shows assay characterization results and immunomodulatory effects by trimodulin and IVIg.

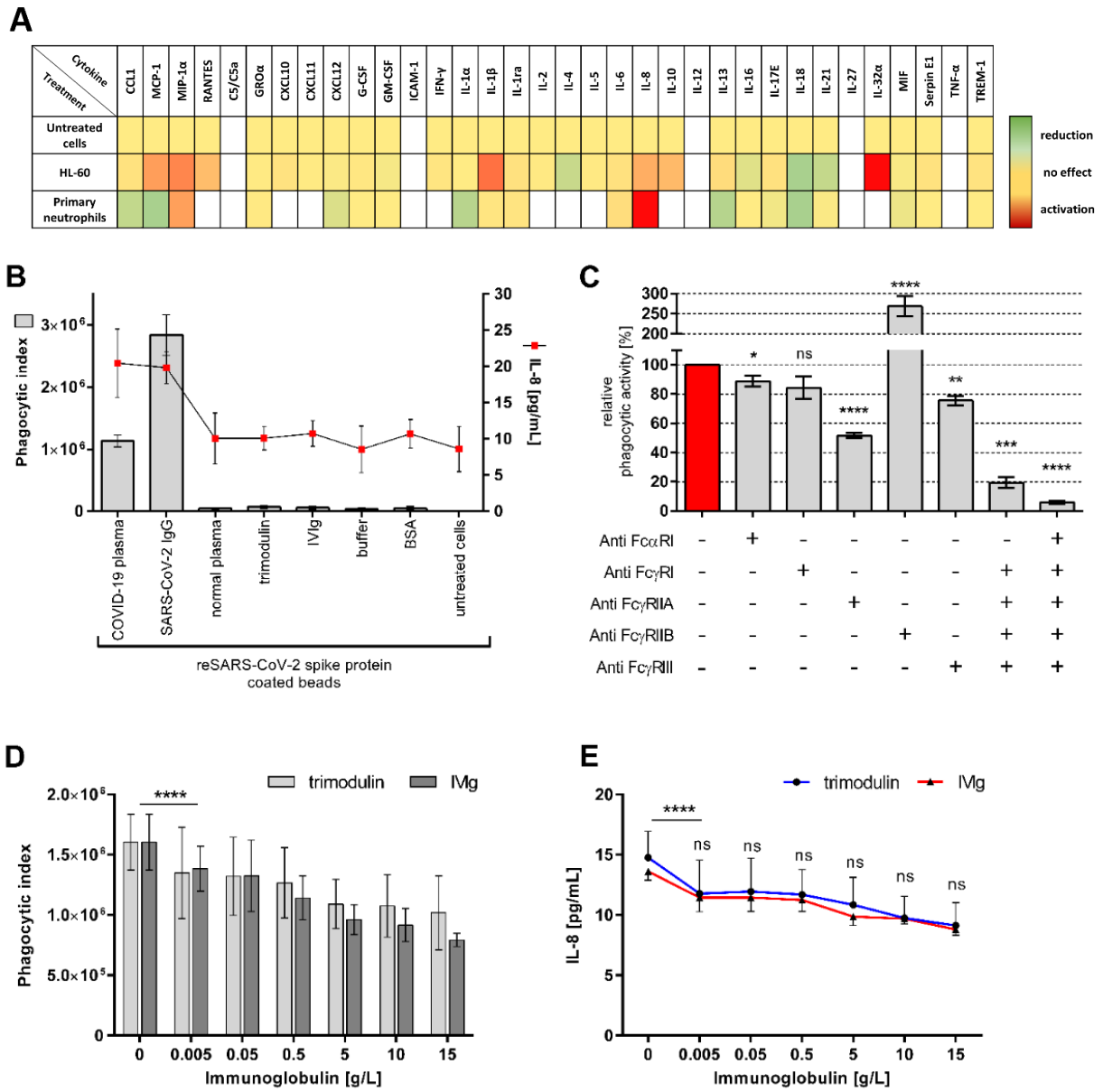

Figure 5-20: COVID-19 inflammation model with primary human neutrophils. **(A)** Heat map of chemokines and cytokines secreted by neutrophil-like HL-60 cells or primary neutrophils after stimulation with anti-SARS-CoV-2 IgG-IC. Cells were stimulated for 18 h at 37 °C with immune complex. Semi-quantitative cytokine secretion was measured by using human cytokine arrays. Relative signal intensities for every measured cytokine of untreated cells were set as 1 (yellow). The x-fold induction (red) or reduction (green) in comparison to untreated cells was calculated. Not detected cytokines are shown in white. Results represent the mean of 3 experiments. **(B)** Evaluation of COVID-19-like inflammation model. Cells were incubated with SARS-CoV-2 spike protein-coated beads opsonized with immunoglobulins or negative controls. Phagocytic index (gray bars, left y-axis) and IL-8 release (red dots, right y-axis) in cell culture supernatant were measured. Data represent the mean of 3 donors. **(C)** FcR blocking experiments with COVID-19 plasma opsonized SARS-CoV-2-like particles. Cells were pre-incubated with 5 µg/mL of indicated blocking antibodies or combinations of those, 20 min before addition of immune complex. The phagocytic index of not blocked cells was referred to as 100 % control and the remaining phagocytic activity is shown as the mean of 4 independent experiments. **(D)** HL-60 cells were incubated with SARS-CoV-2 spike protein-coated beads opsonized with COVID-19 plasma. Trimodulin or IVIg were added in the indicated concentrations to the cell immune complex mixture. Phagocytosis of immune complex was measured with trimodulin (light gray bars) or IVIg (dark gray bars) addition. **(E)** Same as (D) instead phagocytosis IL-8 release into the cell culture supernatant was measured with trimodulin (dots, blue line) or IVIg (triangle, red line) addition. Data represent the mean of 4 independent experiments. Statistics: One way ANOVA, Dunnett's multiple comparisons test.

As seen for HL-60 cells, specific phagocytosis of the SARS-CoV-2-like immune complex results in inflammatory activation of primary human neutrophils (Figure 5-20A/B). Nevertheless, phagocytic activity was higher for primary human neutrophils. FcR blocking revealed small differences: FcγRIII blocking reduces phagocytosis stronger, FcαRI blocking, in contrast, reduced phagocytosis lower than on HL-60 cells (Figure 5-20C). FcγRIIA blocking and combinations of blocking antibodies lead to the strongest reduction of phagocytosis. Like on HL-60 cells blocking of inhibitory FcγRIIB enhanced phagocytosis significantly, whereas the effects are stronger on primary cells (compare Figure 5-17B).
Similar to neutrophil-like HL-60 cells, primary neutrophils show reduced phagocytosis and a decreased IL-8 release by trimodulin and IVIg addition, however, no difference between both preparations was observed (Figure 5-20D/E).

6. Discussion

The human immune system is a complex network of adaptive and innate immunity that defeats invading pathogens. Inflammatory activation of the immune system is crucial for pathogen clearance, but the shift back into a resting state with homeostatic conditions is of major concern. Therefore, a fine-tuned network modulates the immune response. Important players in this network are antibodies and their FcR [44,46,167].

Severe infection diseases, like sepsis, sCAP or COVID-19, disturb the balance of our immune system, leading to systemic inflammation and overwhelming immune response [62,67,132]. While neutrophils are central players in inflammation, they can also mediate crucial damage when exhausted [6,100,101]. A possible treatment for the exhausted immune system is modulation by immunoglobulin preparations [56,63,196]. Immunoglobulin preparations can target multiple immunomodulatory modes of action by interacting with immune cell FcR or inflammatory mediators [63,69].

Our previous knowledge of immunoglobulin preparation modes of action mainly arises from studies using classical IVIg (~98 % IgG). Open questions remain for the modes of action of the, even more, complex IgM- and IgA-enriched immunoglobulin trimodulin (~23 % IgM, 21 % IgA and 56 % IgG). In these preparations, some modes of action could be attributed to the IgG or IgM component, whereas the role of IgA is so far unidentified.

In this thesis, the HL-60 cell line was verified as an appropriate neutrophil model system (chapter 6.1). Multiple immunomodulatory modes of action were investigated on resting HL-60 cells (chapter 6.2), in the context of bacterial- (chapter 6.3 and 6.4) and COVID-19 inflammation (chapter 6.5).

Within these cellular models, five distinct immunomodulatory functions were investigated: (1) interaction with soluble cytokines and modulation of cytokine release, (2) activation of ITAMi signaling, (3) targeting of FcγRIIB and ITIM signaling, (4) Modulation of FcR expression and (5) displacement of immune complex from activating FcR. By comparison between different immunoglobulin preparations and detailed characterization of underlying mechanisms, the functional relevance of IgM, IgA and IgG components in trimodulin was identified.

6.1. The HL-60 cell line is a suitable neutrophil model system

For such detailed investigations, a defined and standardized cellular system is required, which makes the usage of a cell line necessary. As effector cells neutrophils were chosen for several reasons: (1) neutrophils have an elementary role in the human innate and adaptive immune system and (2) mediate antibody-mediated effector functions which play a central role in severe infection diseases [5,101,138]. (3) Neutrophils are poorly studied in conjunction with viral respiratory diseases and COVID-19 [6,100]. (4) *In vivo* studies using mice in the context of neutrophil FcR functions are limited because of crucial differences between mice and humans: neutrophil abundance in mice is lower,

neutrophil-related chemokines like IL-8 are missing. Furthermore, FcαRI, FcγRIIA and FcγRIIC are not expressed in mice and IgG, as well as IgA, antibody classes differ [197,198].

However, the use of primary neutrophils is restricted by the short half-life of several hours [199]. For a better standardization and simplicity in handling the well-characterized HL-60 cell line was used; this cell line is utilized for a variety of phagocytosis assays [200,201]. To ensure that differentiated HL-60 cell line has the desired neutrophil-like phenotype, surface marker and FcR expression were analyzed (chapter 5.1). Neutrophil-like HL-60 cells were compared with primary human neutrophils, as well as not differentiated HL-60 cells. Typical neutrophil phenotype markers for this cell line and FcR expression pattern changed during differentiation to a neutrophil-like phenotype, as reported by others (Figure 5-1) [200–204].

Neutrophil-like HL-60 cells express high levels of FcαRI, FcγRI and FcγRIIA. Expression of FcγRIII and FcγRIIB is lower. The numbers of FcαRI, FcγRI, FcγRIIA and FcγRIIB per neutrophil are in a similar scale as described in literature [41,44,55]. FcμR expression is low on neutrophils and neutrophil-like HL-60 cells indicating no IgM FcR mediated effector functions [59]. For studies aiming to analyze IgM mediated effects, this is a limitation but in the context of this work a benefit. Because IgM is of minor importance in this cell model, the role of IgA can be explored.

Nevertheless, the expression, and especially the number of FcγRIII, was lower on neutrophil-like HL-60 cells in comparison to primary neutrophils. However, due to genetic modifications in tumor cell lines differences were expected [191]. Despite these differences in FcγR expression antibody-mediated effector functions can, also with slightly smaller intensity than on primary cells, investigated with HL-60 cells [199,201,205,206].

Monitoring of surface marker expression reveals that on the one hand, longer differentiation (< 5 days) leads to more neutrophil-like phenotype, on the other hand, cell number, inflammatory IL-8 increases and viability decreases with longer differentiation times (Figure 8-1). Therefore, as a compromise, cells were differentiated for 4 days for functional assays.

As an additional parameter, cytokine release of primary neutrophils and the HL-60 cell line was compared to ensure the significance of cytokine release as effector readout (Figure 5-2). The generated data only allow a semi-quantitative comparison of the detected cytokines (e.g. MIP-1α, IL-1β, IL-8), but these clearly show that both cell types secrete the same cytokine pattern. The detected cytokines are typical for neutrophilic cells and experimentally well-characterized [207,208]. The inflammatory chemokine IL-8 was quantitatively investigated more in detail for the establishment of the following experimental models, because of its elementary role for neutrophil migration and inflammatory activation [6,100,103,209].

Summarized, these data clearly show that neutrophil-like HL-60 cells are a suitable and easy to handle alternative to native neutrophils, justifying the use in these *in vitro* experiments.

6.2. Immunoglobulins facilitate immune homeostatic conditions

Interaction of monomeric immunoglobulins with resting or activated immune cells is an important regulatory step in maintaining immune homeostasis. While immunoglobulins opsonize invading pathogens and interact as a multimeric immune complex with FcR during infection, monomeric immunoglobulin IgG or IgA bind with low affinity on FcR and mediate inhibitory signals leading to anti-inflammatory effects during homeostasis [42,56,174].

The basis for immunoglobulin-mediated effects is the interaction between immunoglobulins and cellular FcR. It is known that increased antibody binding on cells leads to enhanced effector outcomes like ADCC [47]. To test the binding strength of neutrophil-like HL-60 cells to different antibody-coated surfaces, binding assays were performed (chapter 5.2.1). The data show a significantly stronger binding of cells to trimodulin coated surface compared to IVIg-, purified monomeric IgA- or purified IgM-preparations (Figure 5-3). Cells show almost no binding to IgM coated surface, which can be due to missing FcμR on neutrophils [59]. Monomeric IgA and IVIg showed similar binding as also reported by Brandsma and colleges [98]. The basis could be similar receptor binding affinities between IgA-FcαRI and IgG-FcγR [33,35]. In comparison, the binding of neutrophil-like cells to trimodulin is significantly stronger. The strong interaction is possibly due to multimeric species, which are absent in IVIg and purified IgA preparations. Trimodulin comprises monomeric, also multimeric IgG and IgA species as well as multimeric IgM (*in house data*). These multimeric species could interact with high valency to the FcγRs and FcαRI causing stronger binding. Increased binding of multimeric IgA forms to FcαRI is described in the literature and mediates enhanced effector functions [90,210–212]. As seen for purified IgM preparations, the trimodulin IgM component does not affect the interaction with neutrophils, because FcμR is missing.

6.2.1. Trimodulin shows stronger neutralization of cytokines and ITAMi signaling than IVIg

To investigate if enhanced binding of HL-60 cells to trimodulin mediates stronger anti-inflammatory effects compared to IVIg, both preparations were added to cells (chapter 5.2.2). The addition of both preparations reduces inflammatory cytokine release and facilitates an anti-inflammatory cell phenotype, which was mediated significantly stronger by trimodulin than IVIg (Figure 5-4). It was shown that several mechanisms were involved in stronger immune modulation by trimodulin:

(1) Trimodulin showed better direct neutralization of cytokines (IL-8) (Figure 5-4), which is likely an effect mediated by multimeric immunoglobulin species [90]. The direct interaction and neutralization of soluble mediators of inflammation, like activated complement factors, toxins or inflammatory cytokines, is an important mode of action of IVIg [80,158,184,185,213]. Superior effects by IgM- and IgA-enriched immunoglobulins were previously shown by inhibiting complement [79], now similarly dampening of inflammatory cytokines was observed for trimodulin.

(2) Activation of inhibitory ITAMi signaling was stronger with trimodulin compared to IVIg (Figure 5-5). The influence of ITAMi signaling was investigated by blocking the central ITAMi phosphatase SHP-1 using the chemical inhibitor NSC-87877 [174]. This mode of action seems to be central for trimodulin mediated immune modulation, as seen by great differences between trimodulin treated cells with or without SHP-1 inhibition. Differences in IVIg treated cells were lower. ITAMi signaling pathway was originally discovered by the interaction of IgA with FcαRI [177] and was also found for IgG-FcR interaction [214]. Strong activation of ITAMi by trimodulin could be induced by targeting FcαRI with IgA- and FcγR with IgG-component simultaneously. Further, IgA could induce stronger signaling due to 2:1 stoichiometry by FcαRI binding, whereas IgG binds FcγR in 1:1 stoichiometry [57,98].

(3) Inhibitory FcR signaling and expression of inhibitory FcγRIIB was stimulated by trimodulin and IVIg treatment. Incubation of cells with monomeric IVIg preparations modulates the balance between activating FcγRIIA and inhibitory FcγRIIB by upregulation of FcγRIIB [62,69,74]. In line with this, significant upregulation of FcγRIIB was observed by incubating cells with trimodulin or IVIg (Figure 5-6). The important role of ITIM signaling for immune cell homeostasis was shown by inhibition of SHIP-1 phosphatase, a key player in ITIM signaling [174]. Inhibition of SHIP-1 strongly upregulates inflammatory cytokine release and was even enhanced when adding trimodulin or IVIg to cells (Figure 5-5). Enhancement due to immunoglobulin addition could be by multimeric binding to activating FcR, leading to similar effects like an immune complex.

To summarize this chapter, it was shown that trimodulin and IVIg can facilitate immune homeostatic conditions on resting neutrophil-like cells. Three mechanisms were identified to be involved in immunomodulation (Table 6-1): (1) direct neutralization of cytokines, (2) inhibitory ITAMi signaling and (3) upregulation of inhibitory FcγRIIB, as well as ITIM signaling. Due to better neutralization of cytokines (by multimeric species) and stronger ITAMi signaling (by additional IgA component) trimodulin showed a better ability to induce immune homeostasis than IVIg.

Table 6-1: Immunomodulatory modes of action shown on resting neutrophils. Each mode of action and the experimental parameters to prove this are compared. The strength of trimodulin or IVIg mediated effects is depicted as followed: +++ strong effects, ++ medium effects, + low effects, - no effects.

Immunomodulation on resting cells (experimental setting):			
Incubation of resting neutrophil-like HL-60 cells with trimodulin or IVIg. IL-8 release and FcR expression as cellular readout.			
Immunomodulatory effector outcome			
Facilitation of immune homeostasis by reduced inflammatory IL-8			
Mode of action	**Experimental parameter**	**Trimodulin (IgG/A/M)**	**IVIg (IgG)**
(1) Direct neutralization	Detection of remaining IL-8 in buffer	++	+
(2) ITAMi signaling	Inhibition of SHP-1 (change in IL-8)	+++	+
(3) ITIM signaling	Inhibition of SHIP-1 Expression of FcγRIIB	++	++

6.3. Modulation of LPS induced inflammation

In severe infection diseases like sepsis, bacterial endo- and exotoxins are critical mediators of systemic inflammation and mortality. Primary treatment of those patients with antibiotics leads to the destruction of bacterial cells, increasing endotoxin load and forcing inflammation. The treatment with immunoglobulin preparations is a promising adjunctive therapy to reduce inflammatory mediators and modulate the overwhelming immune system [67,104,109].

Before testing the immunomodulatory effects of trimodulin, the inflammatory effects of endotoxin (using LPS) derived from *E.coli* on neutrophil-like HL-60 cells were characterized (chapter 5.3.1).

6.3.1. LPS induced cytokine release

LPS stimulation leads to dose- and time-dependent increase of pro-inflammatory cytokine release by neutrophil-like HL-60 cells (Figure 5-7). Several of these cytokines, like IL-6, IL-8, MIP-1α or IL1ra are known as inflammatory markers and predictors for sepsis severity and mortality [103,105]. Those effects were shown to be induced by TLR signaling (Figure 5-7). PRR like TLR are expressed on immune cells (e.g. neutrophils, macrophages or NK-cells) to detect PAMPs like LPS. They are an effective primary line in defense when pathogen-specific antibodies are absent [37,67,186]. LPS induced IL-8 release was strongly reduced by inhibiting TLR4 pathways with chemical inhibitor CLI-095. Also blocking of TLR2 (with inhibitor C29) and MyD88 (with inhibitor ST2825) diminished LPS induced IL-8 release significantly. Besides the TLR4 receptor, LPS can also be recognized by TLR2 [187,215]. Almost all TLR act via MyD88 dependent signaling pathways to activate inflammatory gene expression, which explains the reduced IL-8 release after inhibition of MyD88 [37,216].

Previously, the phosphorylation of SYK kinase was reported after treating neutrophils and macrophages with LPS [216–218]. Similar effects were observed for the here used HL-60 cell line; stimulation with LPS induced activation of SYK, as seen on increased phosphorylation at specific tyrosine (Figure 8-2). This highlights the complexity and interplay between different receptors and signaling cascades (reviewed in Lowell [178]).

6.3.2. LPS induced changes in FcR expression

Another example of the complex interactions between TLR and FcR is the LPS induced upregulation of FcR (FcαRI, FcγRI and FcγRIIA/B) and TLR (Figure 5-8). Upregulation of activating FcR by LPS is reported in literature [31,33,43,219]. The cellular basis for endotoxin-mediated upregulation of FcR is the FcR-TLR cross-talk [37,42,186]. Invading bacteria release endotoxins like LPS, which are recognized by TLR on immune cells, leading to the expression of pro-inflammatory cytokines (e.g. TNF-α, IL-8) and increased FcR levels on the cell surface. Increased number of FcR make the cells more prone to neutralize antibody

opsonized pathogens [42]. FcR-TLR cross-talk induces potent inflammation as recently shown for co-stimulation of IgA- and IgG-immune complex with LPS [89,171].

In contrast to the other analyzed FcRs (FcαRI, FcγRI, FcγRIIA, FcγRIIB), FcγRIII showed a contrary expression change (Figure 5-8). FcγRIII detection was reduced after LPS stimulus. For neutrophils, this phenomenon is reported [49,220]. In accordance with the absence of FcγRIIIA in neutrophils [181], the reported mechanism is based on proteolytic cleavage of FcγRIIIB by metalloprotease A disintegrin and metalloprotease 17 (ADAM17) from the neutrophil surface. Soluble FcγRIIIB interacts with other immune cells, e.g. macrophages, in the circulation and causes the release of pro-inflammatory cytokines like IL-6 or IL-8, promoting further inflammation [46,48].

In conclusion, the treatment of neutrophil-like HL-60 cells with LPS induces an inflammatory phenotype, as seen by major changes in FcR expression and a strong increase in inflammatory cytokine release. The LPS stimulated neutrophil-like HL60-cells are therefore a suitable model to investigate hereafter the immunomodulatory properties of trimodulin.

6.3.3. Modulation of inflammation by trimodulin and IVIg

Anti-inflammatory effects of immunoglobulin preparations on LPS induced cytokine release were investigated by several studies. Trimodulin was tested in a rabbit model [81] and in a macrophage second-hit model *in vitro* [84]. Effects of serum IgA [91,221], IVIg as well as IgM- and IgA- enriched immunoglobulins on cytokine release were tested *in vitro* [80,185,192]. However, those studies lack a comprehensive identification of the underlying modes of action. The immunomodulatory effects of trimodulin on LPS stimulated cells, as well as the underlying mechanism, were analyzed by modulation of FcR expression and pro-inflammatory IL-8 release (chapter 5.3.2).

Besides the interaction with toxin-induced cytokines, IVIg can directly neutralize endotoxin by anti-LPS antibodies [80]. This was also seen in the here used experimental setup, trimodulin and IVIg were able to neutralize ~30 EU/mL. (Figure 5-9). Nevertheless, the relevance for the here used cellular assays is low, because cells were stimulated with >3000 EU/mL endotoxin to induce powerful inflammation.

To simulate adjunctive therapy of severe sepsis or sCAP patients, neutrophil-like HL-60 cells were pre-stimulated with LPS to induce strong inflammation (discussed above) before the addition of trimodulin or IVIg [62,67]. The data show that trimodulin can reduce LPS induced IL-8 release in high dosage (> 5 g/L) significantly stronger than classical IVIg (Figure 5-9). Elevated IL-8 levels are found in patients with sepsis or severe COVID-19 and are associated with disease severity. IL-8 is from major importance for neutrophil migration (and so neutrophilia), inflammatory activation (e.g. induction of NETs) and neutrophil-mediated tissue damage [6,100,103,209]. The stronger reduction of IL-8 release by trimodulin could therefore explain the benefits of IgM- and IgA-enriched immunoglobulins in the treatment of severe sepsis cases [74,110,111].

Targeting FcR of resting neutrophil-like HL-60 cells with IgA or IgG of trimodulin activates strong inhibitory ITAMi signaling (compare 6.2). The same effects were observed in studies with LPS induced inflammation using monocytic cells [172,175].

LPS stimulated HL-60 cells express higher levels of FcαRI, FcγRI and FcγRIIA (Figure 5-8). The modulation of this LPS induced FcR expression by trimodulin and IVIg was investigated in the neutrophil-like HL-60 cell system. It was shown that trimodulin elicits strong modulation of FcR expression, whereas IVIg did not. Trimodulin can reduce the expression of activating FcαRI, FcγRIIA and FcγRIII, while inhibitory FcγRIIB was upregulated (Figure 5-9).

Monomeric and especially multimeric forms of IgA are known to bind to FcαRI, induce receptor aggregation and leading to receptor internalization [31,222,223]. Similar the IgA antibodies in trimodulin (which are not in IVIg) can bind to FcαRI, thereby reducing available FcαRI on the cell surface. This is the first proof for the involvement of IgA-FcαRI pathway in trimodulin modes of action.

Trimodulin also showed a better capability to shift the balance between the expression of activating and inhibitory FcγRIIA and FcγRIIB. FcγRIIA expression was significantly reduced by trimodulin, whereas inhibitory FcγRIIB was significantly elevated after trimodulin treatment.

The differences in FcγR modulation could be due to IgG-subclass distribution in the products. IgG subclasses IgG1-IgG4 differ in their binding affinity to FcγR and conduct different effector functions [50,168]. IVIg preparations have IgG subclass distribution similar to serum source ([69] and *in house data*). In comparison, trimodulin has a higher portion of IgG4, which has a minimal binding affinity to FcγRIIA and FcγRIII but a relatively high affinity to inhibitory FcγRIIB [50]. Because both, trimodulin and IVIg, were used in the same total protein concentration, IgG concentration is differing and could be a further reason for differences in FcγR modulation.

Comparing these results with the data from resting cells (compare results chapter 5.2.2 and discussion 6.2), the stronger immunomodulatory effects of trimodulin on LPS stimulated neutrophil-like HL-60 cells can be attributed to four modes of action (Table 6-2). (1) direct cytokine interaction and LPS neutralization, (2) ITAMi signaling, (3) interaction with inhibitory FcγRIIB and ITIM signaling, (4) modulation of activating FcR expression.

Table 6-2: Immunomodulatory modes of action in endotoxin model. Each mode of action and the experimental parameters to prove them are compared. The strength of trimodulin or IVIg mediated effects is depicted as followed: +++ strong effects, ++ medium effects, + low effects, - no effects.

Immunomodulation in endotoxin model (experimental setting):			
Pre-incubation of neutrophil-like HL-60 cells with LPS, the addition of trimodulin or IVIg. IL-8 release and FcR expression as cellular readout.			
Immunomodulatory effector outcome			
Modulation of LPS induced IL-8 release and FcR expression			
Mode of action	**Experimental parameter**	**Trimodulin (IgG/A/M)**	**IVIg (IgG)**
(1) Direct neutralization	Detection of remaining IL-8 in buffer	Not tested	Not tested
(2) ITAMi signaling	Inhibition of SHP-1 (change in IL-8)	Not tested	Not tested
(3) ITIM signaling	Expression of FcγRIIB	+++	-
(4) Phenotype modulation	Expression of FcαRI, FcγRI, FcγRIIA, FcγRIII	+++	-

6.4. Immunoglobulins elicit a dual function on phagocytosis

ADCP is a crucial mechanism in antibody and neutrophil-mediated pathogen clearance [5]. ADCP can be directly mediated by immunoglobulin preparations and induce potent inflammatory activation of immune cells [39,62]. The anti-pathogenic effects of immunoglobulin preparations can be investigated by ADCP, but as indicated in the introduction, immunoglobulin preparations can additionally inhibit phagocytosis in high dosage, therefore, representing a dual function [63,69]. Generally, anti-inflammatory effects of IVIg are observed at high dose treatment (1-3 g immunoglobulin per kg body weight [65,224]) when the supplemented immunoglobulins compete with immunoglobulins present in the patient [63]. In this work, the potential dual function of trimodulin and IVIg was explored by investigating the phagocytosis of *S.aureus*.

S.aureus is a widespread bacterium and a leading cause of many infection diseases like sepsis or pneumonia [225–228]. Also in COVID-19 diseases bacterial co-infection with *S.aureus* worsen clinical outcomes [155,157,229–231]. The bacterium developed several mechanisms to evade the innate immune response, therefore, defeating *S.aureus* is a major issue in public health [225,226].

Neutrophils can recognize *S.aureus* via several receptors, attach and ingest the invading organism. The internalized particle is trapped into a phagosome where anti-pathogenic granula and ROS eliminate the threat [226]. Receptors responsible for pathogen recognition include PRR, like TLRs, which bind directly to PAMPs and initiate neutralization, a process called opsonin-independent phagocytosis [227,232]. In comparison, opsonization of *S.aureus* with different opsonins like complement, acute phase proteins or antibodies induce more effective phagocytosis [225].

6.4.1. Immunoglobulins induce phagocytosis of *S.aureus*

The anti-pathogenic properties of immunoglobulin preparations against *S.aureus* were investigated by comprehensive characterization of antibody-mediated phagocytosis (chapter 5.4.1).

Phagocytosis was measured by uptake of immunoglobulin opsonized *S.aureus* particles by neutrophil-like HL-60 cells. The results show that neutrophil-like HL-60 cells can directly phagocytose *S.aureus* without opsonins. These results can be explained by binding and phagocytosis of *S.aureus* via PRR independent of opsonins [227,232]. But importantly, the phagocytosis was strongly enhanced by immune complex formation with different immunoglobulin preparations (Figure 5-10). Immunoglobulin preparations contain specific antibodies against various pathogens (including *S.aureus*). Based on the broad spectrum of antibody specificity in the donor plasma [64,66,67], opsonization and enhanced phagocytosis can be explained.

Phagocytosis of immune complex induces inflammation as seen by the secretion of several pro-inflammatory cytokines like MCP-1, MIP-1α, RANTES, IL-1β, IL-6, IL-8, IL-32a and TNFα by neutrophil-

like HL-60 cells. Further, the amount of secreted IL-8 correlated with phagocytic activity (Figure 5-10). The basis for inflammatory activation is the intracellular signaling via ITAM and the central SYK kinase [175,178]. Experiments inhibiting SYK function by chemical inhibitor Piceatannol [233] showed diminished phagocytosis and IL-8 release (Figure 5-11). Also, the activation of SYK by immune complex due to phosphorylation at specific tyrosine's was shown as reported (Figure 8-3) [175,234,235]. This demonstrates the correlation between phagocytosis, inflammatory activation and SYK/ITAM signaling.
As described in the previous chapter, there is a link between TLR recognized LPS stimulation and FcR expression as well as FcR-signaling. This interplay is known in the literature as FcR-TLR cross-talk [37,42,186].
To show the effects of FcR-TLR cross-talk on functional level LPS stimulated HL-60 cells were used for *S.aureus* phagocytosis assay. LPS stimulated neutrophils showed increased phagocytosis in comparison to not stimulated cells (Figure 5-10). These observations are in accordance with previous data [89,236,237] and confirm that the immune response is induced by a collaboration of several receptors and stimuli [42].

6.4.2. FcR and immunoglobulin species relevant for phagocytosis

In the previous chapter, basic aspects of *S.aureus* ADCP were discussed for the neutrophil-like HL-60 cell model. In this chapter, differences between immunoglobulin preparations, the functional relevant immunoglobulin species, as well as the relevant FcR for phagocytosis were in focus (chapter 5.4.2).
The phagocytic capacity of several immunoglobulin preparations was compared by incubating immune complex (consisting of *S.aureus* opsonized with corresponding immunoglobulins) with neutrophil-like HL-60 cells. Phagocytosis was highest for *S.aureus* opsonized with standard IVIg, followed by purified IgA and trimodulin. *S.aureus* opsonized with purified IgM preparation showed phagocytosis comparable to not opsonized *S.aureus* (Figure 5-10).
To check which immunoglobulin classes opsonize *S.aureus,* immunological detection of IgG, IgA and IgM were performed (Figure 5-12). Functional relevant immunoglobulins and FcRs were identified by pre-incubating neutrophil-like HL-60 cells with specific blocking antibodies (Figure 5-12). Antibodies against FcγRI (clone 10.1), FcγRIIA (clone IV.3), FcγRIIB (clone 2B6), FcγRIII (clone 3G8) or FcαRI (clone MIP8α) were used to inhibit the binding of IgG or IgA to their respective receptors [45,89,238–240]. In the next paragraphs, the results of these experiments were discussed for *S.aureus* without opsonin and each *S.aureus* immune complex:

***S.aureus* without opsonin**

Although opsonin independent phagocytosis of *S.aureus* via PRR was expected [227,232], blocking experiments show decreased phagocytosis when FcαRI is blocked (Figure 5-12). This indicates FcαRI dependent phagocytosis of *S.aureus*. Similarly, De Tymowski *et al*. were able to show that direct binding of *Streptococcus pneumoniae* or *E.coli* by FcαRI leads to phagocytosis of pathogens, representing host defense in an early phase of infection [241].

Purified IgM immune complex

The purified IgM preparation showed no anti-pathogenic activity (Figure 5-10), though IgM species of IgM- and IgA-enriched immunoglobulins have titers against common pathogen surface proteins and IgM was detected on purified IgM and trimodulin immune complex (Figure 5-12) [228]. The reason for none phagocytic capacity is the absence of complement and FcμR [59,242].

Purified IgA immune complex

Opsonization of *S.aureus* with IgA antibodies and complete FcαRI dependency was shown for purified monomeric IgA preparation (Figure 5-12), as described by others [89,92,243–245].

The results indicate that antibodies of IgA class show lower phagocytic activity against *S.aureus* than IgG (Figure 5-10). There a two reasons which could explain these data. (1) the number of available FcRs on the cell surface is an important regulator of phagocytic activity [46]. The sum of FcγR expressed on the neutrophil surface is much higher than FcαRI expression alone [41,44,55]. (2) *S.aureus* has several anti-opsonic strategies to prevent and influence immunoglobulin opsonization. *S.aureus* produces strong IgG-Fc-part binding protein A [225]. To enhance phagocytosis of *in vitro* phagocytosis assays the manufacturer removes protein A. Other virulence factors like IgA binding *Staphylococcal* superantigen-like protein 7 (SSL7) remain [246,247]. Therefore, IgG may have a better ability to bind these *S.aureus* particles than IgA.

IVIg immune complex

IgG-mediated opsonization was observed for IVIg preparation, blocking IgG FcγRI and FcγRIIA and combinations of those reduced phagocytosis (Figure 5-12). The importance of low-affinity FcγRIIA for phagocytosis of IgG immune complex was emphasized before [164,237–239]. More contrary is the role of high-affinity FcγRI: Under homeostatic conditions, FcγRI expression and role in cellular effector functions are low, whereas under inflammatory conditions expression and immune complex phagocytosis are strongly upregulated [44,248]. As the HL-60 cell line is derived from tumor cells [200] and differentiation induces cellular stress, the relatively strong expression and influence of FcγRI in immune complex phagocytosis can be explained. The blockade of FcγRIII was of minor importance in the HL-60 cell model; based on the low expression of this receptor (compare chapter 5.1, Figure 5-1). Besides blocking of FcγR, also the blocking of IgA specific FcαRI slightly decreased IVIg immune complex phagocytosis. This could be due to small amounts of IgA in IVIg preparations (<2 %) [64] or direct binding and phagocytosis of *S.aureus* via FcαRI (see above).

Trimodulin immune complex

The incubation of *S.aureus* with trimodulin leads to opsonization with IgG, IgA and IgM antibodies (Figure 5-12), which is according to data showing neutralizing antibody titers of all three classes against *S.aureus* proteins in IgM- and IgA-enriched immunoglobulins ([228] and *in house data*).

Trimodulin immune complex phagocytosis was dependent on FcαRI and FcγRI or combinations with both. Although lower levels of IgA (compared to IgG and IgM) were found on the trimodulin immune complex; FcR blocking experiments reveal similar importance for phagocytosis. An explanation could be that IgA interacts with two FcαRI molecules thereby mediating stronger ADCP compared to IgG [86,98,99]. The possible importance of IgA in IgM- and IgA-enriched immunoglobulin preparations was previously mentioned [64,73]. The results of this work confirm this hypothesis and show the potential of IgA enriched immunoglobulin preparations, like trimodulin.

Based on IgA and IgM antibodies in trimodulin phagocytic activity is lower compared to IVIg (Figure 5-10). Opsonization with IgM species of trimodulin negatively influences phagocytosis, because IgM covers with high avidity [8] binding sites (for IgG or IgA species) and cannot mediate phagocytosis. In a different experimental setting, adding complement could enhance trimodulin mediated anti-pathogenic effects. In this setting, the IgM and IgA components could expand IgG-mediated functions, resulting in better pathogen clearance, as shown in literature [15,76].

A further reason for lower phagocytosis could be the IgG subclass distribution in both products. The higher portion of IgG4 in trimodulin could negatively affect effector functions like phagocytosis by relatively high affinity to FcγRIIB [50]. Further reasons could be competition between IgA- and IgG-immune complex. Downregulation of IgG-mediated phagocytosis by IgA is known in literature [249], suggesting an interplay between both immunoglobulin species in trimodulin.

The combination of FcR number for IgG and IgA, the different immunoglobulin species and higher IgG4 portion leads to the lower phagocytic activity of trimodulin in comparison to standard IVIg in this experimental setup. As discussed in the previous chapters (chapter 6.2 and 6.3.3), this could induce stronger inhibitory FcR-signaling and therefore better immunomodulation.

In contrast to blockade of activating FcαRI or FcγRs, blocking of inhibitory FcγRIIB increased phagocytosis mediated by IgG-containing immunoglobulin preparations (Figure 5-12). This highlights the inhibitory effect of this receptor and ITIM signaling on cellular effector functions (like ADCP) and immune cell homeostasis (compare chapters 5.2.2 and 6.2) [42,174].

Summarized the results shed light on phagocytosis mediated by trimodulin. The work unravels in detail which FcRs were responsible and extends the knowledge of immunoglobulin-FcR interaction [176,192,250]. The comparison of trimodulin with purified IgM, IgA and IgG preparations shows that IgA plays an important role in trimodulin modes of action.

6.4.3. Dose dependency – from phagocytosis to immunomodulation

After detailed investigations to understand phagocytosis of *S.aureus* mediated by immunoglobulin preparations, next immunomodulation was assessed. Based on clinical observations for the usage of IVIg preparations anti-pathogenic activity was seen at low doses, whereas immunomodulatory activity appears at high doses [63,65,181]. Generally, the immune response depends on the antibody to antigen ratio. When the immunoglobulin amount is lower than the antigen amount, antibody-mediated effector outcome is low. With increasing antibody amount, the ratio of antibody to antigen shifts to a distribution where optimal cross-linking of the immune complex is achieved. The immune response reaches a peak. With further increase in antibody concentration, the ratio shifts to immune inhibition, because excessive antibodies block FcR and disrupt immune complex formation. The immune response is down-modulated [39]. This mechanism is an important step to prevent excessive inflammation and shift the immune system to homeostatic conditions [44,46].

To investigate this possible dual function of immunoglobulins, phagocytosis of *S.aureus* and inflammatory cell activation were investigated with varying concentrations of IVIg or trimodulin (chapter 5.4.3). The data show increasing phagocytic index and correlating IL-8 level with low concentrations up to a peak value. Higher concentrations of immunoglobulins cause immunomodulation by decreased phagocytic activity and down-modulation of IL-8 release (Figure 5-13). IVIg mediated *S.aureus* phagocytosis peaked earlier (~ 0.5 g/L IVIg) than trimodulin (~ 5 g/L trimodulin), but this can be explained based on the above described stronger opsonic capacity of IVIg against *S.aureus* particles. These *in vitro* data are in alliance with the knowledge from treating patients with autoimmune or inflammatory diseases [63,65,66,68,69]. Patients were typically treated with high doses of 1-3 g immunoglobulin per kg body weight in inflammatory diseases, whereas lower doses of 200-400 mg/kg were used in substitution therapy [65,224]. The study doses were specified for the period of typically 5 days [82,149,152]. Assuming that a mean adult comprises 48.5 mL plasma per kg body weight [251], a plasma concentration of 8 g/L immunoglobulin preparations is achieved. Exactly in these doses, immunomodulatory effects were observed. The *in vitro* data are, therefore, suitable to substantiate clinical results.

A benefit of the here used *in vitro* system compared to clinical studies is the opportunity to investigate underlying modes of action for immune modulation in high-dose treatment. Again, it was shown that multiple modes of action act synergistically to mediate immune modulation (chapter 5.4.3):

(1) direct binding and neutralization of pro-inflammatory cytokines (not shown for *S.aureus* phagocytosis model, compare chapter 5.2.2, Figure 5-4).

(2) Activation of inhibitory ITAMi signaling by trimodulin and IVIg was shown by inhibiting SHP-1 and measuring site-specific phosphorylation of SHP-1 (Figure 5-14). After treating neutrophil-like HL-60 cells with *S.aureus* and different concentrations of trimodulin or IVIg, phosphorylation of SHP-1 was

measured. Phosphorylation of ITAMi phosphatase SHP-1 at specific tyrosine 536 indicates activation of ITAMi pathway [175]. IVIg and trimodulin treatment induce dose-dependently phosphorylation of SHP-1, whereas IVIg induced stronger phosphorylation (significant at doses above 0.5 g/L) compared to trimodulin (significant above 5 g/L). This is likely because of stronger phagocytic effects mediated by IVIg. To further demonstrate the importance of ITAMi, SHP-1 was inhibited by chemical inhibitor NSC-87877 [252] before the addition of *S.aureus* and immunoglobulins to the cells. Increased IL-8 levels compared to not inhibited cells show the anti-inflammatory effects of ITAMi. These findings indicate that monomeric binding of IgG and IgA species from trimodulin or IVIg can reduce phagocytosis and lead to cell inhibition via ITAMi, as described [174,176,177].

(3) The inhibitory role of FcγRIIB on phagocytosis was demonstrated by blocking this receptor before immune complex addition. Blocking of FcγRIIB increased phagocytosis of trimodulin- and IVIg- immune complex (Figure 5-12). Co-ligation of immune complex on activating receptors with inhibitory FcγRIIB is known to inhibit cell activation [31,173,174]. This work confirmed this knowledge.

(4) Reduction of activating FcR expression (not shown for *S.aureus* phagocytosis model, compare chapter 5.3.2, Figure 5-9).

(5) Blocking of activating FcRs and displacement of immune complex was shown by reduced phagocytosis with high dosage (>5 g/L) trimodulin or IVIg (Figure 5-13). Reduced phagocytosis induces less pro-inflammatory ITAM signaling [63,69]. Based on higher avidity of multimeric IgM- and IgA-species beneficial effect of trimodulin for immune complex displacement were expected [62,90], but not observed. The reason could be the IgG dependency of *S.aureus* phagocytosis.

Table 6-3 summarizes the immunomodulatory modes of action relevant for the *S.aureus* phagocytosis model.

Table 6-3: Immunomodulatory modes of action in *S.aureus* phagocytosis model. Each mode of action and the experimental parameters to prove them are compared. The strength of trimodulin or IVIg mediated effects is depicted as followed: +++ strong effects, ++ medium effects, + low effects, - no effects.

Immunomodulation in *S.aureus* phagocytosis model (experimental setting):			
Opsonization of ***S.aureus*** with of different doses trimodulin or IVIg. IL-8 release and phagocytic activity as cellular readout.			
Immunomodulatory effector outcome			
Reduction of phagocytic activity and IL-8 release in high doses.			
Mode of action	**Experimental parameter**	**Trimodulin (IgG/A/M)**	**IVIg (IgG)**
(1) Direct neutralization	Detection of remaining IL-8 in buffer	Not tested	Not tested
(2) ITAMi signaling	Inhibition of SHP-1 (change in IL-8) Phosphorylation of SHP-1 at pY536	++	+++
(3) ITIM signaling	Blocking of FcγRIIB	+	+
(4) Phenotype modulation	Expression of FcαRI, FcγRI, FcγRIIA, FcγRIII	Not tested	Not tested
(5) Displacement of immune complex	Reduced phagocytosis	++	++

Although, IgA-FcαRI was clearly shown to be important for trimodulin mediated *S.aureus* phagocytosis and FcαRI can mediate strong anti-inflammatory signaling [31,98,253] no differences between immune complex displacement and immunomodulation were observed. Likely, this might be by the excessive importance of IgG in this *S.aureus* phagocytosis model (see chapter 6.4.2). Experiments using native *S.aureus* particles with Protein G could qualify the IgG effects and highlight IgA effects in trimodulin regarding immunomodulation.

6.5. Immunomodulation in a COVID-19 model

The rapid global spread of SARS-CoV-2 virus-induced COVID-19 disease led to an urgent need for appropriate therapeutics. The major issue for severe COVID-19 patients is a dysregulated immune system with hyper-inflammation, cytokine storm, ARDS and ultimately respiratory failure [132,141,254]. Previous data indicate that in severe cases excessive immune response, mediated by neutrophils [138], is of greater importance for COVID-19 progression than virus-induced damage alone, highlighting the importance of immune modulators [66]. Clinical efficiency and *in vitro* as well as the data in this work showed that trimodulin is a promising immunomodulatory drug in bacterial-induced inflammation [82,84]. In contrast, the knowledge about immunomodulation in viral-induced inflammation is limited. Immunomodulatory activity of Pentaglobin® in SARS-CoV-virus-induced inflammatory disease was reported [120]. Furthermore, first clinical studies showed promising results in treatment of COVID-19 patients with IVIg preparations [149,151–153].

Clinical studies are essential for investigating the efficiency of immune modulators. Besides clinical studies, there is an urgent need for powerful models estimating immunomodulatory potency and modes of action of potential therapeutics. Because severe COVID-19 cannot yet be depicted in animal models [255], an *in vitro* model to reduce this gap was developed.

6.5.1. An easy to use COVID-19 model

As a basis to study immunomodulation on a cellular level a bead platform with fluorescent latex beads was chosen. This platform is an easy-to-use and versatile option to pro-inflammatory activate immune cells [92,226,244]. The bead system has the advantage to easily monitor inflammatory and anti-inflammatory processes under standard laboratory conditions. To associate the bead system with COVID-19, beads were coated with recombinant full-length SARS-CoV-2 spike protein. The SARS-CoV-2 spike protein was selected because it is responsible for virus infectivity and mediates antibody-dependent immune response against the virus *in vivo* [136,256]. It was shown that disease severity is linked to anti-SARS-CoV-2 spike protein-specific antibody levels, corresponding FcR mediated antibody functions and inflammatory cytokine release [136,143,144,146,257]. Furthermore enhanced binding of the SARS-CoV-2 spike protein to ACE-II receptor compared to SARS-CoV is a reason for the fast spreading of SARS-CoV-2 [123,126].

The difference in size between latex bead (~1 μm) and SARS-CoV-2 virus (~100 nm) [123,124,258] is of minor importance for the informative value of the assay. Because the virus-like beads are only on the scope for inducing inflammation. The usage of ~1 μm beads is in this context more suitable because optimal phagocytosis and inflammation are induced with particles of 0.5-2 μm in diameter [259,260].

With this model system, it is possible to unravel in detail the mechanism relevant for the induction of inflammation and furthermore the immunomodulatory modes of action by immunoglobulin preparations (that are so far unknown in the context of COVID-19). As in the here used bacterial models, the role of IgA antibodies was investigated with a particular focus.

Inflammatory activation by SARS-CoV-2-like immune complex

To understand the mechanism of SARS-CoV-2-like particle uptake via immunoglobulin opsonization, IgG, IgA and IgM binding on the particle surface was analyzed (chapter 5.5.1). The phagocytosis of the resulting immune complex and subsequent inflammatory activation of neutrophil-like HL60 cells was investigated in line with this (chapter 5.5.2).

It was shown that the convalescent COVID-19 plasma opsonized beads exhibit binding of IgG, IgA and IgM classes to the SARS-CoV-2 spike protein on the bead (Figure 5-15). This is in accordance with ELISA data showing antibodies of IgG, IgA and IgM class against SARS-CoV-2 surface proteins [257,261,262]. Besides IgG, neutralizing antibodies from IgA and IgM class are important, especially in the early immune response. Nevertheless, they were often not monitored in patients [145,261–265].

The basis for COVID-19-like inflammation in the studied *in vitro* model is FcR-dependent phagocytosis of SARS-CoV-2-like immune complex by immune effector cells. Stimulation of neutrophil-like HL-60 cells with SARS-CoV-2-like immune complex resulted in the secretion of several pro-inflammatory chemokines and cytokines like MCP-1, MIP-1α, IL-1β, IL-8 or IL-10 (Figure 5-16). Upregulation of these inflammatory mediators was also observed in patients with severe COVID-19 (reviewed in Noroozi *et al.* [266]). For more detailed investigations of the here used model phagocytosis and IL-8 release was monitored. An increase in IL-8 level was reported for COVID-19 patients by various studies [133,267,268]. Control experiments showed that only opsonization with SARS-CoV-2 specific antibodies leads to uptake of the fluorescent particles and successive pro-inflammatory cell activation. Negative controls without SARS-CoV-2 spike protein-specific antibodies show no binding of antibodies to bead surface (Figure 5-15) and no phagocytosis or inflammatory IL-8 release (Figure 5-16). This demonstrates high specificity and low background signal of the assay.

The phagocytosis of SARS-CoV-2-like immune complex was linked to a reproducible increase in IL-8 release by neutrophil-like HL-60 cells. The inflammatory activation is similar to native SARS-CoV-2 virus infection: The plasma IL-8 levels measured in patients with SARS-CoV and SARS-CoV-2 induced pneumonia range around 30- 60 pg/mL [133,269]. Similarly, the levels of other inflammatory cytokines are in the pg/mL range instead of ng/mL like in other *in vitro* settings [270]. These data confirm the suitability of the model system to depict severe COVID-19.

The reliance on specific immunoglobulins for particle uptake indicates FcR dependency, as reported for SARS-CoV by others [271,272]. SARS-CoV-2 like particles without specific opsonin showed almost no phagocytosis. This indicates that HL-60 neutrophil-like cells express low levels of ACE-II receptor which

is responsible for SARS-CoV-2 spike protein binding and virus uptake [256]. Low expression of ACE-II receptor was found on neutrophil-like HL-60 cells (Figure 8-5), in accordance with literature [195,273].
The phagocytosis of COVID-19 plasma opsonized particles was dependent on FcαRI, FcγRIIA or combinations of both (Figure 5-17). This dependency shows that IgA and IgG are functionally relevant in this complement-free setup. No influence on particle uptake was detected for FcγRIII. This could be due to lower expression in neutrophil-like HL-60 cells compared to primary neutrophils (chapter 5.1). FcR blocking on primary cells revealed that even though the highly expressed FcγRIII is part of immune complex phagocytosis, the lower expressed FcγRIIA is functional of greater importance (Figure 5-20), as reported in literature [44,47,239]. Furthermore, neutrophils of severe COVID-19 patients exhibit lower levels of FcγRIII [274–276]. This highlights the suitability of neutrophil-like HL-60 cells as a model system for COVID-19. Contrarily to activating FcR, blocking of inhibitory FcγRIIB increased phagocytosis of SARS-CoV-2-like immune complex (Figure 5-17); this is known to correspond to inhibitory ITIM signaling [42,44].
The observed phagocytosis and inflammatory activation are known for FcR and corresponding inflammatory signaling via ITAM and SYK kinase [42,174]. Inhibition of SYK by chemical inhibitor Piceatannol decreased phagocytosis and IL-8 release dose-dependent (Figure 5-17). Confirming SYK and ITAM signaling for the here used setting. In a recent study, Hoepel *et al.* [131] investigated the influence of convalescent plasma on macrophage inflammatory response. They showed in accordance with the here generated data that macrophage inflammation is dependent on anti-SARS-CoV-2 IgG, which mediates immune response via FcγRII and SYK signaling. In comparison, they found no influence on FcαRI blocking. This can be due to the donor plasma, which may have no anti-SARS-CoV-2 IgA antibodies, however, antibody levels were not provided [131].

Plasma donors show varying activation of the cell system

Furthermore, convalescent plasma from six different donors was tested with respect to immunoglobulin binding to spike protein, the induced phagocytosis rate, as well as corresponding IL-8 release. The varying levels of IgM, IgA and IgG antibodies found on the SARS-CoV-2-like particles (Figure 5-15) can be explained by the immune response which changes from IgM to IgG and IgA in the latter phase [257,277,278]. Especially neutralizing IgM levels, but also IgA and IgG levels decline several weeks after infection [277,278]. Nevertheless, this hypothesis cannot be confirmed as donations were randomized and no information regarding the time point of plasma donation after infection, sex, age or diseases severity are available. Studies investigating antibody-mediated effector functions of convalescent COVID-19 plasma donations are available [136,143–146] and could be a possible aim of further studies using this bead system.
As shown by others the antibody-dependent neutralization of SARS-CoV-2 correlates with specific IgG, IgA and IgM antibody levels against viral surface proteins [279]. In accordance with the IgG, IgA and IgM levels detected on the bead surface, varying phagocytosis of immune complex generated with plasma

from different donors was found. The correlation between antibody distribution (IgG, IgA or IgM) and level of phagocytosis is remarkable. Donors with high IgM levels showed lower phagocytosis and IL-8 release than donors with the same IgA or IgG but lower IgM (Figure 5-16). The effect can be explained by the assay setup and the high avidity of IgM [8]. Only antibodies from IgG or IgA class can mediate antibody-dependent phagocytosis via their FcR on neutrophils [242]. There is no IgM FcμR on neutrophils [59] (as well as on the here used neutrophil-like HL-60 cells) and COVID-19 convalescent plasma was heat-inactivated to inhibit classical or alternative complement pathway [280].

COVID-19 model can be transferred to primary neutrophils

As discussed above, the neutrophil-like phenotype of HL-60 cells is comparable to primary human neutrophils based on surface marker staining and cytokine release (compare chapter 6.1). Similarly, stimulation of neutrophil-like HL-60 cells or primary human neutrophils with SARS-CoV-2-like immune complex resulted in the secretion of several pro-inflammatory chemokines and cytokines (Figure 5-20). Specific inflammatory activation by SARS-CoV-2-like immune complex was also shown for primary neutrophils. Negative controls showed no phagocytosis and inflammatory activation (Figure 5-20). Observed differences in phagocytic activity and cytokine profile of primary neutrophils and neutrophil-like HL60 cells arise mainly due to enhanced phagocytic potency and short half-life of primary cells as reported [199,206,281,282]. This data justifies the suitability of the model system to depict severe COVID-19 and the usage of HL60 cells as an alternative to primary neutrophils on a functional level.

To summarize the results, high specificity and low background signal was demonstrated, making this assay a powerful platform to study virus- and bacterial-induced inflammation. It is possible to coat every pathogen-associated protein of interest onto the beads, studying relevant viruses like influenza or other coronaviruses [283]. Further studies using autoimmune targets, an important field of IVIg therapy, are possible [65,72].

The *in vitro* data from several donors show that immunoglobulin classes IgG and IgA are important for antibody-dependent phagocytosis of SARS-CoV-2 virus-like particles. This is consistent with clinical data showing antibody response from IgG and IgA type against SARS-CoV-2. Although again underestimated, IgA seems to have an important role, especially in the early immune response [261–264].

6.5.2. Trimodulin induces strong immune modulation in the COVID-19 model

As discussed above, immunoglobulin preparations are a fast available and long used therapeutic option in the treatment of inflammatory diseases [66]. Optimal therapy of COVID-19 with immunoglobulin preparations depends on the severity of the disease. COVID-19 can be divided into three stages with increasing severity (see introduction 1.3.4) [122,127]. In this work, the focus is on the treatment of severe

COVID-19 patients (stage III) with an exhausted immune system and hyperinflammation. Targeting of inflammatory host immune system is in this stage from greater importance than virus-induced damage [66]. Neutrophils are poorly studied in conjunction with viral respiratory diseases [6]. But a detrimental role of neutrophils in the context of hyperinflammation and COVID-19 is under discussion [6,137,284,285]. Therefore targeting inflammatory neutrophils of severe COVID-19 patients with immunoglobulin preparations could be beneficial [132]. The efficiency of trimodulin in severe infection diseases was shown in sCAP [82] and is now under clinical investigation for severe COVID-19 [83].

To underpin the clinical studies of trimodulin, immunomodulatory effects in comparison to IVIg were investigated in this work in the context of neutrophil inflammation and COVID-19 *in vitro* (chapter 5.5.3 and 5.5.4).

Modulation of cytokine release

The addition of therapeutically used concentrations of IVIg [65,224] or trimodulin similarly blocks the binding and uptake of SARS-CoV-2-like immune complex by FcR, as seen by the subsequent reduction of phagocytosis (Figure 5-18). However, the corresponding effector outcome (release of IL-1ra, IL-10, MCP-1, MIP-1α and IL-8) shows a significantly stronger immune modulation by trimodulin, which was shown to be in part FcαRI-dependent. The corresponding cytokine release was modulated as seen by increased levels of anti-inflammatory and decreased levels of pro-inflammatory cytokines (Figure 5-18), which were chosen based on characterization data (Figure 5-16) and COVID-19 literature [133–135].

The reduction of pro-inflammatory cytokines like IL-6, IL-8 and MCP-1 are commonly known aims of severe COVID-19 therapy, as elevation of these cytokines correlate with disease severity [134,141,286]. Therefore, antagonists of inflammatory cytokines, such as IL-6 receptor inhibitor (tocilizumab) or anti-IL-8 antibody (HuMax-IL-8) are in clinical testing for treatment of COVID-19 patients [287–289]. Also, the blockade of inflammatory IL-1 pathways with IL-1 receptor antagonists (anakinra) is a promising therapeutic option [141,162,290]. The strong upregulation of IL-1ra by trimodulin treatment could lead to similar effects. In contrast, the role of commonly known as anti-inflammatory IL-10 is under discussion. COVID-19 patients show elevated IL-10 levels which are known to correlate with disease severity and mortality [284,291]. Increasing evidence suggests IL-10 as a promotor of inflammation similar to IL-6 [292–294]. The reduction of IL-10 levels due to trimodulin treatment could be, therefore, beneficial for severe COVID-19 patients. Trimodulin showed immunomodulatory properties on the detection of COVID-19 relevant cytokines. The simultaneous modulation of several neutrophil-relevant cytokines could be an advantage compared to targeting one cytokine response (like IL-6, IL-8 inhibitors or IL-1 antagonists) [100,162]. Especially in systemic inflammatory diseases with cytokine storm, it could be important to target several mediators simultaneously to get neutrophil exhaustion under control.

Differences between primary cells and cell line

Immunomodulation was observed with the HL-60 cell model and primary human neutrophils treated with trimodulin or IVIg. In contrast to the cell line, primary cells show comparable IL-8 modulation by trimodulin and IVIg (Figure 5-20). This could be due to: (1) primary neutrophils express more IgG FcR, especially FcγRIII, in relation to IgA FcαRI (compare Figure 5-1). (2) The HL-60 cells are tumor cells with a more inflammatory basal phenotype than neutrophils directly isolated from healthy donors [200]. Increased expression and enhanced avidity between FcαRI and IgA are known as inside-out signaling for an inflammatory environment [21,36,52–54]. The more powerful immunomodulation elicited by trimodulin is, therefore, especially relevant in an inflammatory environment (like in sepsis, sCAP or COVID-19) when the additional IgA component can interact more strongly with its receptor FcαRI.

Strong ITAMi signaling induced by trimodulin

In the here established COVID-19 model trimodulin shows stronger immunomodulation compared to IVIg (Figure 5-18). As underlying mechanism ITAMi signaling was investigated:

Trimodulin induces a more powerful ITAMi signaling than IVIg resulting in stronger immune modulation. The activation of ITAMi signaling was demonstrated by measuring SHP-1 phosphorylation at side specific tyrosine after incubating cells with COVID-19 plasma immune complex and different concentrations of trimodulin or IVIg. Trimodulin showed in all concentrations stronger phosphorylation of SHP-1 than IVIg (Figure 5-19). Furthermore, SHP-1 was inhibited before the addition of immune complex and immunoglobulins. IL-8 release of SHP-1 inhibited cells (treated with immune complex and trimodulin) was compared to not inhibited cells significantly higher, indicating strong immunomodulation by ITAMi (Figure 5-19).

The stronger immunomodulatory effects of trimodulin lead to the hypothesis that neutralizing IgA species in convalescent plasma induce inflammation. In turn, this can be counteracted by the additional IgA component of trimodulin. The data from this work substantiate the theory of IgA as a promising immune modulator in COVID-19 therapy [23,87]. The stronger activation of inhibitory ITAMi signaling could be due to simultaneous targeting of FcγR and FcαRI, as well as bivalent binding of IgA to FcαRI [57,98]. Comments to first clinical trials of high dose IVIg treatment in COVID-19 patients mention these modes of action [194,295] however, this work provides the first *in vitro* data confirming this hypothesis.

The lots of these products were manufactured from plasma collected before COVID-19 pandemic and had no anti-SARS-CoV-2 neutralizing antibodies ([154] and *in house data*). In future lots, SARS-CoV-2 titers will rise. Therefore, a dual function, as seen for commonly known pathogens, like *S.aureus*, is expected (discussed in chapter 6.4.3). Phagocytosis would be enhanced during low-dose trimodulin addition, but in high doses, immunomodulation would still the central therapeutic effect.

As detailed discussed in the previous chapters (6.2.1, 6.3.3 and 6.4.3) the modulation of the immune response by immunoglobulin preparations is a combination of several modes of action. Blocking of

activating FcR, targeting of inhibitory FcR-signaling, modulation of FcR-expression or the interaction with soluble inflammatory molecules (complement factors, cytokines) are ways how immunoglobulins modulate the immune response [63,69,174]. Table 6-4 gives an overview of the relevant modes of action and the benefits of trimodulin for immunomodulation in the COVID-19 model.

Table 6-4: Immunomodulatory modes of action relevant in COVID-19 model. Each mode of action and the experimental parameters to prove this are compared. The strength of trimodulin or IVIg mediated effects is depicted as followed: +++ strong effects, ++ medium effects, + low effects, - no effects.

Immunomodulation in COVID-19 model (experimental setting):			
Reduction of SARS-CoV-2-like particle phagocytosis with different doses trimodulin or IVIg. Cytokine release (IL-8, IL-1ra, MCP-1, MIP1α, IL-10) and phagocytic activity as cellular readout.			
Immunomodulatory effector outcome			
Reduction of phagocytic activity and cytokine release.			
Mode of action	**Experimental parameter**	**Trimodulin (IgG/A/M)**	**IVIg (IgG)**
(1) Direct neutralization	Detection of remaining IL-8 in buffer	Not tested	Not tested
(2) ITAMi signaling	Inhibition of SHP-1 (change in IL-8) Phosphorylation of SHP-1 at pY536	+++	+
(3) ITIM signaling	Blocking of FcγRIIB	Not tested	Not tested
(4) Phenotype modulation	Expression of FcαRI, FcγRI, FcγRIIA, FcγRIII	Not tested	Not tested
(5) Displacement of immune complex	Reduced phagocytosis	+++	+++

6.5.3. Further aspects in COVID-19 therapy

If the immunomodulatory treatment with trimodulin is beneficial for severe COVID-19 patients is under evaluation in ESsCOVID-study [83]. A first case report using Pentaglobin®, another IgA- and IgM enriched immunoglobulin preparation, showed decreased inflammatory markers (CRP and IL-6) [296], confirming the here depicted hypothesis of IgA containing immunoglobulins as immune modulators. Monitoring of IgA antibody response in COVID-19 patients is neglected in many studies. Although especially in the early weeks after infection and in severe cases the IgA response seems to be important [261–264,267,297]. By screening patients with strong IgA mediated inflammatory response, trimodulin therapy could be particularly promising.

The phenomenon of antibody-dependent enhancement (ADE) of viral infection is known for multiple viruses such as dengue, flavivirus and influenza virus [298]. ADE is a possible mechanism of SARS-CoV-2 infection and exacerbation of COVID-19 symptoms [299]. Studies trying to investigate the role of ADE for viral infection showed the central role of FcγRI and FcγRIIA for this process [271,272,300]. The importance of FcγRI and FcγRIIA for SARS-CoV-2 infection was shown in this work and by Hoepel and colleagues [131] although the link to ADE is yet missing.

The treatment of severe COVID-19 patients (or other viral infections) with IVIg preparations could inhibit ADE by blocking FcR availability [61,66,148,194,301]. The data in this work strongly support the hypothesis of FcR blocking and displacement of the viral immune complex; leading to inhibition of ADE. Besides IgG also IgM or IgA antibodies can mediate ADE [298]. The here shown targeting of FcαRI by IgA coated virus-like particles indicates superior effects of trimodulin over standard IVIg in treatment of a possibly SARS-CoV-2 induced ADE.

Another threat for severe COVID-19 patients are co-infections, which were shown to worsen the clinical outcome. Different studies highlighting that a relevant portion of COVID-19 patients suffers from bacterial or viral co-infections [155,157,229–231]. Immunoglobulin preparations combine several modes of action and could be, therefore, immunomodulatory and simultaneously fight co-infections [66,156]. The dual function of trimodulin was shown in this work. On the one hand, trimodulin has anti-pathogenic activity against common pathogens (in this work shown for *S.aureus*); on the other hand, trimodulin can powerfully modulate the inflammatory cell response induced by SARS-CoV-2 like immune complex. These results are hints that trimodulin could improve the clinical outcome of co-infected COVID-19 patients.

6.5.4. Concluding remarks COVID-19

It is important to say that the whole immune system is modified and exhausted in severe COVID-19 patients, adaptive and innate immunity are affected [66,302]. The here developed neutrophil *in vitro* model cannot depict this complexity. It is rather one instrument to understand processes in the fight against COVID-19. Besides COVID-19, the inflammation model can be easily adapted to every pathogen or immune cell of interest, making it a versatile platform for immunological investigations.

The here demonstrated immunomodulation related to IVIg and trimodulin treatment could be beneficial for COVID-19 patients. The data indicate the benefits of trimodulin above standard IVIg treatment. Advantages were shown to be due to the additional IgA component and ITAMi signaling. Particularly in the focus of respiratory diseases, like COVID-19, IgA seems to be an important therapeutic molecule. The observed immunomodulatory effects have yet to be tested in clinical studies to demonstrate the efficacy of this product class.

6.6. Comparative discussion

When comparing the results of this work recurring insights become obvious. One major finding is that trimodulin and IVIg mediate anti-inflammatory effects in all tested settings by a combination of several modes of action. The identified modes of action were summarized in Table 6-5.

Table 6-5: Overview of immunomodulatory modes of action demonstrated for trimodulin or IVIg in different model systems. Each mode of action and the experimental parameters to prove them are listed. It is indicated for which model system each mode of action was proven. The strength of trimodulin or IVIg mediated effects is depicted as followed: +++ strong effects, ++ medium effects, + low effects, - no effects, n.t not tested.

Immunomodulatory effector outcomes mediated by trimodulin					
• **Facilitation of immune homeostatic conditions on resting cells** • **Modulation of LPS induced inflammation** • **Reduced phagocytosis of *S.aureus* in high doses** • **Modulation of COVID-19-like inflammation**					
Mode of action	**Experimental parameter**	**Shown in model system**		**Trimodulin (IgG/A/M)**	**IVIg (IgG)**
(1) Direct neutralization	Detection of IL-8 in buffer	Resting cells (5.2)	X	++	+
		Endotoxin (5.3)	n.t		
		S.aureus phagocytosis (5.4)	n.t		
		COVID-19 (5.5)	n.t		
(2) ITAMi signaling	Inhibition of SHP-1 Phosphorylation of SHP-1 at pY536	Resting cells (5.2)	X	+++	+
		Endotoxin (5.3)	n.t		
		S.aureus phagocytosis (5.4)	X	++	+++
		COVID-19 (5.5)	X	+++	+
(3) ITIM signaling	Inhibition of SHIP-1 Expression /Blocking of FcγRIIB	Resting cells (5.2)	X	++	++
		Endotoxin (5.3)	X	+++	-
		S.aureus phagocytosis (5.4)	X	+	+
		COVID-19 (5.5)	n.t		
(4) Phenotype modulation	Expression of FcαRI, FcγRI, FcγRIIA, FcγRIII	Resting cells (5.2)	X	+	+
		Endotoxin (5.3)	X	+++	-
		S.aureus phagocytosis (5.4)	n.t		
		COVID-19 (5.5)	n.t		
(5) Displacement of immune complex	Reduced phagocytosis	Resting cells (5.2)	n.t		
		Endotoxin (5.3)	n.t		
		S.aureus phagocytosis (5.4)	X	++	++
		COVID-19 (5.5)	X	+++	+++

Modes of action like the direct binding of cytokines or toxins by immunoglobulins have an influence on the cellular environment of each *in vitro* setting. Also binding of immunoglobulins to cellular-FcR occur in every experiment and influences the cellular effector outcome. For example by activation of ITAMi signaling, induction of FcR internalization or upregulation of inhibitory FcγRIIB. Other modes of action are more specific, like the displacement of immune complex from activating FcR. This mode of action can only occur when immune complex are available.

Although the human immune system is a highly complex network with multiple players, this work shows fundamental mechanisms, which seemed to be transferable between different pathogens. Implicating, that these modes of action can be assumed as general mechanisms for immunomodulation by immunoglobulin preparations.

Important to say is, that the measured effector outcome (e.g. cytokine release or phagocytosis) is an offsetting effect of inflammatory- and immunomodulatory- stimuli to the cell [42]. During the treatment with immunoglobulin preparations, the balance can be shifted to one or the other side. The experiments show that high dosages of trimodulin or IVIg were able to shift the balance to the side of immunomodulation, facilitating immune homeostatic conditions. When extending the view apart from immunomodulation, immunoglobulins can mediate further anti-pathogenic effects in a lower dosage. These could be especially beneficial when co-infections occur. In sepsis, sCAP or COVID-19 co-infections are a major problem affecting many patients [112,116,157].

Therefore, optimal treatment dosage and characterization of patients' immune status is elementary.

The multiplicity of modes of action mediated by immunoglobulin preparations could have a benefit in complex diseases, like severe infection diseases when the whole immune system is exhausted [104,127]. Many pathways were triggered simultaneously thereby mediating stronger effects, in comparison to target only one single pathway.

7. Conclusion and outlook

This work aimed to unravel the immunomodulatory properties of the IgM- and IgA-enriched immunoglobulin preparation trimodulin. Therefore, four central questions should be answered:

Can trimodulin induce immune modulation on neutrophils? Trimodulin shows multiple immunomodulatory activities on neutrophils in several experimental settings. Among them is facilitating the anti-inflammatory phenotype of resting neutrophils, shown by reduced cytokine release and modulation of cell phenotype. The reduction of inflammation in bacterial context was demonstrated by counteracting LPS induced effects and the reduction of *S.aureus* phagocytosis in high doses. Further strong anti-inflammatory properties against SARS-CoV-2-virus-like inflammation in the context of COVID-19 were presented.

In the context of severe infection diseases, the results of this work indicate the possible effects of trimodulin in the therapy of patients with a hyperinflammatory immune system. Clinical phase II study revealed the efficacy of trimodulin in severe bacterial-induced sCAP [82], further studies in sCAP and COVID-19 patients will demonstrate the relevance of these *in vitro* data. The monitoring of inflammatory markers, as well as immunoglobulin status of the patients within these clinical studies, could help to compare *in vitro* with *in vivo* data and improve immunoglobulin therapy. As the *in vitro* data indicate, it could be important to access the immune status of the patient for optimal therapeutic dosage.

Which pathways induce immune modulation? This work shows that several modes of action are important for the observed immunomodulation on neutrophil cells. For the first time, this work shed light on the complex immunomodulatory mechanism of trimodulin. It was demonstrated that five modes of action were targeted by trimodulin and work synergistically (compare Figure 7-1). Inflammatory mediators (here inflammatory IL-8) were directly bound by trimodulin and cannot induce further inflammation (1). Inhibitory ITAMi signaling was activated by monomeric immunoglobulins in trimodulin (2). Targeting of inhibitory FcγRIIB and corresponding ITIM signaling counteracts inflammatory FcR signaling (3). The cellular phenotype was modulated by the interaction of immunoglobulins with their FcR. Trimodulin reduced the expression of activating FcR (FcαRI, FcγRIIA) (4). Particularly high doses of trimodulin could displace, compete or block the binding of immune complex to activating FcR, which leads to reduced phagocytosis and subsequent less inflammatory cell activation. Presumably, multimeric species of trimodulin could mediate these effects (5).

These pathways were observed for several inflammatory stimuli followed by trimodulin-mediated immunomodulation. Therefore, these pathways can be attributed as fundamental immunomodulatory modes of action. The data show the central role of the immunoglobulin-FcR interaction and corresponding signaling events for the immune response. This highlights the need to understand and target immunomodulatory pathways in future therapy.

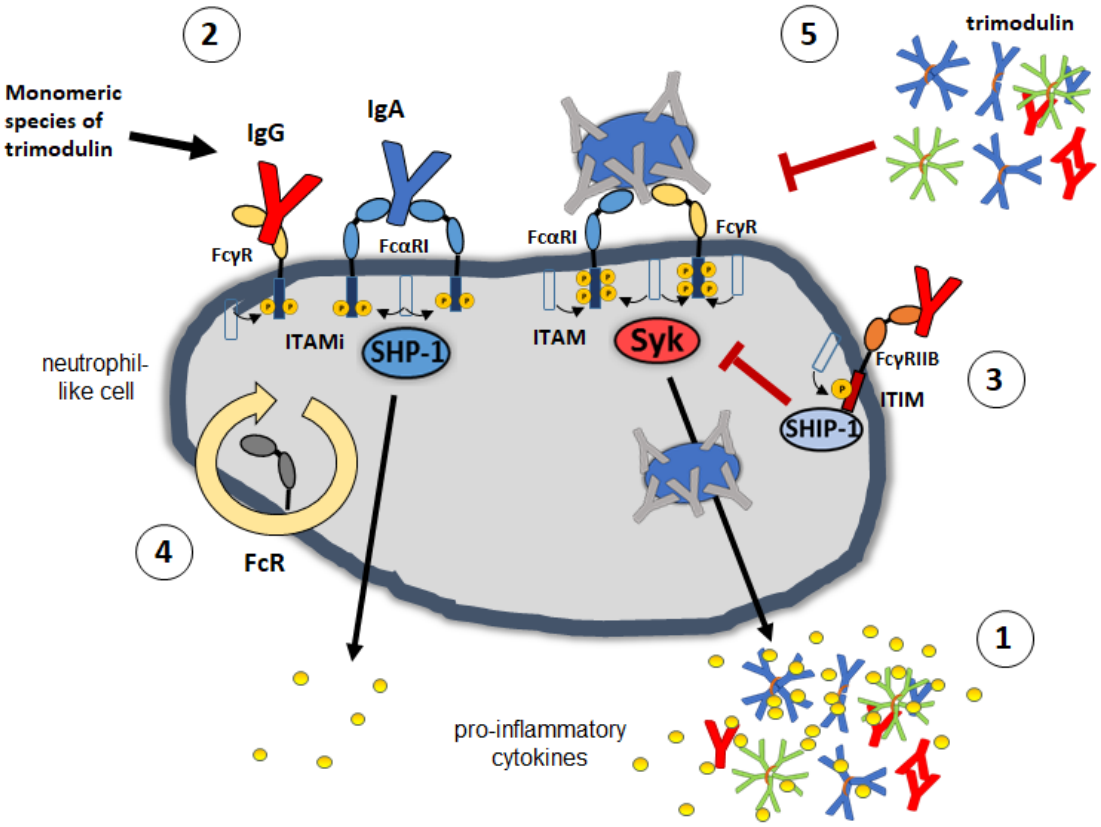

Figure 7-1: Schematic overview of trimodulin modes of action resulting in immunomodulation. **(1)** Direct binding and possible neutralization of cytokines by immunoglobulins. **(2)** Targeting of Fc-receptors (FcR) by monomeric IgA or IgG components of trimodulin induces inhibitory immunoreceptor tyrosine-based activation motif (ITAMi) signaling, resulting in reduced pro-inflammatory cytokine release. **(3)** Interaction with FcγRIIB and inhibitory immunoreceptor tyrosine-based inhibition motif (ITIM) signaling inhibits inflammatory signaling pathways. **(4)** Trimodulin modulates FcR expression. **(5)** Presumably, multimeric immunoglobulin species limit the access of immune complex to activating FcRs due to displacement, competition or blocking. Reduced immune complex binding decreases the pro-inflammatory cytokine release. Immunoglobulins indicated in red represent IgG, blue IgA and green IgM species of trimodulin. Gray represents immunoglobulins from IgG or IgA species.

Has trimodulin superior immunomodulatory effects in comparison to standard IVIg? Superior immunomodulation of trimodulin was demonstrated on resting neutrophils induced by stronger direct binding of inflammatory IL-8 and more powerful activation of ITAMi signaling. In addition, LPS induced inflammation was more efficiently counteracted by trimodulin in comparison to IVIg. Trimodulin shows a better ability to modulate the cellular phenotype, as seen by targeting FcαRI, FcγRIIA and FcγRIIB expression. Counteracting of immune complex-induced inflammation was shown in high doses for *S.aureus* and COVID-19 model system. Although no differences in blocking immune complex uptake was observed, the inflammatory cytokine release was stronger reduced by trimodulin.

Previous data from *in vitro*, as well as clinical studies, indicate superior effects of IgM- and IgA-enriched immunoglobulins [15,67,74,75,77,184,185]. Although the data generated in this work unravel some detailed mechanism for improved immunomodulation, further studies are required to understand the benefits of these highly complex IgM- and IgA-enriched immunoglobulins in severe infection diseases.

What is the functional relevance of IgA in immune modulation? The interactions of trimodulin with FcαRI were demonstrated in several experiments, highlighting the important role of IgA in trimodulin mediated immunomodulation. Based on experimental design, the role of IgM in trimodulin is of minor importance for FcR mediated effector functions on neutrophils, therefore the beneficial immunomodulatory effects can be attributed to the IgA component.

In this work, IgA was identified (besides IgM and IgG) as an active component in IgM- and IgA-enriched immunoglobulins. Further, this seems to enhance immunomodulatory properties. Due to ongoing research in the field, a growing number of inflammatory and anti-inflammatory functions of IgA in serum were identified [21]. IgA functions in plasma products are similarly a beginning research field with many remaining questions.

However, also synergistic effects between monomeric and multimeric IgG, IgA and IgM species or differences in IgG subclasses could promote benefits in trimodulin-induced immunomodulation. Currently, an adequate separation of functional IgM, IgA and IgG species (and therefore a direct proof for the importance of each species) is not possible. Commercially available purified IgM, IgA and IgG preparations are also not suited for comparison based on a different manufacturing process and biochemical characteristics. Enlarged knowledge of the functions of each immunoglobulin component, like multimeric IgA or IgM might be helpful for the development of new plasma products. For example, personalized products for patients with low IgG, IgA or IgM levels or specific therapeutic indications. Therefore, trimodulin has to be tested, concerning the single components, more comprehensively.

The polyclonal nature of trimodulin enables multiple effector functions, by immunomodulation on the one hand and anti-pathogenic effects on the other hand. In comparison to broad immune inhibitors, dampening the complete immune system [156], it seems beneficial to treat complex diseases with polyfunctional immunoglobulin preparations. In the human immune system, every immunoglobulin class has multiple receptors and important effector functions [8]. A preparation like trimodulin can rely on mechanisms and receptors of IgG, IgA and IgM class enabling to target more pathways than classical IgG containing IVIg.

In summary, the given questions were answered successfully within the experiments of this PhD thesis. The immunomodulatory properties of trimodulin were successfully shown. This work demonstrates that multiple modes of action work synergistically to mediate the observed immunomodulation on neutrophils. Finally, the work sheds light on the importance of serum IgA-induced immunomodulation and the capabilities of IgA as an active ingredient in pharmaceutical plasma products like trimodulin.

Outlook

IgM- and IgA-enriched immunoglobulins are a highly complex class of therapeutics [62,64,73]. While several modes of action were attributed to the IgG and IgM components, the role of IgA was not clarified. The results of this work indicate that the importance of serum IgA is underrated. Therefore, further research on IgA is necessary to identify the entire functional spectrum of this immunoglobulin class.

In contrast, the crucial role of IgA in mucosal immunity is well known [27]. Also in pulmonary diseases like sCAP or COVID- 19 IgA seems to be an important player, but comprehensive studies are lacking [23,87,303]. In line with this, it would be interesting if IgA species from trimodulin can reach the lung and support the defense against pathogens on the mucosa.

As mentioned throughout this thesis the immune system is a complex network with multiple interacting cell types and proteins [1,2]. In this work, solely neutrophils (and mainly a neutrophil-like cell line) were used as immune effector cells with a limited number of inflammatory stimuli and effector readouts. Therefore, several other immune cell lines or primary cells could be tested, for example, macrophages, B-cells, T-cells, NK-cells or dendritic cells. Besides LPS further bacterial toxins (e.g. of gram$^+$ bacteria, like lipoteichoic acid) or viral stimuli could be tested. The anti-pathogenic properties of trimodulin could be investigated with other pathogens commonly known to be involved in severe infection diseases (e.g. *Streptococcus pneumoniae*). In addition, there are much more effector outcomes (and the modulation of these effector outcomes) that can be studied, as ADCC, granula-, ROS- or NET-release.

Besides this research on inflammatory diseases, the efficiency of IgM- and IgA-enriched immunoglobulins in autoimmune diseases could be a future research topic. In autoimmune diseases, modes of action like neutralization of autoantibodies or interaction with FcRn could be analyzed.

The heterogeneity of natural immunoglobulins by post-translational modifications is also a research field that enables therapeutic opportunities. Antibody glycosylation for example is a key player that influences the immunoglobulin FcR interaction and corresponding effector functions [46,68,304]. Altered antibody glycosylation is known for many diseases including autoimmune and infection diseases [305,306]. In further research, it could be addressed if immunoglobulin preparations can help to circumvent problems arising with aberrant antibody glycosylation profiles.

The identification of modes of action for the human immunoglobulins and immunoglobulin preparations is an ongoing research topic during the last decades and a lot of knowledge was generated during this time [63,65,69]. This fact demonstrates the complexity and diversity of this product class. Further, the complexity of the immunoglobulin interaction partners and the human immune system increase the possibilities in this research field.

To sum up this chapter, there are many interesting research questions, which can be addressed by further *in vitro* and *in vivo* studies. There is still a lot to do to understand the multifaceted functions and the interplay between all immunoglobulin components and the immune system. Finally, this knowledge will help to treat patients with multiple diseases.

8. Appendix

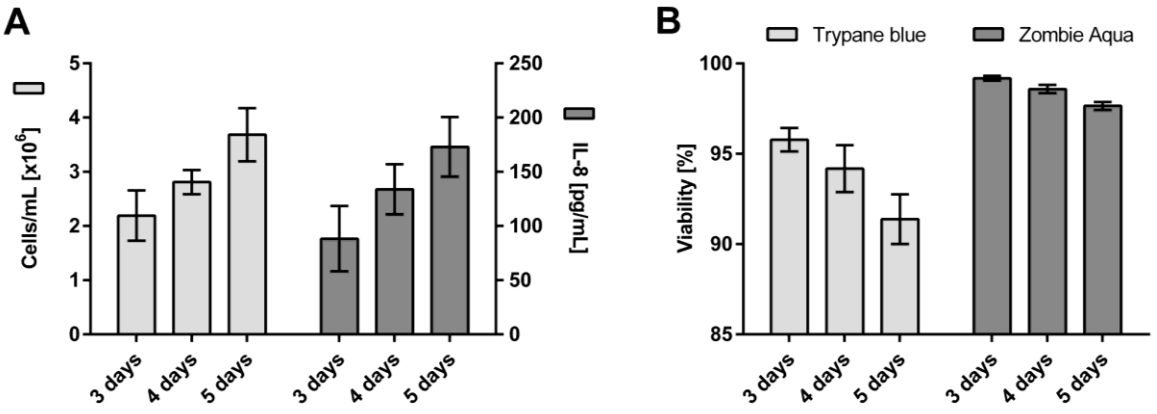

Figure 8-1: Cell number, IL-8 release and cell viability during the HL-60 cell differentiation process. **(A)** Cell number and IL-8 release. HL-60 cells were cultivated for indicated days with 1.3 % (v/v) dimethylsulfoxide (DMSO) at 37 °C. Cell number was determined by Neubauer-improved chamber, IL-8 release in cell culture supernatant was determined by ELISA kit. **(B)** Cell viability of HL-60 cells. Same as in (A), cells were incubated after cultivation with 0.2 % trypane blue, dead cells were counted. Viability with zombie-aqua was determined via flow-cytometry staining as described.

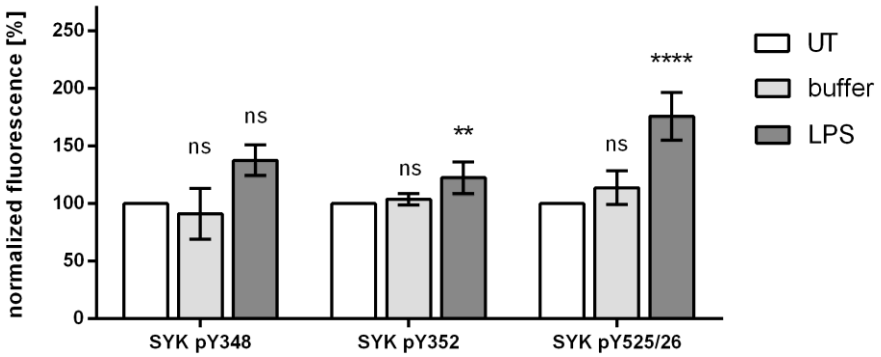

Figure 8-2: LPS treatment induces ITAM signaling by phosphorylation of SYK at tyrosine 348 (pY536), 352 (pY352) and 525/526 (pY525/26). Cells were treated for 30 min with 500 ng/mL LPS. Cells were fixed, permeabilized and stained with indicated anti-phospho-SYK antibodies. The fluorescence signal was measured by flow cytometry and normalized to buffer treated cells. Values represent mean of 6 independent experiments. Statistics: Two-way ANOVA; Tukey's multiple comparisons test.

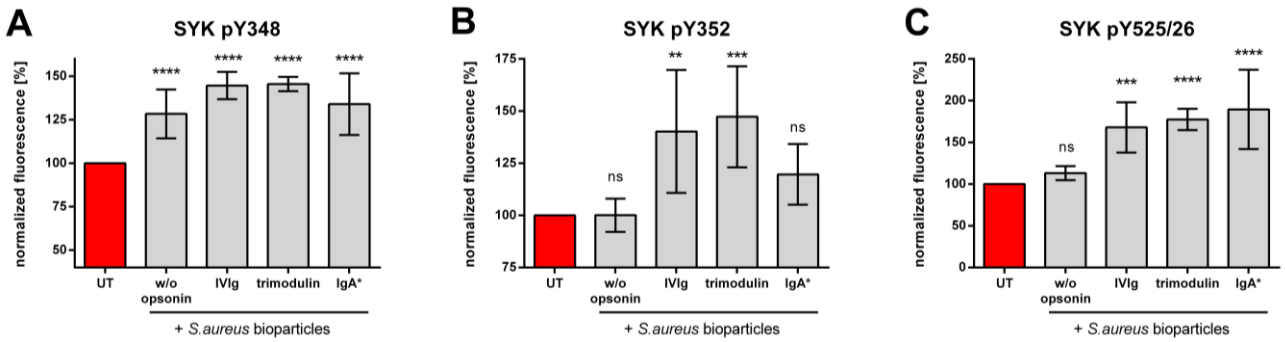

Figure 8-3: *S.aureus* immune complex treatment induce ITAM signaling by phosphorylation of SYK at **(A)** tyrosine 348 (pY536), **(B)** tyrosine 352 (pY352) and **(C)** tyrosine 525/526 (pY525/26). Cells were treated for 30 min with *S.aureus* without (w/o) opsonin, *S.aureus*-IVIg, -trimodulin, or IgA-IC. *Purified monomeric IgA from human serum (Sigma-Aldrich). Cells were fixed,

permeabilized and stained with indicated anti-phospho-SYK antibodies. The fluorescence signal was measured by flow cytometry and normalized to buffer treated cells. Data show the mean of 6 independent experiments. Statistics: One way ANOVA; Dunnett's multiple comparisons test.

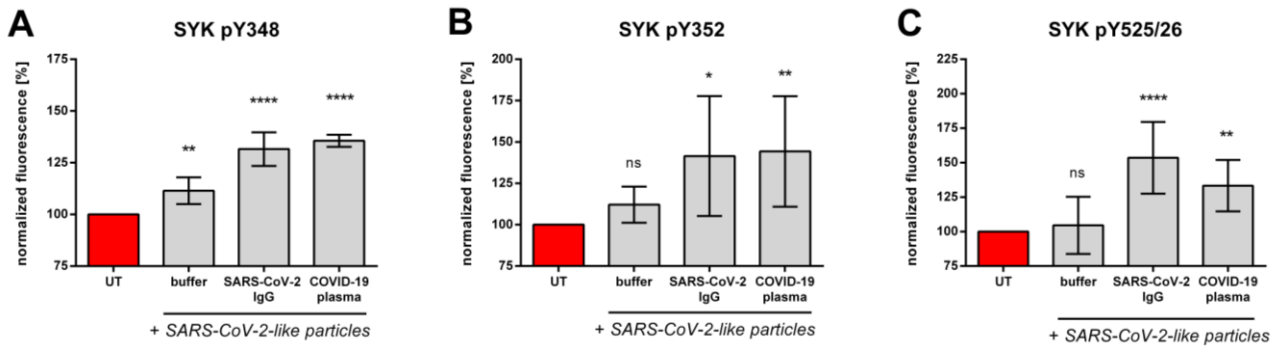

Figure 8-4: SARS-CoV-2-like immune complex treatment induces ITAM signaling by phosphorylation of SYK at **(A)** tyrosine 348 (pY536), **(B)** tyrosine 352 (pY352) and **(C)** tyrosine 525/526 (pY525/26). Cells were treated for 30 min with buffer, SARS-CoV-2-IgG-IC or COVID-19 plasma-IC. Cells were fixed, permeabilized and stained with indicated anti-phospho-SYK antibodies. The fluorescence signal was measured by flow cytometry and normalized to buffer treated cells. Data show the mean of 6 independent experiments. Statistics: One way ANOVA; Dunnett's multiple comparisons test.

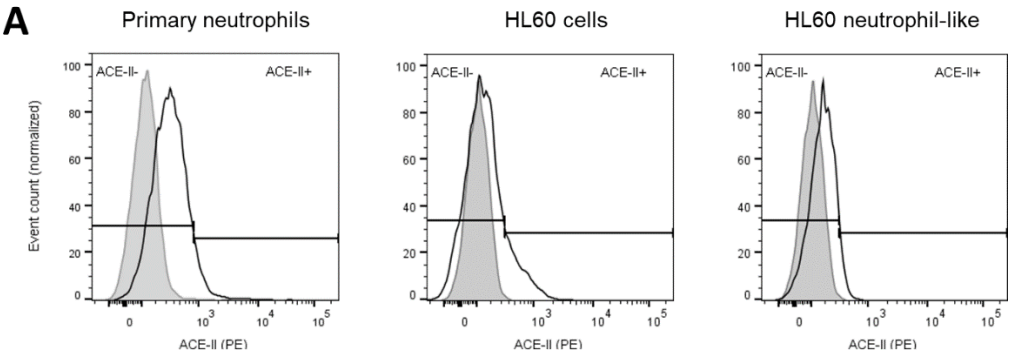

B

Cell type	ACE-II positive cells [%]
HL60 cells	7.4
HL60 neutrophil-like (4 days DMSO)	14.6
Primary neutrophils	12.5

Figure 8-5: ACE-II expression on neutrophil-like HL-60 cells and primary neutrophils. **(A)** Exemplary data showing histograms of ACE-II receptor staining for indicated cell types. HL-60 cells were differentiated by adding 1.3 % (v/v) dimethylsulfoxide (DMSO) into cell culture medium for 4 days, primary neutrophils were isolated from human blood donations. Cells were washed, stained with ACE-II detection antibodies and analyzed by flow cytometry. **(B)** Mean values of ACE-II receptor-positive cells. Data show the mean of 3 independent experiments.

List of abbreviations

Abbreviation	Advertised
° C	Degree celsius
μg	Micro gram
ABC	Antibody binding capacity
ADAM17	A disintegrin and metalloprotease 17
ADCC	Antibody-dependent cell-mediated cytotoxicity
ADCP	Antibody-dependent cellular phagocytosis
ADE	Antibody-dependent enhancement
AF	Alexa fluor™
AmCyan	*Anemonia majano* Cyan
ANOVA	Analysis of variance
APC	Allophycocyanin
ARDS	Acute respiratory distress syndrome
ATCC	American Type Culture Collection
BCR	B-cell receptor
BSA	Bovine serum albumin
BV	Brilliant Violet™
CAP	Community-acquired pneumonia
CDC	Complement-dependent cytotoxicity
COVID-19	Coronavirus disease 2019
DMSO	Dimethyl sulfoxide
D-PBS	Dulbecco's PBS
E. coli	Escherichia coli
e.g.	Exempli Gratia
ELISA	Enzyme-linked Immunosorbent Assay
et al.	et alii/aliae (and others)
Fab	Fragment antigen-binding
FACS	Fluorescence-activated cell sorter
FBS	Fetal bovine serum
Fc	Fragment crystallizable
FcμR	Fcμ receptor
FcR	Fc-receptor
FcγR	Fcγ-receptor
FcγRIIB	Fcγ-receptor II B

Abbreviation	Advertised
FcαRI	Fcα-receptor I
FcγRIIA	Fcγ-receptor II A
FcγRIII	Fcγ-receptor III
FITC	Fluorescein isothiocyanate
FSC	Forward scatter
g	gram
h	Hour
hi	Heat-inactivated
IC	Immune complex
ICU	Intensive care unit
Ig	Immunoglobulin
IgA	Immunoglobulin A
IgG	Immunoglobulin G
IgM	Immunoglobulin M
IL	Interleukin
IL-1ra	Interleukin-1 receptor antagonist
ITAM	Immunoreceptor tyrosine-based activation motif
ITAMi	Inhibitory immunoreceptor tyrosine-based activation motif
ITIM	Immunoreceptor tyrosine-based inhibition motif
ITP	Immune thrombocytopenia purpura
IV	Intravenous
IVIg	Intravenous immunoglobulin
kDa	Kilo Dalton
L	liter
LPS	Lipopolysaccharide
LTA	Lipoteichoic acid
MERS	Middle East respiratory syndrome
MFI	Median fluorescence intensity
min	Minute
mL	Milli-liter
MoAModes of action	Mode of ActionModes of action
MS	multiple sclerosis
NET	Neutrophil extracellular traps
NK cell	Natural killer cell

Abbreviation	Advertised
OD	Optical density
PAMP	Pathogen-associated molecular patterns
PBS	Phosphate-buffered saline
PE	Phycoerythrin
PerCP	Peridinin-chlorophyll-protein complex
pIgR	Polymeric Ig receptor
PMN	Polymorphonuclear
PRR	Pattern recognition receptor
RA	Rheumatoid arthritis
ROS	Reactive oxygen species
RT	Room temperature
S. aureus	*Staphylococcus aureus*
SARS	Severe acute respiratory syndrome
SARS-CoV-2	Severe acute respiratory syndrome coronavirus 2
sCAP	Severe community-acquired pneumonia
SEM	Standard error of the mean
SIgA	Secretory IgA
SLE	Systemic lupus erythematosus
SSC	Sideward scatter
TLR	Toll-like receptor
TNF	Tumor necrosis factor
w/o	Without
x g	x-times gravity

List of figures

List of tables

References

1. Marshall, J. S., Warrington, R., Watson, W. & Kim, H. L. An introduction to immunology and immunopathology. *Allergy Asthma Clin. Immunol.* 14, 49 (2018).
2. Chaplin, D. D. Overview of the immune response. *J. Allergy Clin. Immunol.* 125, S3–S23 (2010).
3. Thompson. The Immune System. *JAMA* 1 (2015).
4. Murphy, K. M. & Weaver, C. *Janeway's immunobiology*. (GS, Garland Science, Taylor & Francis Group, 2017).
5. Wang, X., Qiu, L., Li, Z., Wang, X.-Y. & Yi, H. Understanding the Multifaceted Role of Neutrophils in Cancer and Autoimmune Diseases. *Front. Immunol.* 9, (2018).
6. Camp, J. V. & Jonsson, C. B. A Role for Neutrophils in Viral Respiratory Disease. *Front. Immunol.* 8, (2017).
7. Lu, L. L., Suscovich, T. J., Fortune, S. M. & Alter, G. Beyond binding: antibody effector functions in infectious diseases. *Nat. Rev. Immunol.* 18, 46–61 (2017).
8. Späth, P. J. Structure and Function of Immunoglobulins. *Sepsis* 197–218 (2000).
9. Schroeder, H. W. & Cavacini, L. Structure and function of immunoglobulins. *J. Allergy Clin. Immunol.* 125, S41–S52 (2010).
10. Johansen, Braathen & Brandtzaeg. Role of J Chain in Secretory Immunoglobulin Formation. *Scand. J. Immunol.* 52, 240–248 (2000).
11. Michaelsen, T. E. *et al.* Human Secretory IgM Antibodies Activate Human Complement and Offer Protection at Mucosal Surface. *Scand. J. Immunol.* 85, 43–50 (2017).
12. Randall, T. D., Brewer, J. W. & Corley, R. B. Direct evidence that J chain regulates the polymeric structure of IgM in antibody-secreting B cells. *J. Biol. Chem.* 267, 18002–18007 (1992).
13. Boes, M. Role of natural and immune IgM antibodies in immune responses. *Mol. Immunol.* 37, 1141–1149 (2000).
14. Ehrenstein, M. R. & Notley, C. A. The importance of natural IgM: scavenger, protector and regulator. *Nat. Rev. Immunol.* 10, 778–786 (2010).
15. Stephan, W. Antibacterial and antitoxic efficancy of an IgM-enriched Intravenous Immunoglobulin Preparation. *Immune Consequences Trauma Shock Sepsis* (1989).
16. Goulet, D. R. & Atkins, W. M. Considerations for the Design of Antibody-Based Therapeutics. *J. Pharm. Sci.* 109, 74–103 (2020).
17. Vidarsson, G., Dekkers, G. & Rispens, T. IgG Subclasses and Allotypes: From Structure to Effector Functions. *Front. Immunol.* 5, (2014).
18. Napodano, C. *et al.* Immunological Role of IgG Subclasses. *Immunol. Invest.* 1–18 (2020) doi:10.1080/08820139.2020.1775643.

19. de Sousa-Pereira, P. & Woof, J. M. IgA: Structure, Function, and Developability. *Antibodies* 8, 57 (2019).
20. Suzuki, T., Ainai, A. & Hasegawa, H. Functional and structural characteristics of secretory IgA antibodies elicited by mucosal vaccines against influenza virus. *Vaccine* 35, 5297–5302 (2017).
21. Bakema, J. E. & van Egmond, M. Immunoglobulin A: A next generation of therapeutic antibodies? *mAbs* 3, 352–361 (2011).
22. Woof, J. M. & Russell, M. W. Structure and function relationships in IgA. *Mucosal Immunol.* 4, 590–597 (2011).
23. Russell, M. W., Moldoveanu, Z., Ogra, P. L. & Mestecky, J. Mucosal Immunity in COVID-19: A Neglected but Critical Aspect of SARS-CoV-2 Infection. *Front. Immunol.* 11, (2020).
24. Strugnell, R. A. & Wijburg, O. L. C. The role of secretory antibodies in infection immunity. *Nat. Rev. Microbiol.* 8, 656–667 (2010).
25. Suzuki, T. *et al.* Relationship of the quaternary structure of human secretory IgA to neutralization of influenza virus. *Proc. Natl. Acad. Sci.* 112, 7809–7814 (2015).
26. Wang, Z. *et al. Enhanced SARS-CoV-2 Neutralization by Secretory IgA in vitro*. http://biorxiv.org/lookup/doi/10.1101/2020.09.09.288555 (2020) doi:10.1101/2020.09.09.288555.
27. Corthésy, B. Multi-Faceted Functions of Secretory IgA at Mucosal Surfaces. *Front. Immunol.* 4, (2013).
28. Diebel, L. N., Liberati, D. M., Diglio, C. A. & Brown, W. J. Immunoglobulin a modulates inflammatory responses in an in vitro model of pneumonia. *J. Trauma* 59, 1099–1106 (2005).
29. Diebel, L. N., Amin, P. B. & Liberati, D. M. Sequence of Immunoglobulin Isotype Exposure Modulates Inflammatory Response to Bacteria and Lipopolysaccharide in Vitro <sup/>. *Surg. Infect.* 11, 145–150 (2010).
30. Longet, S. *et al.* Human Plasma-derived Polymeric IgA and IgM Antibodies Associate with Secretory Component to Yield Biologically Active Secretory-like Antibodies. *J. Biol. Chem.* 288, 4085–4094 (2013).
31. Breedveld, A. & van Egmond, M. IgA and FcαRI: Pathological Roles and Therapeutic Opportunities. *Front. Immunol.* 10, 553 (2019).
32. van Gool, M. M. J. & van Egmond, M. IgA and FcαRI: Versatile Players in Homeostasis, Infection, and Autoimmunity. *ImmunoTargets Ther.* Volume 9, 351–372 (2021).
33. Mkaddem, S. B. *et al.* IgA, IgA Receptors, and Their Anti-inflammatory Properties. in *Fc Receptors* (eds. Daeron, M. & Nimmerjahn, F.) vol. 382 221–235 (Springer International Publishing, 2014).
34. Roos, A. *et al.* Human IgA Activates the Complement System Via the Mannan-Binding Lectin Pathway. *J. Immunol.* 167, 2861–2868 (2001).

35. Hogarth, P. M. & Pietersz, G. A. Fc receptor-targeted therapies for the treatment of inflammation, cancer and beyond. *Nat. Rev. Drug Discov.* 11, 311–331 (2012).
36. Koenderman, L. Inside-Out Control of Fc-Receptors. *Front. Immunol.* 10, (2019).
37. van Egmond, M., Vidarsson, G. & Bakema, J. E. Cross-talk between pathogen recognizing Toll-like receptors and immunoglobulin Fc receptors in immunity. *Immunol. Rev.* 268, 311–327 (2015).
38. Rosales, C. Fcγ Receptor Heterogeneity in Leukocyte Functional Responses. *Front. Immunol.* 8, (2017).
39. Lu, L. L., Suscovich, T. J., Fortune, S. M. & Alter, G. Beyond binding: antibody effector functions in infectious diseases. *Nat. Rev. Immunol.* 18, 46–61 (2018).
40. Kubagawa, H. *et al.* Functional Roles of the IgM Fc Receptor in the Immune System. *Front. Immunol.* 10, (2019).
41. Kerntke, C., Nimmerjahn, F. & Biburger, M. There Is (Scientific) Strength in Numbers: A Comprehensive Quantitation of Fc Gamma Receptor Numbers on Human and Murine Peripheral Blood Leukocytes. *Front. Immunol.* 11, (2020).
42. Vogelpoel, L. T. C., Baeten, D. L. P., de Jong, E. C. & den Dunnen, J. Control of Cytokine Production by Human Fc Gamma Receptors: Implications for Pathogen Defense and Autoimmunity. *Front. Immunol.* 6, (2015).
43. Nimmerjahn, F. & Ravetch, J. V. Fc-Receptors as Regulators of Immunity. in *Advances in Immunology* vol. 96 179–204 (Elsevier, 2007).
44. Wang & Jönsson. Expression, Role, and Regulation of Neutrophil FcγReceptors. *Front. Immunol.* 10, 1958 (2019).
45. Matlung, H. L. *et al.* Neutrophils Kill Antibody-Opsonized Cancer Cells by Trogoptosis. *Cell Rep.* 23, 3946-3959.e6 (2018).
46. Patel, K. R., Roberts, J. T. & Barb, A. W. Multiple Variables at the Leukocyte Cell Surface Impact Fc γ Receptor-Dependent Mechanisms. *Front. Immunol.* 10, 223 (2019).
47. Barb, A. W. Fc γ receptor compositional heterogeneity: considerations for immunotherapy development. *J. Biol. Chem.* jbc.REV120.013168 (2020) doi:10.1074/jbc.REV120.013168.
48. Huizinga, T. W. J. *et al.* The Pi-linked receptor FcRIII is released on stimulation of neutrophils. *Nature* 333, 667–669 (1988).
49. Middelhoven, P. J., Van Buul, J. D., Hordijk, P. L. & Roos, D. Different proteolytic mechanisms involved in FcgammaRIIIb shedding from human neutrophils. *Clin. Exp. Immunol.* 125, 169–175 (2001).
50. Chenoweth, A. M., Wines, B. D., Anania, J. C. & Mark Hogarth, P. Harnessing the immune system *via* FcγR function in immune therapy: a pathway to next-gen mAbs. *Immunol. Cell Biol.* 98, 287–304 (2020).

51. Leong, K. W. & Ding, J. L. The Unexplored Roles of Human Serum IgA. *DNA Cell Biol.* 33, 823–829 (2014).
52. Bakema, J. E. & van Egmond, M. The human immunoglobulin A Fc receptor FcαRI: a multifaceted regulator of mucosal immunity. *Mucosal Immunol.* 4, 612–624 (2011).
53. Bakema, J. E. *et al.* Inside-Out Regulation of FcαRI (CD89) Depends on PP2A. *J. Immunol.* 181, 4080–4088 (2008).
54. Heineke, M. H. & van Egmond, M. Immunoglobulin A: magic bullet or Trojan horse? *Eur. J. Clin. Invest.* 47, 184–192 (2017).
55. Monteiro, R. C. Role of IgA and IgA Fc Receptors in Inflammation. *J. Clin. Immunol.* 30, 1–9 (2010).
56. Ben Mkaddem, S., Benhamou, M. & Monteiro, R. C. Understanding Fc Receptor Involvement in Inflammatory Diseases: From Mechanisms to New Therapeutic Tools. *Front. Immunol.* 10, 811 (2019).
57. Herr, A. B., White, C. L., Milburn, C., Wu, C. & Bjorkman, P. J. Bivalent Binding of IgA1 to FcαRI Suggests a Mechanism for Cytokine Activation of IgA Phagocytosis. *J. Mol. Biol.* 327, 645–657 (2003).
58. Kubagawa, H. *et al.* Identity of the elusive IgM Fc receptor (FcμR) in humans. *J. Exp. Med.* 206, 2779–2793 (2009).
59. Kubagawa, Kubagawa, Torii & Kang. Kubagawa et al. - 2014 - The Long Elusive IgM Fc Receptor, FcμR. *J. Clin. Immunol.* (2014).
60. Liu, J. *et al.* Role of the IgM Fc Receptor in Immunity and Tolerance. *Front. Immunol.* 10, (2019).
61. Rojas, M. *et al.* Convalescent plasma in Covid-19: Possible mechanisms of action. *Autoimmun. Rev.* 102554 (2020) doi:10.1016/j.autrev.2020.102554.
62. Esen, F. & Tugrul, S. IgM-enriched Immunoglobulins in Sepsis. *Intensive Care Med* S.102-10 (2009).
63. Gelfand, E. W. Intravenous Immune Globulin in Autoimmune and Inflammatory Diseases. *N. Engl. J. Med.* 367, 2015–2025 (2012).
64. Späth, P. J., Schneider, C. & von Gunten, S. Clinical Use and Therapeutic Potential of IVIG/SCIG, Plasma-Derived IgA or IgM, and Other Alternative Immunoglobulin Preparations. *Arch. Immunol. Ther. Exp. (Warsz.)* 65, 215–231 (2017).
65. Galeotti, C., Kaveri, S. V. & Bayry, J. IVIG-mediated effector functions in autoimmune and inflammatory diseases. *Int. Immunol.* 29, 491–498 (2017).
66. Liu, X., Cao, W. & Li, T. High-Dose Intravenous Immunoglobulins in the Treatment of Severe Acute Viral Pneumonia: The Known Mechanisms and Clinical Effects. *Front. Immunol.* 11, (2020).
67. Nierhaus, A., Berlot, G., Kindgen-Milles, D., Müller, E. & Girardis, M. Best-practice IgM- and IgA-enriched immunoglobulin use in patients with sepsis. *Ann. Intensive Care* 10, (2020).

68. Lünemann, J. D., Nimmerjahn, F. & Dalakas, M. C. Intravenous immunoglobulin in neurology—mode of action and clinical efficacy. *Nat. Rev. Neurol.* 11, 80–89 (2015).
69. Schwab, I. & Nimmerjahn, F. Intravenous immunoglobulin therapy: how does IgG modulate the immune system? *Nat. Rev. Immunol.* 13, 176–189 (2013).
70. Perricone, C. *et al.* Intravenous Immunoglobulins at the Crossroad of Autoimmunity and Viral Infections. *Microorganisms* 9, 121 (2021).
71. Zuercher, A. W., Spirig, R., Baz Morelli, A. & Käsermann, F. IVIG in autoimmune disease — Potential next generation biologics. *Autoimmun. Rev.* 15, 781–785 (2016).
72. Zuercher, A. W., Spirig, R., Baz Morelli, A., Rowe, T. & Käsermann, F. Next-generation Fc receptor–targeting biologics for autoimmune diseases. *Autoimmun. Rev.* 18, 102366 (2019).
73. Langereis, J. D., van der Flier, M. & de Jonge, M. I. Limited Innovations After More Than 65 Years of Immunoglobulin Replacement Therapy: Potential of IgA- and IgM-Enriched Formulations to Prevent Bacterial Respiratory Tract Infections. *Front. Immunol.* 9, (2018).
74. Kakoullis, L. *et al.* The use of IgM-enriched immunoglobulin in adult patients with sepsis. *J. Crit. Care* 47, 30–35 (2018).
75. Berlot, G. *et al.* Effects of the timing of administration of IgM- and IgA-enriched intravenous polyclonal immunoglobulins on the outcome of septic shock patients. *Ann. Intensive Care* 8, (2018).
76. Garbett, N. D. & Munro, C. S. Opsonic activity of a new intravenous immunoglobulin preparation: Pentaglobin compared with Sandoglobulin. 5 (1989).
77. Nachbaur, D., Herold, M., Gächter, A. & Niederwieser, D. Modulation of alloimmune response *in vitro* by an IgM-enriched immunoglobulin preparation (Pentaglobin). *Immunology* 94, 279–283 (1998).
78. Norrby-Teglund, A. *et al.* Relative Neutralizing Activity in Polyspecific IgM, IgA, and IgG Preparations against Group A Streptococcal Superantigens. *Clin. Infect. Dis.* 31, 1175–1182 (2000).
79. Rieben, R. *et al.* Immunoglobulin M-enriched human intravenous immunoglobulin prevents complement activation in vitro and in vivo in a rat model of acute inflammation. *Blood* 93, 942–951 (1999).
80. Trautmann *et al.* Bacterial lipopolysaccharide (LPS)-specific antibodies in commercial human immunoglobulin preparations: superior antibody content of an IgM-enriched product. *Clin. Exp. Immunol.* 111, 81–90 (1998).
81. Shmygalev, S. *et al.* IgM-enriched solution BT086 improves host defense capacity and energy store preservation in a rabbit model of endotoxemia. *Acta Anaesthesiol. Scand.* 60, 502–512 (2016).
82. Welte, T. *et al.* Efficacy and safety of trimodulin, a novel polyclonal antibody preparation, in patients with severe community-acquired pneumonia: a randomized, placebo-controlled, double-blind, multicenter, phase II trial (CIGMA study). *Intensive Care Med.* 44, 438–448 (2018).

83. U.S. National Libary of Medicine. Efficacy and Safety of Trimodulin in Subjects With Severe COVID-19 (ESsCOVID) Identifier: NCT04576728. *ClinicalTrials.gov* (2020) doi:NCT04576728.
84. Duerr, C. *et al.* The novel polyclonal Ab preparation trimodulin attenuates *ex vivo* endotoxin-induced immune reactions in early hyperinflammation. *Innate Immun.* 25, 374–388 (2019).
85. Jahn, K. *et al.* Pneumolysin induces platelet destruction, not platelet activation, which can be prevented by immunoglobulin preparations in vitro. *Blood Adv.* 4, 6315–6326 (2020).
86. Kelton, W. *et al.* IgGA: A "Cross-Isotype" Engineered Human Fc Antibody Domain that Displays Both IgG-like and IgA-like Effector Functions. *Chem. Biol.* 21, 1603–1609 (2014).
87. Sterlin, D. & Gorochov, G. When Therapeutic IgA Antibodies Might Come of Age. *Pharmacology* 1–11 (2020) doi:10.1159/000510251.
88. van Tetering, G., Evers, M., Chan, C., Stip, M. & Leusen, J. Fc Engineering Strategies to Advance IgA Antibodies as Therapeutic Agents. *Antibodies* 9, 70 (2020).
89. Hansen, I. S., Hoepel, W., Zaat, S. A. J., Baeten, D. L. P. & den Dunnen, J. Serum IgA Immune Complexes Promote Proinflammatory Cytokine Production by Human Macrophages, Monocytes, and Kupffer Cells through FcαRI–TLR Cross-Talk. *J. Immunol.* 199, 4124–4131 (2017).
90. Longet, S. *et al.* Reconstituted Human Polyclonal Plasma-derived Secretory-like IgM and IgA Maintain the Barrier Function of Epithelial Cells Infected with an Enteropathogen. *J. Biol. Chem.* 289, 21617–21626 (2014).
91. Wolf, H. M. *et al.* Anti-inflammatory properties of human serum IgA: induction of IL-1 receptor antagonist and Fc alpha R (CD89)-mediated down-regulation of tumour necrosis factor-alpha (TNF-alpha) and IL-6 in human monocytes. *Clin. Exp. Immunol.* 105, 537–543 (1996).
92. Aleyd, E. *et al.* IgA Enhances NETosis and Release of Neutrophil Extracellular Traps by Polymorphonuclear Cells via Fcα Receptor I. *J. Immunol.* 192, 2374–2383 (2014).
93. Wolf, H. M. *et al.* Inhibition of Receptor-Dependent and Receptor-Independent Generation of the Respiratory Burst in Human Neutrophils and Monocytes by Human Serum IgA. *Pediatr. Res.* 36, 235–243 (1994).
94. Pfirsch-Maisonnas, S. *et al.* Inhibitory ITAM Signaling Traps Activating Receptors with the Phosphatase SHP-1 to Form Polarized 'Inhibisome' Clusters. *Sci. Signal.* 4, ra24–ra24 (2011).
95. van Egmond, M. & Bakema, J. E. Neutrophils as effector cells for antibody-based immunotherapy of cancer. *Semin. Cancer Biol.* 23, 190–199 (2013).
96. Lobo, P. I. Role of Natural Autoantibodies and Natural IgM Anti-Leucocyte Autoantibodies in Health and Disease. *Front. Immunol.* 7, (2016).
97. Panda, S. & Ding, J. L. Natural Antibodies Bridge Innate and Adaptive Immunity. *J. Immunol.* 194, 13–20 (2015).

98. Brandsma, A. M. *et al.* Potent Fc Receptor Signaling by IgA Leads to Superior Killing of Cancer Cells by Neutrophils Compared to IgG. *Front. Immunol.* 10, (2019).
99. Treffers, L. W. *et al.* IgA-Mediated Killing of Tumor Cells by Neutrophils Is Enhanced by CD47–SIRPα Checkpoint Inhibition. *Cancer Immunol. Res.* 8, 120–130 (2020).
100. Didangelos, A. COVID-19 Hyperinflammation: What about Neutrophils? *mSphere* 5, (2020).
101. Futosi, K., Fodor, S. & Mócsai, A. Neutrophil cell surface receptors and their intracellular signal transduction pathways. *Int. Immunopharmacol.* 17, 638–650 (2013).
102. Singer, M. *et al.* The Third International Consensus Definitions for Sepsis and Septic Shock (Sepsis-3). *JAMA* 315, 801 (2016).
103. Chaudhry, H. *et al.* Role of cytokines as a double-edged sword in sepsis. *Vivo Athens Greece* 27, 669–684 (2013).
104. Hotchkiss, R. S. *et al.* Sepsis and septic shock. *Nat. Rev. Dis. Primer* 2, (2016).
105. Schulte, W., Bernhagen, J. & Bucala, R. Cytokines in Sepsis: Potent Immunoregulators and Potential Therapeutic Targets—An Updated View. *Mediators Inflamm.* 2013, 1–16 (2013).
106. Cao, C., Yu, M. & Chai, Y. Pathological alteration and therapeutic implications of sepsis-induced immune cell apoptosis. *Cell Death Dis.* 10, (2019).
107. Hotchkiss, R. S., Coopersmith, C. M., McDunn, J. E. & Ferguson, T. A. The sepsis seesaw: tilting toward immunosuppression. *Nat. Med.* 15, 496–497 (2009).
108. Boomer, J. S., Green, J. M. & Hotchkiss, R. S. The changing immune system in sepsis: Is individualized immuno-modulatory therapy the answer? *Virulence* 5, 45–56 (2014).
109. Busani, S., Damiani, E., Cavazzuti, I., Donati, A. & Girardis, M. Intravenous immunoglobulin in septic shock: review of the mechanisms of action and meta-analysis of the clinical effectiveness. *Minerva Anestesiol.* 82, 14 (2016).
110. Alejandria, M. M., Lansang, M. A. D., Dans, L. F. & Mantaring, J. B. Intravenous immunoglobulin for treating sepsis, severe sepsis and septic shock. *Cochrane Database Syst. Rev.* CD001090 (2013) doi:10.1002/14651858.CD001090.pub2.
111. Cui, J. *et al.* The clinical efficacy of intravenous IgM-enriched immunoglobulin (pentaglobin) in sepsis or septic shock: a meta-analysis with trial sequential analysis. *Ann. Intensive Care* 9, (2019).
112. Morgan, A. & Glossop, A. Severe community-acquired pneumonia. *BJA Educ.* 16, 167–172 (2016).
113. Sibila, O., Rodrigo-Troyano, A. & Torres, A. Nonantibiotic Adjunctive Therapies for Community-Acquired Pneumonia (Corticosteroids and Beyond): Where Are We with Them? *Semin. Respir. Crit. Care Med.* 37, 913–922 (2016).
114. Woodhead, M., Welch, C. A., Harrison, D. A., Bellingan, G. & Ayres, J. G. Community-acquired pneumonia on the intensive care unit: secondary analysis of 17,869 cases in the ICNARC Case Mix Programme Database. *Crit. Care Lond. Engl.* 10 Suppl 2, S1 (2006).

115. Meijvis, S. C. A. *et al.* Therapy in pneumonia: What is beyond antibiotics? 69, 6 (2011).
116. Morris, A. C. Management of pneumonia in intensive care. *J. Emerg. Crit. Care Med.* 2, 101–101 (2018).
117. Woods, D. R. & José, R. J. Current and emerging evidence for immunomodulatory therapy in community-acquired pneumonia. *Ann. Res. Hosp.* 1, 1–1 (2017).
118. Sibila, O., Restrepo, M. I. & Anzueto, A. What is the Best Antimicrobial Treatment for Severe Community-Acquired Pneumonia (Including the Role of Steroids and Statins and Other Immunomodulatory Agents). *Infect. Dis. Clin. North Am.* 27, 133–147 (2013).
119. de la Torre, M. C. *et al.* Serum levels of immunoglobulins and severity of community-acquired pneumonia. *BMJ Open Respir. Res.* 3, e000152 (2016).
120. Ho, J. C. *et al.* Pentaglobin in steroid-resistant severe acute respiratory syndrome. *INT J TUBERC LUNG DIS* 8(10):1173–1179 (2005).
121. Tagami, T., Matsui, H., Fushimi, K. & Yasunaga, H. Intravenous Immunoglobulin and Mortality in Pneumonia Patients With Septic Shock: An Observational Nationwide Study. *Clin. Infect. Dis.* 61, 385–392 (2015).
122. dos Santos, W. G. Natural history of COVID-19 and current knowledge on treatment therapeutic options. *Biomed. Pharmacother.* 129, 110493 (2020).
123. Wang, M.-Y. *et al.* SARS-CoV-2: Structure, Biology, and Structure-Based Therapeutics Development. *Front. Cell. Infect. Microbiol.* 10, (2020).
124. Mittal, A. *et al.* COVID-19 pandemic: Insights into structure, function, and hACE2 receptor recognition by SARS-CoV-2. *PLOS Pathog.* 16, e1008762 (2020).
125. Saghazadeh, A. & Rezaei, N. Towards treatment planning of COVID-19: Rationale and hypothesis for the use of multiple immunosuppressive agents: Anti-antibodies, immunoglobulins, and corticosteroids. *Int. Immunopharmacol.* 84, 106560 (2020).
126. Kumar, A. *et al.* SARS-CoV-2-specific virulence factors in COVID-19. *J. Med. Virol.* 93, 1343–1350 (2021).
127. Siddiqi, H. K. & Mehra, M. R. COVID-19 illness in native and immunosuppressed states: A clinical–therapeutic staging proposal. *J. Heart Lung Transplant.* 39, 405–407 (2020).
128. Henss, L. *et al.* Analysis of Humoral Immune Responses in Patients With Severe Acute Respiratory Syndrome Coronavirus 2 Infection. *J. Infect. Dis.* 223, 56–61 (2021).
129. Wu, Z. & McGoogan, J. M. Characteristics of and Important Lessons From the Coronavirus Disease 2019 (COVID-19) Outbreak in China: Summary of a Report of 72 314 Cases From the Chinese Center for Disease Control and Prevention. *JAMA* 323, 1239 (2020).
130. Zhang, Y., Chen, Y. & Meng, Z. Immunomodulation for Severe COVID-19 Pneumonia: The State of the Art. *Front. Immunol.* 11, (2020).

131. Hoepel, W. *et al. Anti-SARS-CoV-2 IgG from severely ill COVID-19 patients promotes macrophage hyper-inflammatory responses*. http://biorxiv.org/lookup/doi/10.1101/2020.07.13.190140 (2020) doi:10.1101/2020.07.13.190140.
132. McGonagle, D., Sharif, K., O'Regan, A. & Bridgewood, C. The Role of Cytokines including Interleukin-6 in COVID-19 induced Pneumonia and Macrophage Activation Syndrome-Like Disease. *Autoimmun. Rev.* 19, 102537 (2020).
133. Gong, J. *et al. Correlation Analysis Between Disease Severity and Inflammation-related Parameters in Patients with COVID-19 Pneumonia*. http://medrxiv.org/lookup/doi/10.1101/2020.02.25.20025643 (2020) doi:10.1101/2020.02.25.20025643.
134. Miao, Y., Fan, L. & Li, J.-Y. Potential Treatments for COVID-19 Related Cytokine Storm - Beyond Corticosteroids. *Front. Immunol.* 11, (2020).
135. Petrey, A. C. *et al.* Cytokine release syndrome in COVID-19: Innate immune, vascular, and platelet pathogenic factors differ in severity of disease and sex. *J. Leukoc. Biol.* (2020) doi:10.1002/JLB.3COVA0820-410RRR.
136. Yates, J. L. *et al. Serological Analysis Reveals an Imbalanced IgG Subclass Composition Associated with COVID-19 Disease Severity*. http://medrxiv.org/lookup/doi/10.1101/2020.10.07.20208603 (2020) doi:10.1101/2020.10.07.20208603.
137. Wang, D. *et al.* Clinical Characteristics of 138 Hospitalized Patients With 2019 Novel Coronavirus–Infected Pneumonia in Wuhan, China. *JAMA* 323, 1061 (2020).
138. Wang, J. *et al.* Excessive Neutrophils and Neutrophil Extracellular Traps in COVID-19. *Front. Immunol.* 11, (2020).
139. Zhao, Y. *et al.* Abnormal immunity of non-survivors with COVID-19: predictors for mortality. *Infect. Dis. Poverty* 9, (2020).
140. Ingraham, N. E. *et al.* Immunomodulation in COVID-19. *Lancet Respir. Med.* 544–546 (2020) doi:10.1016/S2213-2600(20)30226-5.
141. Mehta, P. *et al.* COVID-19: consider cytokine storm syndromes and immunosuppression. *The Lancet* 395, 1033–1034 (2020).
142. Shi, Y. *et al.* COVID-19 infection: the perspectives on immune responses. *Cell Death Differ.* 27, 1451–1454 (2020).
143. Adeniji, O. S. *et al.* COVID-19 Severity Is Associated with Differential Antibody Fc-Mediated Innate Immune Functions. 12, 8 (2021).
144. Atyeo, C. *et al.* Distinct Early Serological Signatures Track with SARS-CoV-2 Survival. *Immunity* 53, 524-532.e4 (2020).

145. Guo, L. *et al.* Profiling Early Humoral Response to Diagnose Novel Coronavirus Disease (COVID-19). *Clin. Infect. Dis.* (2020) doi:10.1093/cid/ciaa310.
146. Natarajan, H. *et al.* Markers of Polyfunctional SARS-CoV-2 Antibodies in Convalescent Plasma. *mBio* 12, (2021).
147. Hong, Y.-N., Xu, J., Sasa, G. B. K., Zhou, K.-X. & Ding, X.-F. Remdesivir as a broad-spectrum antiviral drug against COVID-19. *Eur. Rev. Med. Pharmacol. Sci.* 25, 541–548 (2021).
148. Fu, Y., Cheng, Y. & Wu, Y. Understanding SARS-CoV-2-Mediated Inflammatory Responses: From Mechanisms to Potential Therapeutic Tools. *Virol. Sin.* (2020) doi:10.1007/s12250-020-00207-4.
149. Cao, W. *et al.* High-Dose Intravenous Immunoglobulin as a Therapeutic Option for Deteriorating Patients With Coronavirus Disease 2019. *Open Forum Infect. Dis.* 7, (2020).
150. Cao, W. *et al.* High-Dose Intravenous Immunoglobulin in Severe Coronavirus Disease 2019: A Multicenter Retrospective Study in China. *Front. Immunol.* 12, (2021).
151. Lanza, M. *et al.* Successful intravenous immunoglobulin treatment in severe COVID-19 pneumonia. *IDCases* 21, e00794 (2020).
152. Xie, Y. *et al.* Effect of regular intravenous immunoglobulin therapy on prognosis of severe pneumonia in patients with COVID-19. *J. Infect.* S0163-4453(20)30172–9 (2020) doi:10.1016/j.jinf.2020.03.044.
153. Zhou, Z.-G. *et al. Short-Term Moderate-Dose Corticosteroid Plus Immunoglobulin Effectively Reverses COVID-19 Patients Who Have Failed Low-Dose Therapy*. https://www.preprints.org/manuscript/202003.0065/v1 (2020) doi:10.20944/preprints202003.0065.v1.
154. Schwaiger, J., Karbiener, M., Aberham, C., Farcet, M. R. & Kreil, T. R. No SARS-CoV-2 neutralization by intravenous immunoglobulins produced from plasma collected before the 2020 pandemic. *J. Infect. Dis.* 222, 1960–1964 (2020).
155. Hughes, S., Troise, O., Donaldson, H., Mughal, N. & Moore, L. S. Bacterial and fungal coinfection among hospitalised patients with COVID-19: A retrospective cohort study in a UK secondary care setting. *Clin. Microbiol. Infect.* (2020) doi:10.1016/j.cmi.2020.06.025.
156. Ritchie, A. I. & Singanayagam, A. Immunosuppression for hyperinflammation in COVID-19: a double-edged sword? *The Lancet* 395, 1111 (2020).
157. Zhu, X. *et al.* Co-infection with respiratory pathogens among COVID-2019 cases. *Virus Res.* 285, 198005 (2020).
158. Basta, M., Kirshbom, P., Frank, M. M. & Fries, L. F. Mechanism of therapeutic effect of high-dose intravenous immunoglobulin. Attenuation of acute, complement-dependent immune damage in a guinea pig model. *J. Clin. Invest.* 84, 1974–1981 (1989).

159. Fang, S., Wang, H., Lu, L., Jia, Y. & Xia, Z. Decreased complement C3 levels are associated with poor prognosis in patients with COVID-19: A retrospective cohort study. *Int. Immunopharmacol.* 89, 107070 (2020).
160. Ram Kumar Pandian, S., Arunachalam, S., Deepak, V., Kunjiappan, S. & Sundar, K. Targeting complement cascade: an alternative strategy for COVID-19. *3 Biotech* 10, (2020).
161. Langarizadeh, M. A. *et al.* A review on function and side effects of systemic corticosteroids used in high-grade COVID-19 to prevent cytokine storms. *EXCLI J. 20Doc339 ISSN 1611-2156* (2021) doi:10.17179/EXCLI2020-3196.
162. Reusch, N. *et al.* Neutrophils in COVID-19. *Front. Immunol.* 12, (2021).
163. Galeotti, C., Kaveri, S. V. & Bayry, J. Intravenous immunoglobulin immunotherapy for coronavirus disease-19 (COVID-19). *Clin. Transl. Immunol.* 9, (2020).
164. Anania, J. C., Chenoweth, A. M., Wines, B. D. & Hogarth, P. M. The Human FcγRII (CD32) Family of Leukocyte FcR in Health and Disease. *Front. Immunol.* 10, (2019).
165. Kara, S. *et al.* Impact of Plasma Membrane Domains on IgG Fc Receptor Function. *Front. Immunol.* 11, (2020).
166. de Taeye, S. W., Rispens, T. & Vidarsson, G. The Ligands for Human IgG and Their Effector Functions. *Antibodies* 8, 30 (2019).
167. Nimmerjahn, F. & Ravetch, J. V. Fcγ Receptors: Old Friends and New Family Members. *Immunity* 24, 19–28 (2006).
168. Castro-Dopico & Clatworthy. Castro-Dopico und Clatworthy - 2019 - IgG and Fcγ Receptors in Intestinal Immunity and I.pdf. *Front. Immunol.* (2019).
169. Bharadwaj, D., Mold, C., Markham, E. & Du Clos, T. W. Serum Amyloid P Component Binds to Fcγ Receptors and Opsonizes Particles for Phagocytosis. *J. Immunol.* 166, 6735–6741 (2001).
170. Lim, B. J., Lee, D., Hong, S. W. & Jeong, H. J. Toll-Like Receptor 4 Signaling is Involved in IgA-Stimulated Mesangial Cell Activation. *Yonsei Med. J.* 52, 610 (2011).
171. Rittirsch, Flierl, Day & Werner. Rittirsch et al. - 2009 - Cross-Talk between TLR4 and FcγReceptorIII (CD16) .pdf. *PLOS Pathog.* (2009).
172. Rossato, E. *et al.* Reversal of Arthritis by Human Monomeric IgA Through the Receptor-Mediated SH2 Domain-Containing Phosphatase 1 Inhibitory Pathway: Antiinflammatory action of monomeric IgA in arthritis. *Arthritis Rheumatol.* 67, 1766–1777 (2015).
173. Hamdan, T. A., Lang, P. A. & Lang, K. S. The Diverse Functions of the Ubiquitous Fcγ Receptors and Their Unique Constituent, FcRγ Subunit. *Pathogens* 9, 140 (2020).
174. Blank, U., Launay, P., Benhamou, M. & Monteiro, R. C. Inhibitory ITAMs as novel regulators of immunity. *Immunol. Rev.* 232, 59–71 (2009).

175. Mkaddem, S. B. *et al.* Lyn and Fyn function as molecular switches that control immunoreceptors to direct homeostasis or inflammation. *Nat. Commun.* 8, (2017).
176. Aloulou, M. *et al.* IgG1 and IVIg induce inhibitory ITAM signaling through Fc RIII controlling inflammatory responses. *Blood* 119, 13 (2012).
177. Pasquier, B. *et al.* Identification of FcαRI as an Inhibitory Receptor that Controls Inflammation. *Immunity* 22, 31–42 (2005).
178. Lowell, C. A. Src-family and Syk Kinases in Activating and Inhibitory Pathways in Innate Immune Cells: Signaling Cross Talk. *Cold Spring Harb. Perspect. Biol.* 3, a002352–a002352 (2011).
179. Ben Mkaddem, S. *et al.* Shifting FcγRIIA-ITAM from activation to inhibitory configuration ameliorates arthritis. *J. Clin. Invest.* 124, 3945–3959 (2014).
180. Jang, J.-E., Hidalgo, A. & Frenette, P. S. Intravenous Immunoglobulins Modulate Neutrophil Activation and Vascular Injury Through FcγRIII and SHP-1. *Circ. Res.* 110, 1057–1066 (2012).
181. Shock, A., Humphreys, D. & Nimmerjahn, F. Dissecting the mechanism of action of intravenous immunoglobulin in human autoimmune disease: lessons from therapeutic modalities targeting Fcγ receptors. *J. Allergy Clin. Immunol.* (2020) doi:10.1016/j.jaci.2020.06.036.
182. Li, N. Complete FcRn dependence for intravenous Ig therapy in autoimmune skin blistering diseases. *J. Clin. Invest.* 115, 3440–3450 (2005).
183. Pan, Y., Yuhasz, S. C. & Amzel, L. M. Anti-idiotypic antibodies: biological function and structural studies. *FASEB J. Off. Publ. Fed. Am. Soc. Exp. Biol.* 9, 43–49 (1995).
184. Basta, M. *et al.* F(ab)′2-mediated neutralization of C3a and C5a anaphylatoxins: a novel effector function of immunoglobulins. *Nat. Med.* 9, 431–438 (2003).
185. Andersson, U., Björk, L., Skansén-Saphir, U. & Andersson, J. Pooled human IgG modulates cytokine production in lymphocytes and monocytes. *Immunol. Rev.* 139, 21–42 (1994).
186. Kawai, T. & Akira, S. Toll-like Receptors and Their Crosstalk with Other Innate Receptors in Infection and Immunity. *Immunity* 34, 637–650 (2011).
187. Takeuchi, O. *et al.* Differential Roles of TLR2 and TLR4 in Recognition of Gram-Negative and Gram-Positive Bacterial Cell Wall Components. *Immunity* 11, 443–451 (1999).
188. Patik, I. *et al.* Identification of novel cell-impermeant fluorescent substrates for testing the function and drug interaction of Organic Anion-Transporting Polypeptides, OATP1B1/1B3 and 2B1. *Sci. Rep.* 8, 2630 (2018).
189. Andersen, M. N., Al-Karradi, S. N. H., Kragstrup, T. W. & Hokland, M. Elimination of erroneous results in flow cytometry caused by antibody binding to Fc receptors on human monocytes and macrophages: FcR-Blocking Eliminates Erroneous Results in Flow Cytometry. *Cytometry A* 89, 1001–1009 (2016).

190. Schmidt, S. R., Schweikart, F. & Andersson, M. E. Current methods for phosphoprotein isolation and enrichment. *J. Chromatogr. B* 849, 154–162 (2007).
191. Kaur, G. & Dufour, J. M. Cell lines: Valuable tools or useless artifacts. *Spermatogenesis* 2, 1–5 (2012).
192. Kozicky, L. K. *et al.* IVIg and LPS Co-stimulation Induces IL-10 Production by Human Monocytes, Which Is Compromised by an FcγRIIA Disease-Associated Gene Variant. *Front. Immunol.* 9, (2018).
193. Lin, L., Lu, L., Cao, W. & Li, T. Hypothesis for potential pathogenesis of SARS-CoV-2 infection–a review of immune changes in patients with viral pneumonia. *Emerg. Microbes Infect.* 9, 727–732 (2020).
194. Nguyen, A. A. *et al.* Immunoglobulins in the treatment of COVID-19 infection: Proceed with caution! *Clin. Immunol.* 216, 108459 (2020).
195. Tomar, B., Anders, H.-J., Desai, J. & Mulay, S. R. Neutrophils and Neutrophil Extracellular Traps Drive Necroinflammation in COVID-19. *Cells* 9, 1383 (2020).
196. Esmaeilzadeh, A. & Elahi, R. Immunobiology and immunotherapy of COVID-19: A clinically updated overview. *J. Cell. Physiol.* (2020) doi:10.1002/jcp.30076.
197. Wagar, L. E., DiFazio, R. M. & Davis, M. M. Advanced model systems and tools for basic and translational human immunology. *Genome Med.* 10, (2018).
198. Mestas, J. & Hughes, C. C. W. Of Mice and Not Men: Differences between Mouse and Human Immunology. *J. Immunol.* 172, 2731–2738 (2004).
199. Rincón, E., Rocha-Gregg, B. L. & Collins, S. R. A map of gene expression in neutrophil-like cell lines. *BMC Genomics* 19, (2018).
200. Fleck, R. A., Romero-Steiner, S. & Nahm, M. H. Use of HL-60 Cell Line To Measure Opsonic Capacity of Pneumococcal Antibodies. *Clin. Diagn. Lab. Immunol.* 12, 19–27 (2005).
201. Kim, K.-H., Seoh, J. Y. & Cho, S. J. Phenotypic and Functional Analysis of HL-60 Cells Used in Opsonophagocytic-Killing Assay for *Streptococcus pneumoniae*. *J. Korean Med. Sci.* 30, 145 (2015).
202. Mullick, A. *et al.* GeneExpression in HL60 Granulocytoids and Human PolymorphonuclearLeukocytes Exposed to Candidaalbicans†. *Infect. Immun.* 72, 414–429 (2004).
203. Trayner, I. D. *et al.* Changes in antigen expression on differentiating HL60 cells treated with dimethylsulphoxide, all-trans retinoic acid, h1,25-dihydroxyvitamin D3 or 12-O-tetradecanoyl phorbol-13-acetate. *Leuk. Res.* 11 (1998).
204. Villamón, E. *et al.* Imiquimod inhibits growth and induces differentiation of myeloid leukemia cell lines. *Cancer Cell Int.* 18, (2018).
205. Chi, M., Tridandapani, S., Zhong, W., Coggeshall, K. M. & Mortensen, R. F. C-Reactive Protein Induces Signaling Through FcγRIIa on HL-60 Granulocytes. *J. Immunol.* 168, 1413–1418 (2002).

206. Yaseen, R. *et al.* Antimicrobial activity of HL-60 cells compared to primary blood-derived neutrophils against Staphylococcus aureus. *J. Negat. Results Biomed.* 16, (2017).
207. Cassatella, M. A. Neutrophil-Derived Proteins: Selling Cytokines by the Pound. in *Advances in Immunology* vol. 73 369–509 (Elsevier, 1999).
208. Tecchio, C., Micheletti, A. & Cassatella, M. A. Neutrophil-Derived Cytokines: Facts Beyond Expression. *Front. Immunol.* 5, (2014).
209. Gupta, A. K., Giaglis, S., Hasler, P. & Hahn, S. Efficient Neutrophil Extracellular Trap Induction Requires Mobilization of Both Intracellular and Extracellular Calcium Pools and Is Modulated by Cyclosporine A. *PLoS ONE* 9, e97088 (2014).
210. Davis, S. K., Selva, K. J., Kent, S. J. & Chung, A. W. Serum IgA Fc effector functions in infectious disease and cancer. *Immunol. Cell Biol.* 98, 276–286 (2020).
211. Janoff, E. N. *et al.* Killing of Streptococcus pneumoniae by capsular polysaccharide–specific polymeric IgA, complement, and phagocytes. *J. Clin. Invest.* 104, 1139–1147 (1999).
212. Wines, B. D., Sardjono, C. T., Trist, H. H., Lay, C. S. & Hogarth, P. M. The interaction of Fc alpha RI with IgA and its implications for ligand binding by immunoreceptors of the leukocyte receptor cluster. *J. Immunol. Baltim. Md 1950* 166, 1781–1789 (2001).
213. Abe, Y., Horiuchi, A., Miyake, M. & Kimura, S. Anti-Cytokine Nature of Natural Human Immunoglobulin: One Possible Mechanism of the Clinical Effect of Intravenous Immunoglobulin Therapy. *Immunol. Rev.* 139, 5–19 (1994).
214. Pinheiro da Silva, F. *et al.* CD16 promotes Escherichia coli sepsis through an FcRγ inhibitory pathway that prevents phagocytosis and facilitates inflammation. *Nat. Med.* 13, 1368–1374 (2007).
215. Yang, R.-B. *et al.* Toll-like receptor-2 mediates lipopolysaccharide-induced cellular signalling. *Nature* 395, 284–288 (1998).
216. Miller, Y. I., Choi, S.-H., Wiesner, P. & Bae, Y. S. The SYK side of TLR4: signalling mechanisms in response to LPS and minimally oxidized LDL: Role of SYK in TLR4 signalling. *Br. J. Pharmacol.* 167, 990–999 (2012).
217. Arndt, P. G., Suzuki, N., Avdi, N. J., Malcolm, K. C. & Worthen, G. S. Lipopolysaccharide-induced c-Jun NH2-terminal Kinase Activation in Human Neutrophils. *J. Biol. Chem.* 279, 10883–10891 (2004).
218. Chaudhary, A., Fresquez, T. M. & Naranjo, M. J. Tyrosine kinase Syk associates with toll-like receptor 4 and regulates signaling in human monocytic cells. *Immunol. Cell Biol.* 85, 249–256 (2007).
219. Loughlin, A. J., Woodroofe, M. N. & Cuzner, M. L. Regulation of Fc receptor and major histocompatibility complex antigen expression on isolated rat microglia by tumour necrosis factor,

interleukin-1 and lipopolysaccharide: effects on interferon-gamma induced activation. *Immunology* 75, 170–175 (1992).

220. Bzowska, M., Hamczyk, M., Skalniak, A. & Guzik, K. Rapid Decrease of CD16 (FcγRIII) Expression on Heat-Shocked Neutrophils and Their Recognition by Macrophages. *J. Biomed. Biotechnol.* 2011, 1–14 (2011).
221. Olas, K., Butterweck, H., Teschner, W., Schwarz, H. P. & Reipert, B. Immunomodulatory properties of human serum immunoglobulin A: anti-inflammatory and pro-inflammatory activities in human monocytes and peripheral blood mononuclear cells. *Clin. Exp. Immunol.* 140, 478–490 (2005).
222. Geissmann, F. *et al.* A Subset of Human Dendritic Cells Expresses IgA Fc Receptor (CD89), Which Mediates Internalization and Activation Upon Cross-Linking by IgA Complexes. *J. Immunol.* 166, 346–352 (2001).
223. Grossetête, B. *et al.* Down-regulation of Fcα receptors on blood cells of IgA nephropathy patients: Evidence for a negative regulatory role of serum IgA. *Kidney Int.* 53, 1321–1335 (1998).
224. Jolles, S. High-dose intravenous immunoglobulin (hdIVIg) in the treatment of autoimmune blistering disorders. *Clin. Exp. Immunol.* 129, 385–389 (2002).
225. Guerra, F. E., Borgogna, T. R., Patel, D. M., Sward, E. W. & Voyich, J. M. Epic Immune Battles of History: Neutrophils vs. Staphylococcus aureus. *Front. Cell. Infect. Microbiol.* 7, (2017).
226. van Kessel, K. P. M., Bestebroer, J. & van Strijp, J. A. G. Neutrophil-Mediated Phagocytosis of Staphylococcus aureus. *Front. Immunol.* 5, (2014).
227. Lu, T., Porter, A. R., Kennedy, A. D., Kobayashi, S. D. & DeLeo, F. R. Phagocytosis and Killing of *Staphylococcus aureus* by Human Neutrophils. *J. Innate Immun.* 6, 639–649 (2014).
228. Stracquadanio, S. *et al.* Titration of Igs contained in an intravenous IgM-enriched preparation against selected pathogens involved in sepsis. *Immunobiology* 225, 151897 (2020).
229. Elabbadi, A. *et al.* Bacterial coinfection in critically ill COVID-19 patients with severe pneumonia. *Infection* 49, 559–562 (2021).
230. Mahmoudi, H. Bacterial co-infections and antibiotic resistance in patients with COVID-19. *GMS Hyg. Infect. Control 15Doc35* (2020) doi:10.3205/DGKH000370.
231. Manohar, P. *et al.* Secondary Bacterial Infections in Patients With Viral Pneumonia. *Front. Med.* 7, (2020).
232. Su, Z., Fortin, A., Gros, P. & Stevenson, M. M. Opsonin-Independent Phagocytosis: An Effector Mechanism against Acute Blood-Stage *Plasmodium chabaudi* AS Infection. *J. Infect. Dis.* 186, 1321–1329 (2002).
233. Oliver, J. M., Burg, D. L., Wilson, B. S., McLaughlin, J. L. & Geahlen, R. L. Inhibition of mast cell Fc epsilon R1-mediated signaling and effector function by the Syk-selective inhibitor, piceatannol. *J. Biol. Chem.* 269, 29697–29703 (1994).

234. Cottat, M. *et al.* Phosphorylation impact on Spleen Tyrosine kinase conformation by Surface Enhanced Raman Spectroscopy. *Sci. Rep.* 7, 39766 (2017).
235. Tsang, E. *et al.* Molecular Mechanism of the Syk Activation Switch. *J. Biol. Chem.* 283, 32650–32659 (2008).
236. Fatehchand, K. *et al.* Toll-like Receptor 4 Ligands Down-regulate Fcγ Receptor IIb (FcγRIIb) via MARCH3 Protein-mediated Ubiquitination. *J. Biol. Chem.* 291, 3895–3904 (2016).
237. Vargas-Hernández, O. *et al.* THP-1 cells increase TNF-α production upon LPS + soluble human IgG co-stimulation supporting evidence for TLR4 and Fcγ receptors crosstalk. *Cell. Immunol.* 355, 104146 (2020).
238. Hart, S. P., Alexander, K. M. & Dransfield, I. Immune Complexes Bind Preferentially to FcγRIIA (CD32) on Apoptotic Neutrophils, Leading to Augmented Phagocytosis by Macrophages and Release of Proinflammatory Cytokines. *J. Immunol.* 172, 1882–1887 (2004).
239. Treffers, L. W. *et al.* FcγRIIIb Restricts Antibody-Dependent Destruction of Cancer Cells by Human Neutrophils. *Front. Immunol.* 9, (2019).
240. Veri, M.-C. *et al.* Monoclonal antibodies capable of discriminating the human inhibitory Fcgamma-receptor IIB (CD32B) from the activating Fcgamma-receptor IIA (CD32A): biochemical, biological and functional characterization. *Immunology* 121, 392–404 (2007).
241. de Tymowski, C. *et al.* CD89 Is a Potent Innate Receptor for Bacteria and Mediates Host Protection from Sepsis. *Cell Rep.* 27, 762-775.e5 (2019).
242. Rumpold, H., Wiedermann, G., Scheiner, O., Kraft, D. & Stemberger, H. Lack of evidence for IgM-induced ADCC: studies with monoclonal and polyclonal antibodies. *Immunology* 43, 161–170 (1981).
243. Bakema, J. E. *et al.* Targeting FcαRI on Polymorphonuclear Cells Induces Tumor Cell Killing through Autophagy. *J. Immunol.* 187, 726–732 (2011).
244. Heineke, M. H. *et al.* Peptide mimetics of immunoglobulin A (IgA) and FcαRI block IgA-induced human neutrophil activation and migration. *Eur. J. Immunol.* 47, 1835–1845 (2017).
245. Lu, J. *et al.* Recognition and functional activation of the human IgA receptor (Fc RI) by C-reactive protein. *Proc. Natl. Acad. Sci.* 108, 4974–4979 (2011).
246. Langley, R. *et al.* The Staphylococcal Superantigen-Like Protein 7 Binds IgA and Complement C5 and Inhibits IgA-FcαRI Binding and Serum Killing of Bacteria. *J. Immunol.* 174, 2926–2933 (2005).
247. Mouratou, B., Béhar, G. & Pecorari, F. Artificial Affinity Proteins as Ligands of Immunoglobulins. *Biomolecules* 5, 60–75 (2015).
248. Akinrinmade, O. A. *et al.* CD64: An Attractive Immunotherapeutic Target for M1-type Macrophage Mediated Chronic Inflammatory Diseases. *Biomedicines* 5, 56 (2017).

249. Wilton, J. M. Suppression by IgA of IgG-mediated phagocytosis by human polymorphonuclear leucocytes. *Clin. Exp. Immunol.* 34, 423–428 (1978).
250. Nagelkerke, S. Q. *et al.* Inhibition of FcγR-mediated phagocytosis by IVIg is independent of IgG-Fc sialylation and FcγRIIb in human macrophages. *Blood* 124, 3709–3718 (2014).
251. Yiengst, M. J. & Shock, N. W. Blood and plasma volume in adult males. *J. Appl. Physiol.* 17, 195–198 (1962).
252. Song, M. *et al.* NSC-87877, inhibitor of SHP-1/2 PTPs, inhibits dual-specificity phosphatase 26 (DUSP26). *Biochem. Biophys. Res. Commun.* 381, 491–495 (2009).
253. Wu, Y., Pan, W., Hu, X., Zhang, A. & Wei, W. The prospects for targeting FcR as a novel therapeutic strategy in rheumatoid arthritis. *Biochem. Pharmacol.* 183, 114360 (2021).
254. Merad, M. & Martin, J. C. Pathological inflammation in patients with COVID-19: a key role for monocytes and macrophages. *Nat. Rev. Immunol.* 20, 355–362 (2020).
255. Ehaideb, S. N., Abdullah, M. L., Abuyassin, B. & Bouchama, A. Evidence of a wide gap between COVID-19 in humans and animal models: a systematic review. *Crit. Care* 24, (2020).
256. Walls, A. C. *et al.* Structure, Function, and Antigenicity of the SARS-CoV-2 Spike Glycoprotein. *Cell* 181, 281-292.e6 (2020).
257. Bruni, M. *et al.* Persistence of Anti-SARS-CoV-2 Antibodies in Non-Hospitalized COVID-19 Convalescent Health Care Workers. *J. Clin. Med.* 9, 3188 (2020).
258. Bar-On, Y. M., Flamholz, A., Phillips, R. & Milo, R. SARS-CoV-2 (COVID-19) by the numbers. *eLife* 9, (2020).
259. Pacheco, P., White, D. & Sulchek, T. Effects of Microparticle Size and Fc Density on Macrophage Phagocytosis. *PLoS ONE* 8, e60989 (2013).
260. Champion, J. A., Walker, A. & Mitragotri, S. Role of particle size in phagocytosis of polymeric microspheres. *Pharm. Res.* 25, 1815–1821 (2008).
261. Yu, H. *et al.* Distinct features of SARS-CoV-2-specific IgA response in COVID-19 patients. *Eur. Respir. J.* 2001526 (2020) doi:10.1183/13993003.01526-2020.
262. Ma, H. *et al.* Serum IgA, IgM, and IgG responses in COVID-19. *Cell. Mol. Immunol.* 773–775 (2020) doi:10.1038/s41423-020-0474-z.
263. Padoan, A. *et al.* IgA-Ab response to spike glycoprotein of SARS-CoV-2 in patients with COVID-19: A longitudinal study. *Clin. Chim. Acta* 507, 164–166 (2020).
264. Sterlin, D. *et al. IgA dominates the early neutralizing antibody response to SARS-CoV-2*. http://medrxiv.org/lookup/doi/10.1101/2020.06.10.20126532 (2020) doi:10.1101/2020.06.10.20126532.
265. Infantino, M. *et al.* Closing the serological gap in the diagnostic testing for COVID-19: The value of anti-SARS-CoV-2 IgA antibodies. *J. Med. Virol.* 1436–1442 (2020) doi:10.1002/jmv.26422.

266. Noroozi, R. *et al.* Altered cytokine levels and immune responses in patients with SARS-CoV-2 infection and related conditions. *Cytokine* 133, 155143 (2020).
267. Li, Y. *et al.* Immune-related Factors Associated with Pneumonia in 127 Children with Coronavirus Disease 2019 in Wuhan. *Pediatr. Pulmonol.* 55, 2354–2360 (2020).
268. Wan, S. *et al. Characteristics of lymphocyte subsets and cytokines in peripheral blood of 123 hospitalized patients with 2019 novel coronavirus pneumonia (NCP)*. http://medrxiv.org/lookup/doi/10.1101/2020.02.10.20021832 (2020) doi:10.1101/2020.02.10.20021832.
269. Wong, C. K. *et al.* Plasma inflammatory cytokines and chemokines in severe acute respiratory syndrome. *Clin. Exp. Immunol.* 136, 95–103 (2004).
270. Liu, J. *et al. Longitudinal characteristics of lymphocyte responses and cytokine profiles in the peripheral blood of SARS-CoV-2 infected patients*. http://medrxiv.org/lookup/doi/10.1101/2020.02.16.20023671 (2020) doi:10.1101/2020.02.16.20023671.
271. Jaume, M. *et al.* Anti-Severe Acute Respiratory Syndrome Coronavirus Spike Antibodies Trigger Infection of Human Immune Cells via a pH- and Cysteine Protease-Independent Fc R Pathway. *J. Virol.* 85, 10582–10597 (2011).
272. Liu, L. *et al.* Anti–spike IgG causes severe acute lung injury by skewing macrophage responses during acute SARS-CoV infection. *JCI Insight* 4, (2019).
273. Qi, F., Qian, S., Zhang, S. & Zhang, Z. Single cell RNA sequencing of 13 human tissues identify cell types and receptors of human coronaviruses. *Biochem. Biophys. Res. Commun.* 526, 135–140 (2020).
274. Kuri-Cervantes, L. *et al.* Comprehensive mapping of immune perturbations associated with severe COVID-19. *Sci. Immunol.* 5, eabd7114 (2020).
275. Lourda, M. *et al. High-dimensional profiling reveals phenotypic heterogeneity and disease-specific alterations of granulocytes in COVID-19*. http://medrxiv.org/lookup/doi/10.1101/2021.01.27.21250591 (2021) doi:10.1101/2021.01.27.21250591.
276. Carissimo, G. *et al.* Whole blood immunophenotyping uncovers immature neutrophil-to-VD2 T-cell ratio as an early marker for severe COVID-19. *Nat. Commun.* 11, (2020).
277. Ma, H. *et al.* Decline of SARS-CoV-2-specific IgG, IgM and IgA in convalescent COVID-19 patients within 100 days after hospital discharge. *Sci. China Life Sci.* (2020) doi:10.1007/s11427-020-1805-0.

278. Orth-Höller, D., Eigentler, A., Stiasny, K., Weseslindtner, L. & Möst, J. Kinetics of SARS-CoV-2 specific antibodies (IgM, IgA, IgG) in non-hospitalized patients four months following infection. *J. Infect.* 82, 282–327 (2020).
279. Beaudoin-Bussières, G. *et al.* Decline of Humoral Responses against SARS-CoV-2 Spike in Convalescent Individuals. *mBio* 11, (2020).
280. Soltis, R. D., Hasz, D., Morris, M. J. & Wilson, I. D. The effect of heat inactivation of serum on aggregation of immunoglobulins. *Immunology* 36, 37–45 (1979).
281. Kim, K.-H., Seoh, J. Y., Cho, S. J. & Hl, D. Phenotypic and Functional Analysis of HL-60 Cells Used in Opsonophagocytic-Killing Assay for Streptococcus pneumoniae. 6 (2015).
282. Kolaczkowska, E. & Kubes, P. Neutrophil recruitment and function in health and inflammation. *Nat. Rev. Immunol.* 13, 159–175 (2013).
283. Ding, Q., Lu, P., Fan, Y., Xia, Y. & Liu, M. The clinical characteristics of pneumonia patients coinfected with 2019 novel coronavirus and influenza virus in Wuhan, China. *J. Med. Virol.* (2020) doi:10.1002/jmv.25781.
284. Huang, C. *et al.* Clinical features of patients infected with 2019 novel coronavirus in Wuhan, China. *The Lancet* 395, 497–506 (2020).
285. Zhou, F. *et al.* Clinical course and risk factors for mortality of adult inpatients with COVID-19 in Wuhan, China: a retrospective cohort study. *The Lancet* 395, 1054–1062 (2020).
286. Peter, A. E., Sandeep, B. V., Rao, B. G. & Kalpana, V. L. Calming the Storm: Natural Immunosuppressants as Adjuvants to Target the Cytokine Storm in COVID-19. *Front. Pharmacol.* 11, (2021).
287. U.S. National Libary of Medicine. Anti-Interleukin-8 (Anti-IL-8) for Patients With COVID-19. *ClinicalTrials.gov* (2020) doi:NCT04347226.
288. Tleyjeh, I. M. *et al.* Efficacy and safety of tocilizumab in COVID-19 patients: a living systematic review and meta-analysis-first update. *Clin. Microbiol. Infect. Off. Publ. Eur. Soc. Clin. Microbiol. Infect. Dis.* (2021) doi:10.1016/j.cmi.2021.04.019.
289. Wei, Q. *et al.* Tocilizumab treatment for COVID-19 patients: a systematic review and meta-analysis. *Infect. Dis. Poverty* 10, 71 (2021).
290. Franzetti, M. *et al.* IL-1 Receptor Antagonist Anakinra in the Treatment of COVID-19 Acute Respiratory Distress Syndrome: A Retrospective, Observational Study. *J. Immunol.* 206, 1569–1575 (2021).
291. Han, H. *et al.* Profiling serum cytokines in COVID-19 patients reveals IL-6 and IL-10 are disease severity predictors. *Emerg. Microbes Infect.* 9, 1123–1130 (2020).
292. Rojas, J. M., Avia, M., Martín, V. & Sevilla, N. IL-10: A Multifunctional Cytokine in Viral Infections. *J. Immunol. Res.* 2017, 1–14 (2017).

293. Lu, L., Zhang, H., Dauphars, D. J. & He, Y.-W. A Potential Role of Interleukin 10 in COVID-19 Pathogenesis. *Trends Immunol.* 42, 3–5 (2021).
294. Lauw, F. N. *et al.* Proinflammatory Effects of IL-10 During Human Endotoxemia. *J. Immunol.* 165, 2783–2789 (2000).
295. Scoppetta, C., Di Gennaro, G. & Polverino, F. Editorial – High dose intravenous immunoglobulins as a therapeutic option for COVID-19 patients. *Eur. Rev. Med. Pharmacol. Sci.* 24, 5178–5179 (2020).
296. Carannante, N. *et al.* Administration of Immunoglobulins in SARS-CoV-2-Positive Patient Is Associated With Fast Clinical and Radiological Healing: Case Report. *Front. Med.* 7, (2020).
297. Huang, Z. *et al.* Characteristics and roles of severe acute respiratory syndrome coronavirus 2-specific antibodies in patients with different severities of coronavirus 19. *Clin. Exp. Immunol.* 202, 210–219 (2020).
298. Kulkarni, R. Antibody-Dependent Enhancement of Viral Infections. in *Dynamics of Immune Activation in Viral Diseases* (ed. Bramhachari, P. V.) 9–41 (Springer Singapore, 2020). doi:10.1007/978-981-15-1045-8_2.
299. Tetro, J. A. Is COVID-19 receiving ADE from other coronaviruses? *Microbes Infect.* 22, 72–73 (2020).
300. Wan, Y. *et al.* Molecular Mechanism for Antibody-Dependent Enhancement of Coronavirus Entry. *J. Virol.* 94, (2019).
301. Yoo, E. M., Trinh, K. R., Lim, H., Wims, L. A. & Morrison, S. L. Characterization of IgA and IgM binding and internalization by surface-expressed human Fcα/μ receptor. *Mol. Immunol.* 48, 1818–1826 (2011).
302. Paces, J., Strizova, Z., Smrz, D. & Cerny, J. COVID-19 and the Immune System. *Physiol. Res.* 379–388 (2020) doi:10.33549/physiolres.934492.
303. Chao, Y. X., Rötzschke, O. & Tan, E.-K. The role of IgA in COVID-19. *Brain. Behav. Immun.* (2020) doi:10.1016/j.bbi.2020.05.057.
304. Chakraborty, S. *et al. Symptomatic SARS-CoV-2 infections display specific IgG Fc structures*. http://medrxiv.org/lookup/doi/10.1101/2020.05.15.20103341 (2020) doi:10.1101/2020.05.15.20103341.
305. Alter, G., Ottenhoff, T. H. M. & Joosten, S. A. Antibody glycosylation in inflammation, disease and vaccination. *Semin. Immunol.* 39, 102–110 (2018).
306. Seeling, M., Brückner, C. & Nimmerjahn, F. Differential antibody glycosylation in autoimmunity: sweet biomarker or modulator of disease activity? *Nat. Rev. Rheumatol.* 13, 621–630 (2017).

Acknowledgments

Zum Abschluss möchte ich mich bei allen bedanken, die mir das Verfassen dieser Arbeit ermöglicht und mich währenddessen unterstützt haben.
Als erstes ist mein Doktorvater Prof. Dr. Harald Kolmar zu nennen, der mich seit meiner Masterarbeit und dem Einstieg bei Biotest von universitärer Seite aus betreut hat. Vielen Dank für die reibungslosen und unkomplizierten Abläufe, diese sind gerade bei Industriekooperationen nicht selbstverständlich. Es war immer bereichernd dir meine neusten Erkenntnisse vorzustellen und mit dir über die Herausforderungen der Biotest-Produkten zu diskutieren.
Als zweites bedanke ich mich herzlich bei meinem Koreferenten PD Dr. Jörg Schüttrumpf, der mich während meiner gesamten Arbeit bei Biotest immer unterstützte und mir vieles in dieser Firma ermöglicht hat. Außerdem bedanke ich mich für die zahlreichen interessanten Diskussionen, die im Rahmen meiner Arbeit aufgekommen sind und mir beim Fortschreiten im Promotionsprozess geholfen haben. Und zuletzt natürlich vielen Dank für die Übernahme des Zweitgutachtens!
Ebenso bedanke ich mich bei PD Dr. Arnulf Kletzin und bei Prof. Dr. Katja Schmitz für die Übernahme der Fachprüfung und die unkomplizierte Organisation dieser, vielen Dank!

Mein besonderer Dank gilt in erster Linie auch meinen Kollegen bei Biotest. Als erstes ist meine interne Betreuerin Dr. Stefanie Faust zu nennen. Vielen Dank, dass du damals bei meinem Bewerbungsgespräch mein Potential erkannt und mich in die Firma geholt hast. Dadurch hast du mir viele Möglichkeiten eröffnet. Danke für die zahlreichen Ideen, Anregungen, Tipps und auch kreativen Ansätze die du mir in den letzten vier Jahren gegeben hast. Diese haben maßgeblich zum Erfolg meiner Arbeit beigetragen. Wir waren ein gutes Team!
Weiterhin möchte ich meine Kollegen Dr. Marcus Gutscher, Dr. Dennis Riehl, Dr. Karina Winterling, Dr. Katharina Heim, Dr. Viola Marshall, Dr. Daniela Rübsamen, Dr. Matthias Germer und Dr. Sabrina Weißmüller erwähnen. Vielen Dank, dass ihr euer Wissen mit mir geteilt, mir bei der Planung und Auswertung meiner Versuche geholfen und mich so bei meiner Arbeit vorangebracht habt. Und natürlich gilt euch besonderer Dank für das Korrekturlesen meiner Berichte, Publikation und nun auch meiner Dissertation, eure Anregungen haben meine Arbeiten definitiv bereichert. Dr. Tobias Roeser gilt mein weiterer Dank für die Beratung und die Durchführung der patentrechtlichen Fragestellungen.
Ebenso bedanke ich mich bei allen Kollegen aus dem Laborbereich der Abteilungen ADV, IAB, Bioanalysis und Prozessentwicklung. Nur mit eurer Unterstützung war die Durchführung meiner Versuche in diesem Maße überhaupt möglich. Danke, dass Ihr Rücksicht auf den Doktoranden genommen habt und mir geholfen habt. Hier möchte ich besonders meine Kollegen Maren Kyris, Yannick Kopper und Steffen Lehmann hervorheben die auch privat zu guten Freunden geworden sind und mit denen die Pausen immer eine willkommene Abwechslung zum Laboralltag waren. Meiner ehemaligen

Doktorandenkollegin Dr. Carolin Schmidt danke ich besonders für die gemeinsamen Diskussionen und die Tipps bei der Bewältigung der organisatorischen Dinge in Bezug auf die Promotion. Ann Marie McCartin danke ich besonders für das Korrekturlesen meiner Publikation im Hinblick auf die englische Sprache.

Zu guter Letzt möchte ich mich auch bei meinem privaten Umfeld bedanken. Durch dessen Unterstützung und den Ausgleich, den ich hatte, wurde diese Arbeit maßgeblich positiv beeinflusst. Meinen Eltern und meiner Familie danke ich besonders für die Unterstützung und Ermöglichung meines Studiums und der Promotion. Ohne euren Rückhalt wäre es viel schwerer geworden!
Meinen Freunden, besonders dem Stammtisch der Rebläuse, muss ich ebenfalls danken für die abwechslungsreiche und immer lustige Freizeitgestaltung! Dieser Ausgleich zum anspruchsvollen Alltag hat mir sehr geholfen.
Schließlich danke ich meiner größten Stütze, meiner besten Freundin und Lebensgefährtin. Deine Liebe, Unterstützung und Aufmunterungen in vielen schwierigen Phasen des Studiums und dieser Arbeit haben mich in den letzten Jahren immer weitermachen lassen und mir dies alles ermöglicht. Danke!